AUGMENTATION OF HEAT TRANSFER IN INTERNAL FLOW

A

THESIS

Submitted in fulfilment of the requirements for the award of the degree of

DOCTOR OF PHILOSOPHY

in

MECHANICAL ENGINEERING

by

SACHIN GUPTA

YMCAUST/ Ph36/ 2012

UNDER THE SUPERVISION OF

Dr. ARVIND GUPTA
Professor
Department of Mechanical Engineering
J.C.B.U.S.T., YMCA, Faridabad

Dr. MUNISH GUPTA
Associate Professor
Department of Mechanical Engineering
G.J.U.S.T., Hissar

DEPARTMENT OF MECHANICAL ENGINEERING

J. C. BOSE UNIVERSITY OF SCIENCE & TECHNOLOGY, YMCA

FARIDABAD-121006, INDIA

JANUARY, 2021

Candidate's Declaration

I hereby certify that the work which is being presented in the thesis, entitled "**Augmentation of Heat Transfer in Internal Flow"** in the fulfillment of the requirements for the award of the degree of Doctor of Philosophy and submitted in the Department of Mechanical Engineering of J. C. Bose University of Science & Technology, YMCA, Faridabad, is an authentic record of my own work carried out under the supervision of Dr. Arvind Gupta, Professor, Department of Mechanical Engineering, J. C. Bose University Of Science & Technology, YMCA, Faridabad.

The matter presented in this thesis has not been submitted by me for the award of any degree of this or any other University/Institute.

Date:

SACHIN GUPTA
Research Scholar
(YMCAUST/Ph36/2012)
Department of Mechanical Engineering
J. C. Bose University of Science & Technology, YMCA, Faridabad

Certificate

This is to certify that the thesis entitled "**Augmentation of Heat Transfer in Internal Flow**", being submitted by Sachin Gupta (Reg. No. YMCAUST/ Ph36/ 2012) to the Department of Mechanical Engineering, J. C. Bose University of Science & Technology, YMCA, Faridabad for the award of Degree of 'Doctor of Philosophy' in Mechanical Engineering, is a bonafide research work carried out by him under my supervision and guidance. His thesis has reached the standard of fulfilling the requirements of regulations relating to a degree. The thesis is an original piece of research work and embodies the findings made by the research scholar himself.

The results presented have not been submitted in part or in full to any other University/ Institute for the award of any degree or diploma.

Dr. ARVIND GUPTA
Professor
Department of Mechanical Engineering
J.C.B.U.S.T., YMCA, Faridabad

Dr. MUNISH GUPTA
Associate Professor
Department of Mechanical Engineering
G.J.U.S.T., Hissar

Acknowledgment

I take the opportunity to express my heartfelt adulation and gratitude to my supervisor, Dr. Arvind Gupta, Professor, Mechanical Engineering Department, J. C. Bose University of Science & Technology, YMCA, Faridabad for his unreserved guidance, constructive suggestions, thought-provoking discussions and unabashed inspiration in nurturing this research work. It has been a benediction for me to spend many opportune moments under the guidance of the perfectionist at the acme of professionalism. The present work is a testimony to his alacrity, inspiration and ardent personal interest, taken by him during the course of this thesis work in its present form.

I am grateful to my co-supervisor, Dr. Munish Gupta, Associate Professor, Mechanical Engineering Department, Guru Jambheshwar University of Science & Technology, Hissar for his timely guidance, support and encouragement during the course of my work.

I am also thankful to Dr. Raj Kumar, Professor, and Head, Mechanical Engineering Department, J. C. Bose University of Science & Technology, YMCA, Faridabad, for providing facilities to carry out the investigations. Thanks are also to Mr. Nitin Panwar, Assistant Professor, Mechanical Engineering Department, J. C. Bose University of Science & Technology, YMCA, Faridabad to facilitate my experimental work.

I am thankful to Dr. Rajeev Saha, Assistant Professor, Mechanical Engineering Department, J. C. Bose University of Science & Technology, YMCA, Faridabad for his timely guidance, support and encouragement during the course of my work. I express my sincere thanks to Dr. Krishan Verma, Assistant Professor Department of Mechanical Engineering, J. C. Bose University of Science & Technology, YMCA, Faridabad for his valuable contributions to execute this research work. I also wish to thank Dr. Nikhil Dev Garg, Assistant Professor, Department of Mechanical Engineering, J. C. Bose University of Science & Technology, YMCA, Faridabad for their constant support during my experimental work.

I am particularly thankful to Dr. Narinder Kaushik, Assistant Professor, Department of Mechanical Engineering, Maharaja Agrasen Institute of Technology, Delhi for providing valuable suggestions concerning this research work.

The services of the staff of Central Workshop and various testing labs, Mechanical Engineering Department, J. C. Bose University of Science & Technology, YMCA, Faridabad are acknowledged with sincere thanks.

It is a pleasure to acknowledge the support and help extended by all my Professional colleagues Dr. Rajesh and Dr. Alok. I cannot close these prefatory remarks without expressing my deep sense of gratitude and reverence to my dear parents for their blessings and endeavor to keep my morale high throughout the period of my work. The author feels extremely happy to express his sincere appreciation to his wife Isha and son Keshav for their understanding, care, support and encouragement.

I want to express my sincere thanks to all those who directly or indirectly helped me at various stages of this work.

Above all, I express my indebtedness to the "**ALMIGHTY GOD**" for all His blessing and kindness.

(SACHIN GUPTA)

Abstract

Heat exchangers are indispensable for achieving heat dissipation from the generation source point in applications such as Heating, Ventilation and Air Conditioning (HVAC), refrigeration devices and automobile radiators. Efforts for improving the transfer of heat between two fluids flowing over and into the heat exchanger have been a topic of research for many years. Fin-tube type of heat exchanger is one of the most commonly used types of heat exchangers and there are numerous studies that have been carried out to increase the air-side heat transfer, all of which involve either the use of active methods or passive methods for heat transfer augmentation. Since making use of passive methods does not require any extra power, they are commonly used and preferred. Among all such methods, Vortex Generators (VGs) are of prime interest. From the available types of VGs, the majority of the studies have been performed considering winglets as VGs because these types of VGs can be easily attached or punched out of fins. Winglets can effectively generate Longitudinal Vortices (LV) which in turn increases convective heat transfer coefficient and at the same time increases pressure drop.

The present study is focused on the development of a new compact heat exchanger by enhancing the local convective heat transfer coefficient. In the present work, we have considered a fin-and-tube heat exchanger for investigations. The vortex generators considered are in the form of a rectangular winglet pair having a circular hole at their center. Experiments were performed on a fin-and-tube heat exchanger installed in a wind tunnel test rig. I have considered two configurations of the winglet during the experimentation i.e. Common Flow Down orientation at the downstream location and Common Flow Up orientation at an upstream location. Numerical simulations have also been performed to investigate the heat transfer and flow resistance characteristics of rectangular winglet type vortex generators (VGs) with a punched hole of circular shape at their center. Investigations have been performed considering Reynolds number in the range of 1400 to 9000, keeping the angle of attack at 45°. The Shear Stress Transport (SST) k-ω turbulence model has been used for performing numerical simulations. Rectangular winglet pair have been placed in Common Flow Down (CFD) and

Common Flow Up (CFU) orientation at downstream as well as upstream location. After comparing the results of experimentation with the numerical simulations results, we found that the error was well within the acceptable limit of 15%.

Firstly, my focus was on to study localized heat transfer augmentation. For this purpose, two points have been taken. One point was 32 mm away from the tube center radially, and the second point was a random point taken downstream of the tube. This point happened to lie after the winglets in all of the four cases. In the case of the common flow down orientation of the winglet located at a downstream position, the point was right near the region where the formation of vortices was most pronounced. The reason behind making such a selection of point location was to study the effect of vortex formation on temperature values over the plate. In other words, the motive was to study the effect of winglets on heat transfer from the fin plate in the wake region. Heat transfer, as well as flow resistance characteristics, have been compared for all the four configurations of winglet viz., CFD and CFU, in downstream as well as upstream location using Colburn's factor(j), friction factor(f) and performance evaluation criterion (PEC) = $(j/j_0)/(f/f_0)^{1/3}$. The punched hole considerably improves the thermal performance and decreases the flow resistance due to the reduction in the face area. It has been observed that CFD orientation at upstream location provides a maximum enhancement in heat transfer characteristics with an average improvement of 55% over baseline case as it offers the highest Nusselt number values out of all the four cases. Additionally, CFD orientation at a downstream position provides the least value of pressure drop whereas CFU orientation at the upstream position has the maximum pressure drop. Moreover, we found that CFD configurations have better thermal performance as compared to CFU configurations irrespective of whether it is located upstream or downstream. Furthermore, we found that positioning of the winglet at the upstream location would have better heat transfer augmentation as compared to the scenario of positioning the same in the downstream position as far as the local heat transfer augmentation is considered.

Secondly, I move on to find the globalized effect of employing a rectangular winglet having a punched hole at its center. Studies have been performed on all the four configurations viz., common flow down (CFD) and common flow up (CFU) orientation at upstream as well as downstream location. Performance characteristics such as Colburn's factor (j), friction factor (f) and performance evaluation criterion (PEC = j/f)

have been considered for evaluating the thermohydraulic performance. Investigations have been performed considering the same Reynolds number i.e. 1400 to 9000, keeping the same angle of attack i.e. 45°. The SST k-ω turbulence model has been used for performing numerical simulations. A significant augmentation of up to 71% in thermal performance of fin-tube heat exchanger was observed with the CFD orientation located upstream over the CFU orientation located upstream which displayed the least improvement.

The present study goes on further to investigate the effect of punching out the VGs from the plate surface. Secondly, three cases have been studied numerically in case of punched out rectangular winglet pair with a circular hole at the center viz., common flow up at the upstream location, common flow down at an upstream location and common flow down at the downstream location. The location of the winglet and its angle of attack in the punched-out case has been kept identical to that in the non-punched case in order to draw coherent comparisons between the performance characteristics of the two. Due to placement of the winglet at the determined location and selected angle of attack, plate punching interferes with the tube placement for the fourth case that is, common flow up at a downstream location. There is a thermohydraulic augmentation of up to 34% for the considered range of Reynolds number in case of fin-tube heat exchanger employing punched rectangular winglet pair with hole at the center, having CFU orientation and located in the upstream location, over the non-punched case of rectangular winglet with hole at the center, in the same orientation and location.

The study shows that the vortex generators when either mounted or punched-out on the fin surface show great promise for enhancing the heat transfer rate in a fin-tube heat exchanger.

Contents

List of Figures

List of Tables

Nomenclature

j	Colburn's factor
A_c	Cross Section Area (m^2)
f	Friction factor
Q	Heat Transfer Capacity (W)
D_h	Hydraulic Diameter (m)
$\dot{m}$	Mass flow rate of air (kg $s^{-1)}$
T_m	Mean temperature for a cross section (K)
$T_{m,in}$	Mean temperature at inlet cross section (K)
$T_{m,out}$	Mean temperature at outlet cross section (K)
$T_{m,wall}$	Mean wall temperature of fin surface (K)
ΔT_m	Mean temperature difference (K)
P_m	Mean Pressure for a cross section (Pa)
ΔP_m	Mean pressure drop (Pa)
Nu	Nusselt number
Pr	Prandtl number
Re	Reynolds number
C_p	Specific heat at constant pressure (J $kg^{-1}K^{-1}$)
A_s	Surface Area (m^2)
k	Thermal conductivity (W m^{-1} K^{-1})

u	Velocity component in x-direction (m s^{-1})
v	Velocity component in y-direction (m s^{-1})
w	Velocity component in z-direction (m s^{-1})

GREEK SYMBOLS

α	Angle of attack of the vortex generator
ρ	Density (kg m^{-3})
μ	Dynamic Viscosity (Pa.s)
ν	Kinematic Viscosity (m^2 s^{-1})

ABBREVIATIONS

CFD	Common Flow Down
CFU	Common Flow Up
CFD_D	Common Flow Down at the downstream location
CFD_U	Common Flow Down at the upstream location
CFU_U	Common Flow Up at the upstream location
CFU_D	Common Flow Up at the downstream location
LV	Longitudinal Vortices
LVG	Longitudinal Vortex Generator
PEC	Performance Evaluation Criterion
RWP	Rectangular winglet pair
RWPH	Rectangular Winglet Pair with a hole
VG	Vortex Generator

CHAPTER - 1

(INTRODUCTION)

1.1. INTRODUCTION

Air acts as a medium of heat exchange in so many thermal equipments. Ordinarily, phase change heat exchanger have high heat transfer coefficient in comparison to air. Heat transfer enhancement devices or methods can help in achieving significant cost reductions and energy in such applications where one fluid's thermal resistance shows dominance. For air side heat transfer enhancement, the development of surfaces with high performance is an area that is important and interesting as the above-described situations are usual and extensively recognized in industries. The heat transfer coefficient of the gas side can be increased by the use of extended surfaces. However, the obtained heat transfer coefficient of the gas side may still be lower than that of the liquid.

Generally, the air side thermal resistance used to be 10 to 50 times as high as compared to liquids so especially, in heat exchangers with gases, improvement of the performance becomes extremely important (Stefan Tiggelbeck, Mitra, & Fiebig, 1992) which, on air side, needs sizeable surface area of heat transfer per unit volume. It will be beneficial, in this case, to consider the use of particularly composed enlarged surfaces or turbulence generations which will yield augmented coefficients of heat transfer. 50 to 150% higher coefficients of heat transfer may be provided by such special surface devices than that of plain extended surfaces. For heat transfer between gases, such arrangements will give a tenable reduction in the size of the heat exchanger.

1.2. TRADITIONAL METHODS OF HEAT TRANSFER AUGMENTATION

Energy and materials prevention considerations have prompted an augmentation of the attempts focused on developing better and extra potent equipment of heat exchanger by heat transfer augmentation during the last fifty years. Externally finned tubes **(Jacobi & Shah, 1995)** are a good example wherein they have provided good advantages in natural and forced convection, pool and forced convection boiling and condensing applications.

The most popular technique is the extended heat transfer surfaces, which cross flow compact heat exchangers use extensively. Either tube-fin or plate-fin heat exchangers are cross-flow compact heat exchangers.

1.2.1. Plate-Fin Heat Exchangers

In this type, spacers or fins separate two plates which are parallel and which define each channel. Formed tubes or parallel plates cram spacers or fins as shown in Figure1.1. Welding, soldering, mechanical fit, extrusion or brazing is used to attach the fin to the plates. Two sides of heat exchangers are formed by connecting alternate passages of fluid, parallelly by ends. In gas-to-gas heat exchangers, on both sides, fins are applied.

The coefficient of heat transfer is lower on the side of gas, so fins are generally commissioned only there, in applications of gas-to-liquid heat exchangers. There is a possibility of fins being plain but wavy fins; straight and plain fins; or interrupted fins such as strip, perforated and, louver, which are used in a plate heat exchanger. Distinct fin configurations used in plate-fin heat exchangers are shown in Figure 1.2.

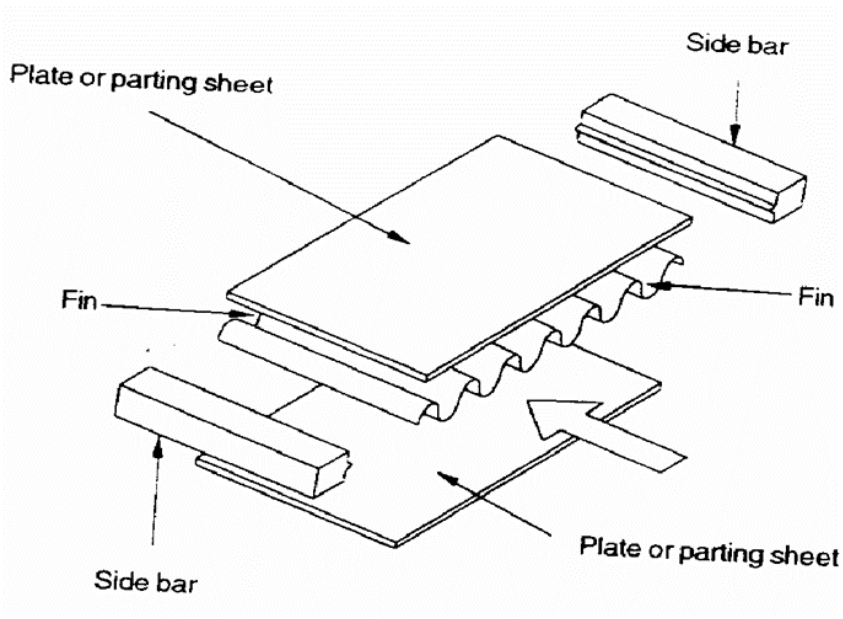

Figure 1.1 Basic components of plate-fin heat exchanger (Lyczkowski, 1984)

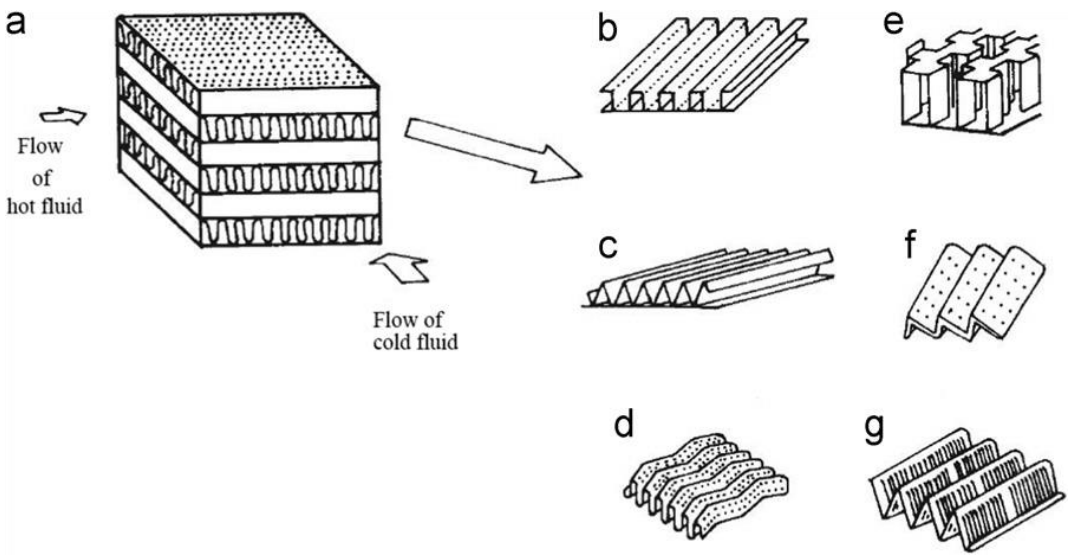

Figure 1.2 (a) Plate-fin heat exchanger and it's surface geometries, (b) plain rectangular fins, (c) plain triangular fins, (d) wavy fins,(e) offsets strip fins, (f) perforated fins and (g) louvered fins (Kakaç, Shah, & Aung, 1987)

1.2.2. Tube-Fin Heat Exchangers

Round, rectangular, and elliptical-shaped tubes are used and depending upon the applications, either on both outside and inside or, on the inside or on the outside, of the tubes fins are employed, in a fin-tube heat exchanger.

Many closely packed heat exchangers with several fin paradigms were produced to reduce the airside thermal resistance, for weight and size reduction of heat exchangers. Fins that are on the outside of the tube can be classified as 1) Longitudinal fins on individual tubes, 2) Normal fins on individual tubes, 3) Flat or continuous (wavy, interrupted, or plain) external fins on arrays of tubes. Owing to its versatility, durability, and simplicity, among these, in the application, the most popular fin pattern is still the plain fin configuration. Drop-in pressure and heat transfer characteristics of a range of configurations of compact heat exchanger matrices have been presented by (Kays and London, 1964). Figure 1.3 shows the distinct types of tube-fin heat exchangers.

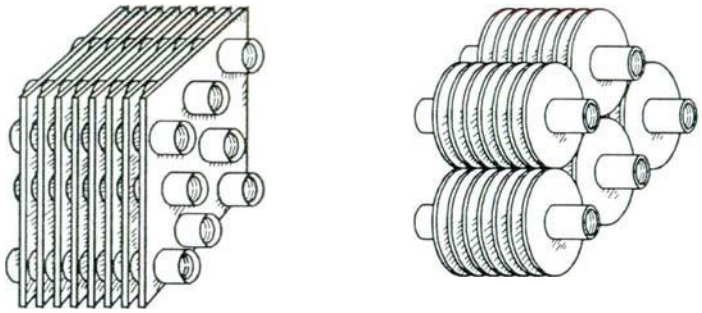

Figure 1.3 Tube-fin type of compact heat exchangers

1.2.3. Applications

In applications where heat exchanger medium is a gas, tube-fin, plate-fin, tube bundles with small diameters and regenerative have exchangers are ordinarily used. Some of the applications are refrigeration, HVAC systems, air-cooled condensers, dry cooling towers, oil heaters, and transportation equipment. Also, in-car radiators, cryogenics process industries, chemicals, electronics and several other areas of industries, compact heat exchangers are used.

1.2.4. Limitation of Traditional Methods of Heat Transfer Augmentation

The above mentioned compact heat exchangers were developed by increasing the heat transfer surface area per unit volume of heat exchangers. On the gas side, there can still be the higher thermal heat transfer resistance, despite the larger heat transfer area. These methods are found to have many advantages and limitations. Fin efficiency gets lower with augmentation of the fin area, so, by increasing the fin area for reducing gas side thermal resistance the potential is constrained. The system becomes spacious, heavier, and costlier because fins are higher in number. Even though a good amount of research work has been carried out on the traditional methods, and endeavor for getting to a wider view on the heat transfer coefficient enhancement is still being studied. In compact heat exchangers, the artificial introduction of vortices on the gas side can be another alternative for augmenting heat transfer.

1.3. WINGLET VORTEX GENERATOR – A DEVICE FOR HEAT TRANSFER AUGMENTATION

In recent years the quest for more efficient compact heat exchanger design has stimulated the interest of investigators in exploring the use of a new technique of augmenting the air-side coefficient of heat transfer. It has been shown by the recent researchers that in enhancing the heat transfer, an important role is played by the vortices. However, by making the flow turbulent the value can be increased of the coefficient of convective heat transfer. The flow can be made more turbulent by artificial vortices into the flow, at a given Reynolds number. These will lead to the generation of more turbulence in the flow and which will improve the rate of transfer of heat, and the heat exchanger's capacity is thereby increased. The introduction of artificial vortices can be done in many ways. One of the ways of increasing the level of turbulence is by attaching or punching protruded surfaces on the heat exchanger's surface in the form of small triangular pieces. With respect to the direction of the main flow, these small protrusions are attached at an angle of attack. These are known as vortex generators, turbulence promoters, or sometimes turbulators. Vortex generators are classified according to their shapes. They are called wing type vortex generators and termed as winglets when its chord is joined to the fin and wings when their trailing edge is joined to the fin. Consideration of ease of fabrication requires the shape of the winglets to be kept simple. They are therefore often either rectangular or triangular. The major distinction between the flow fields of the winglet and of the wings is because a trailing edge wake cannot be generated by the attached wings. Main flow direction and the trailing edge form strong shear layers near the plane and the winglet wake is characterized by these strong shear layers. Study of the influence of longitudinal vortices embedded by vortex generator having types as wing and winglet and on the loss of pressure and transfer of heat is related to the present-day development of high-performance heat exchangers.

Figure 1.4 shows the vortex generators' different geometries. Longitudinal streamwise vortices are induced by these vortex generators in the flow field. Because of the difference of the pressure between the back surface and the front surface which faces the flow, the vortices are developed along the vortex generator's edge. Due to the reason

that the direction of the main flow has an angle of inclination with their axes of rotation, so, these vortices are called longitudinal vortices.

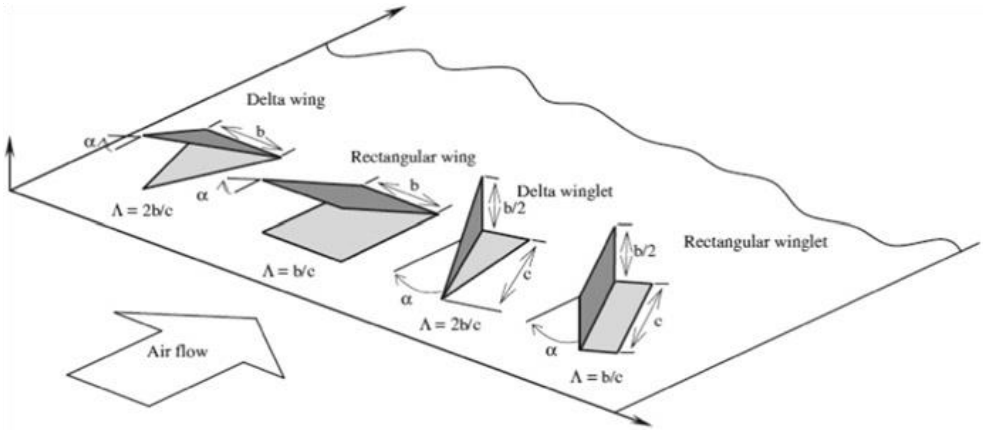

Figure 1.4 Types of longitudinal vortex generators (Aris, Owen, & Sutcliffe, 2011)

Figures 1.5 shows the vortices produced by a vortex generator along the cross-section. On a flat plate, in a laminar boundary, a sketch of longitudinal vortices behind a vortex generator placed is presented in Figure 1.6 (Kahoru Torii, Nishino, & Nakayama, 1994). The near-wall fluid is mixed with the free stream by a three-dimensional swirling flow which is produced by these streamwise vortices which associate with an otherwise boundary layer which is two dimensional. High heat transfer augmentation is caused by this mechanism, as the fluid exchange, between the wall and the region of the core of the flow field, is enhanced by this mechanism. The use of longitudinal vortices for boundary layer control is well known (Pearcy, 1961) and the vortex generators are commonly used in commercial airplanes for this purpose. Several investigations were carried out by (M. Fiebig, Güntermann, & Mitra, 1995), both experimental as well as computational so that the basic mechanism for enhancement of transfer of heat by longitudinal vortices can be understood, and also to predict quantitatively the range of increment of transfer of heat which can be attained by the use of distinct vortex generators' types viz., delta winglet pairs, delta wings, and rectangular wings. The vortex generator obstructs the flow and hence adds to the pumping cost. However, because of the longitudinal vortex generators' use, the additional loss of pressure is very ordinary, because, for these slender bodies, the form drag is low. Further, when the absolute ducting of the equipment is contemplated, this elevation in pumping power will be trivial.

Figure 1.5 Longitudinal vortices along the cross-section (Dyke, 1988)

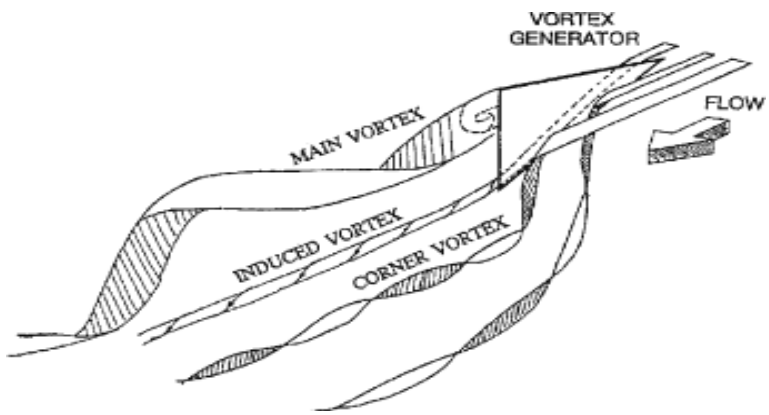

Figure 1.6 Longitudinal streamwise vortices generated with delta winglet type vortex generator (Kahoru Torii et al., 1994)

1.3.1. Concept of Generation of Vortices in a Flow

Turbulent flows are known for having high rates of momentum and heat transfer. Internal turbulent flows will have a high drop in pressure and a high value of convective heat transfer coefficient. Detailed studies about turbulent flow reveal that turbulent flow consists of a set of eddies of (vortices) varying size and strength. The level of local

momentum transfer and heat transfer depends on the structure of the vortex flow.

The understanding of vertical motion in turbulent flows developed two ideas, (i) controlling the sizes and strength of these vortices and (ii) artificial introduction of selected vortices into an existing flow to achieve a specific objective. Vortices can be generated in many ways, some popular methods are mentioned below. The vortices can be introduced by locating protrusive surfaces in a flow field. Vortices can also be generated by introducing sound waves into a flow field. In acoustics, the theory of aerodynamic sound generation is based on vertical motion in an unsteadying flow. In 1908, (BENARD & H., 1908) related the vortex concept to sound for the first time. Another research that was carried out by (Wendt & Hingst, 1994) closely related to vertical sound generation is the vortex-induced vibration of bodies.

1.3.2. Counter-rotating and Co-rotating Vortices

A horseshoe vortex system's form is usually taken by a secondary flow which is introduced by a tube when it is present in a plain passage. At the stagnation zone, the transfer of heat is enhanced by the horseshoe vortex system. It has been shown by several studies (Saboya & Sparrow, 1974) that of the order of several hundred percent enhancement of local transfer of heat can be ascribed to the horseshoe vortex system.

Additionally, the flow field is seen in sets or pairs, in vortices, usually, for instance when a blunt protuberance from a surface produces the horseshoe vortex pair. On the basis of their corresponding ways of rotation, the interaction between adjacent vortices can be split into two paradigms, co-rotating (common flow up) and counter-rotating (common flow down). The secondary flow direction between them, that is able to be conducted away from or towards the wall, can identify counter-rotating vortices. A vortex pair is created when two vortex generators are positioned together as depicted in figures 1.7(a) and 1.7(b). When the apex of each vortex generator is in close proximity to the centerline than the trailing edge, this creates a Common Flow Down (CFD) between the two vortices in a pair, as Figure1.7 (a) shows. When the apex of each vortex generator is further away from the

tube centerline than the trailing edge, then between the two vortices in a pair the opposite effect of a Common Flow Up (CFU) is created, as Figure1.7 (b) shows.

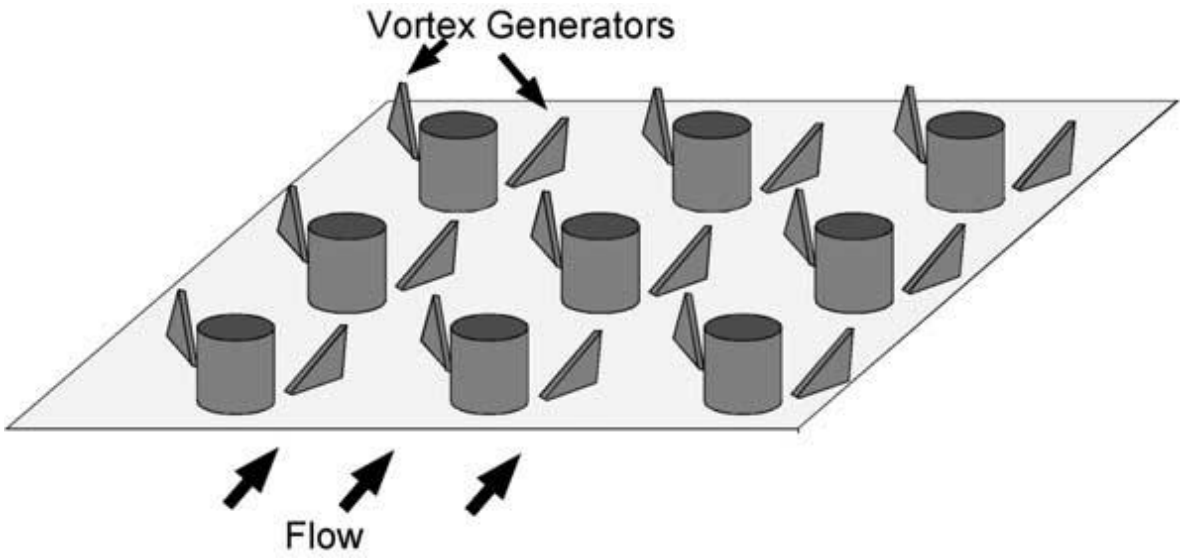

(a) Common Flow Down configuration

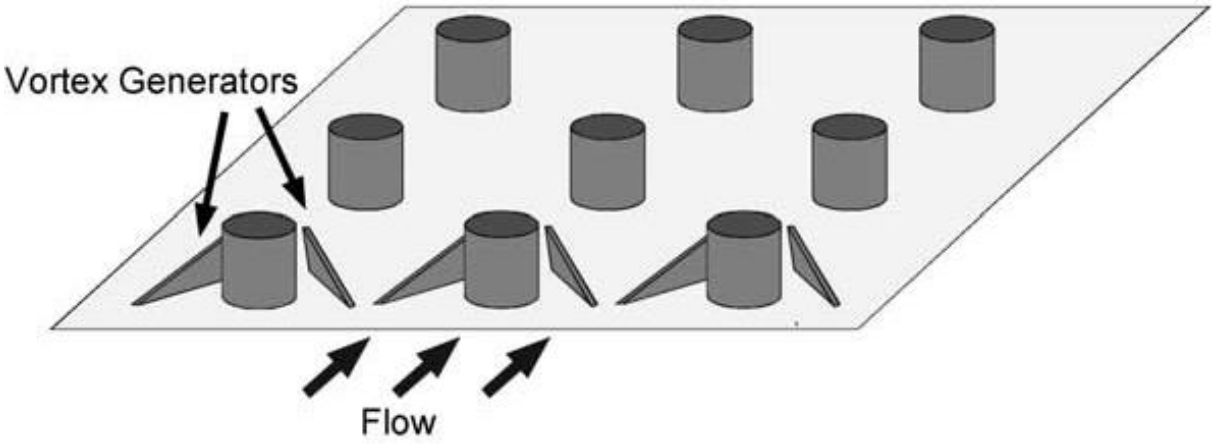

(b) Common Flow Up configuration.

Figure 1.7 Configuration of winglet type vortex generator (K. Torii, Kwak, & Nishino, 2002)

1.4. MOTIVATION FOR THE WORK

As mentioned before, on the gas side the thermal resistance in the heat exchangers is very high. So, even while having an extended surface, this high resistance causes low heat transfer coefficients. Schemes and approaches must be produced to bring about considerable heat transfer enhancement. So, finding the augmentation of the heat transfer on the gas side, is the motivation behind the present work, with longitudinal vortex generator's use which is mounted as well as stamped out of the fin plate surface in a fin-tube heat exchanger.

1.5. OBJECTIVES OF THE WORK

In the proposed study the attempt has been made to achieve the following objectives by doing analysis on a fin-tube heat exchanger which has very wide applications in the Refrigeration and Air-Conditioning (RAC) industry. These are as follows

1) To have an understanding of flow characteristics for different values of Reynolds no. using winglet as a vortex generator that is mounted as well as punched out of the fin surface in a fin-tube heat exchanger.
2) To analyze numerically the behavior of pressure drop along the length of the fluid flow using winglet as a vortex generator which is mounted as well as punched out of the fin surface in a fin-tube heat exchanger.
3) To analyze experimentally as well as numerically heat transfer characteristics (which is of paramount importance while designing the heat exchangers for refrigeration and air-conditioning devices) with or without the winglet as a heat transfer enhancement device in a fin-tube heat exchanger.
4) To evaluate analytically the overall thermohydraulic performance (for making a relative comparison between different heat exchangers which can be used for a particular application) of the fin-tube heat exchanger using winglet as a vortex generator which is mounted as well as punched out of the fin plate surface and compare it with the baseline case having no vortex generator.

1.6. ORGANIZATION OF THE THESIS

There are eight chapters in this thesis. Following is a synopsis of each chapter

Chapter 1-Introduction

Heat exchangers are introduced and classified in this chapter. There is a brief introduction of compact heat exchangers. The concept of generation of vortices is also discussed. Finally, the motivation for the research and objectives of this research are presented.

Chapter 2-Literature Review

Presentation of results of broad literature research in the area of augmentation of heat transfer with higher attention on vortex generators use is done in this chapter. A special focus has been given to the vortex generator's use for augmentation of heat transfer. This chapter presents the details of work undertaken by different scientists and engineers in the field of augmentation of heat transfer with vortex generator's use. The review includes numerical along with the time to time undertaken experimental work**.** The gaps are identified for the present research work, depending upon the literature review.

Chapter 3- Research Methodology

A detailed description of the problem statement is given, in this chapter. The experimental test-rig used and the procedure followed have been explained clearly. Various elements of the numerical simulation viz., selection of turbulence model, grid independence and validation of simulation with the experimentation have also been presented. Various performance parameters used have been explained clearly including a note on uncertainty analysis. Moreover, a section on the sample calculation has also been added to clearly explain the various performance parameters calculated during the entire investigations.

Chapter 4- Performance of the Rectangular Winglet (Localized study)

This chapter discusses the advancement in the fin-tube heat exchanger's performance in the wake region, using a rectangular winglet having a circular hole at its

center, over the baseline case having no vortex generator. It also explains the effects of punched holes on the rectangular winglet's surface over the winglet having no punched hole. The performance of various configurations of vortex generators viz., Common Flow Down (CFD) and Common Flow Up (CFU) configuration at an upstream and downstream location of flow have been presented with the help of various performance parameters. Studies have also been done on the selection of optimum configuration of vortex generator for maximum augmentation of transfer of heat and minimum resistance of flow.

Chapter 5- Performance of the Rectangular Winglet (Globalized study)

A study on the globalized effect (i.e. considering the entire fin plate surface for study; rather than limiting to the point study (localized study) only) of employing a rectangular winglet having a punched hole at its center as the vortex generator, in a fin-tube heat exchanger, is contained in this chapter. Firstly, the vortex generator's orientation effect has been presented and afterward the effect of the location of the same has been discussed in detail. The performance of various configurations of vortex generators viz., CFU and CFD configuration at upstream and downstream locations of flow have been presented with the help of various performance parameters. The study has also been done on the selection of optimum configuration of vortex generator for maximum augmentation of transfer of heat as well as minimum resistance to flow.

Chapter 6- Performance of the Punched-out Winglet

This chapter presents the effect of a punched-out / stamped-out rectangular winglet having a circular hole at its center from the fin plate surface. In addition to that a relative comparison between the performances of punched-out winglets over non-punched winglets in the three different configurations viz., CFD configuration at downstream as well as upstream location and CFU at the upstream location have also been presented with the help of various performance parameters.

Chapter 7- Conclusion and Future Scope

Present work's conclusions along with the opportunity and scope for future work in the same field, are contained in this chapter.

Figure 1.8 represents the chapter plan of the thesis which gives us a quick idea of how the entire thesis has been arranged. Moreover, it also tells us briefly about how the entire investigation has been made.

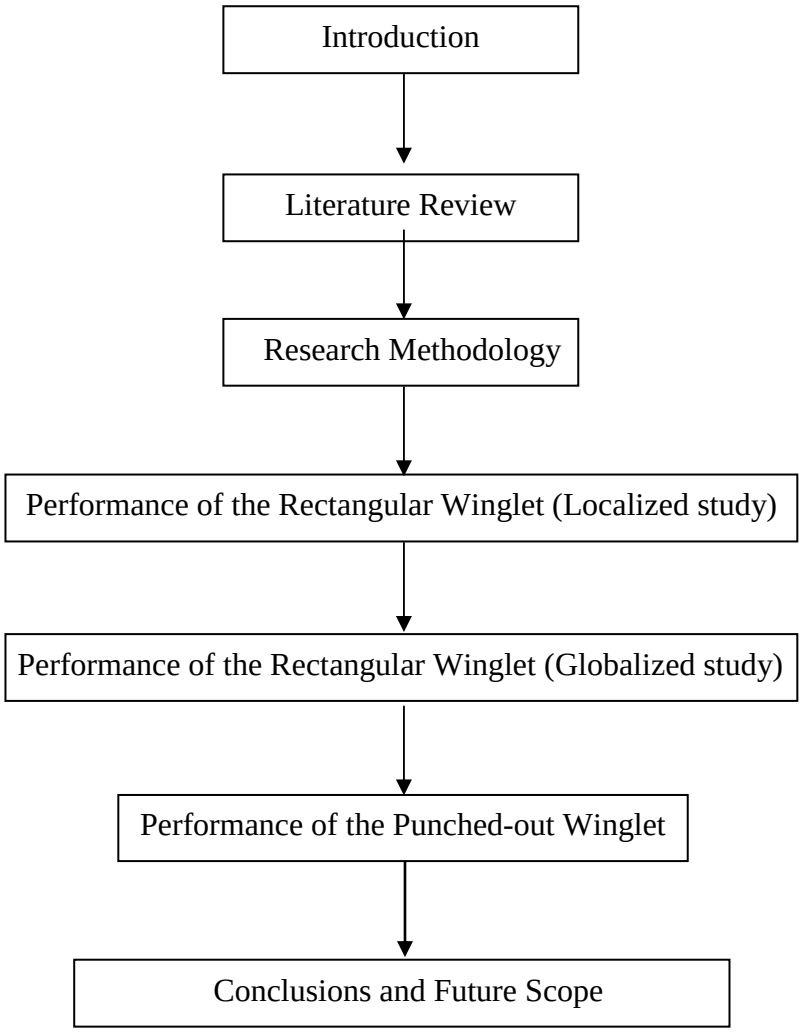

Figure1.8 Chapter plan of the thesis

CHAPTER - 2

(LITERATURE REVIEW)

2.1. INTRODUCTION

In this chapter, the results of extensive literature research in the field of heat transfer enhancement with more emphasis on the use of vortex generators are presented. Special focus will be given on the use of a vortex generator for heat transfer augmentation. This chapter presents the details of work undertaken by different scientists and engineers in the field of heat transfer enhancement with the use of vortex generators. It also discusses the literature review encompassing different shapes of winglet (vortex generator), method of attachment, a different arrangement of winglet with regard to single or multi winglet pair and also optimization of various input parameters related to the shape and size of the winglet. The review includes numerical as well as the experimental work undertaken from time to time. Depending upon the literature review the gaps are identified for the present research work.

Heat exchangers are indispensable for achieving heat dissipation from the generation source point in applications such as Heating, Ventilation and Air Conditioning (HVAC), refrigeration devices and automobile radiators. Efforts for improving the transfer of heat between two fluids flowing over and into the heat exchanger have been a topic of research for many years. The fin-tube type of heat exchanger is one of the most commonly used types of heat exchangers. Figure 2.1 shows a fin tube heat exchanger.

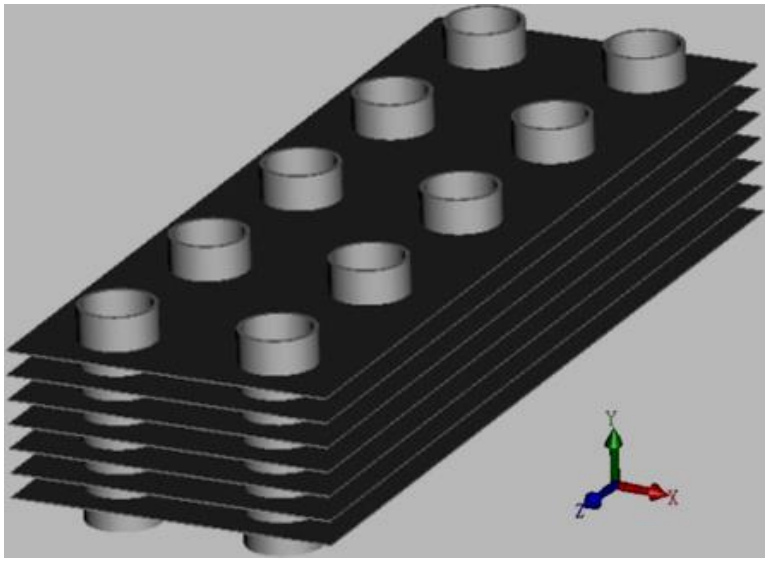

Figure 2.1 Fin tube heat exchanger (Y. L. He, Han, Tao, & Zhang, 2012)

There are numerous studies that have been carried out to increase the air-side heat transfer, all of which involve either the use of active methods or passive methods for heat transfer augmentation. Since making use of passive methods does not require any extra power, they are commonly used and preferred. Among all such methods, vortex generators (VGs) are of prime interest. Various studies have been performed over the years which make use of various types of vortex generators for increasing air-side convective heat transfer coefficient in a heat exchanger. As the name suggests, the primary task of a vortex generator is to create longitudinal vortices (LV) that delay the separation of the boundary layer from the wall and simultaneously guide the fluid having more kinetic energy to wake the region for minimizing the recirculation zone, thereby enhancing heat transfer. From the available types of VGs, the majority of the studies have been performed considering winglets because these types of VGs can be easily attached or punched out of fins. Winglets can effectively generate LV which in turn increases convective heat transfer coefficient and at the same time increases pressure drop. Figure 2.2 shows the formation of longitudinal vortices.

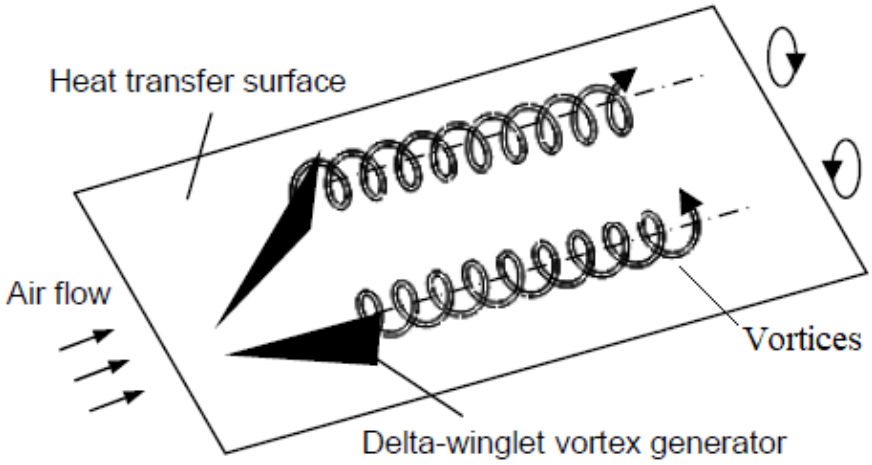

Figure 2.2 Formation of longitudinal vortices

2.2. HEAT TRANSFER AUGMENTATION IN THE CHANNEL FLOW

Numerous studies, both numerical and experimental have been performed in recent times considering winglet as the vortex generator for investigating the thermo-hydraulic behavior of heat exchangers, particularly channel flow.

(**Jacobi & Shah, 1995**) presented an exhaustive review of thermo-hydraulic characteristics for a channel flow by using delta and rectangular winglets as VGs.

(Valencia, Fiebig, & Mitra, 1996) performed a number of experiments and concluded that by using vortex generators on the fin surface, there was a considerable improvement in the heat transfer. This was in agreement with the findings of (Biswas, Mitra, & Fiebig, 1994).

(M. Fiebig, 1998) performed numerical simulation and experimentation for a channel flow considering rectangular and delta wings as well as winglet both and concluded that winglets furnished superior heat transfer characteristics. In his study, he also observed that for identical dimensionless parameters, the performance of rectangular and delta winglets was the same.

(St. Tiggelbeck, Mitra, & Fiebig, 2008) considered channel flow to compare the performance of winglets and wings and concluded that winglets outperformed wings for heat transfer enhancement.

(PAULEY & EATON, 2008) made experimental investigations and proposed two configurations for winglets known as common flow down (CFD) and common flow up (CFU). In CFD configuration leading edge of the winglet is closer than the trailing edge with respect to the tube in a fin-tube heat exchanger. On the contrary, in CFU configuration trailing edge of the winglet is closer than the leading edge with respect to the tube in a fin-tube heat exchanger.

(L. T. Tian, He, Lei, & Tao, 2009) performed numerical investigations for both the aforementioned configurations, which is CFU and CFD for rectangular as well as delta

winglet and reported that better results are realized using rectangular winglet as compared to the latter in terms of superior heat transfer augmentation.

(Min, Qi, Kong, & Dong, 2010) also proposed a new configuration replacing rectangular winglet pair (RWP) with modified rectangular winglet pair (MRWP) which was developed by cutting four corners of the rectangular winglet and reported that MRWP has better thermohydraulic performance than RWP. The same has been depicted in figure 2.3.

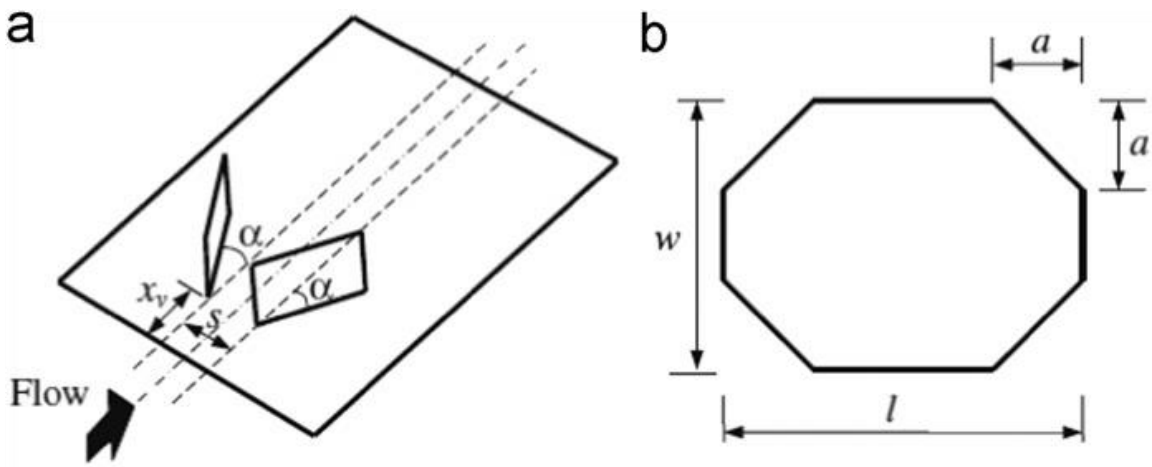

Figure 2.3 Schematic view (a) Rectangular Winglet (b) Modified rectangular winglet (Min et al., 2010)

(Oneissi, Habchi, Russeil, Bougeard, & Lemenand, 2016) numerically investigated and proposed a new winglet VG pair named as inclined projected winglet pair (IPWP) which gives a better thermohydraulic performance as compared to delta winglet pair for fluid in a channel flow. The proposed vortex generator gives a significant drop in the pressure drop penalty because of its aerodynamic design.

(J. M. Wu & Tao, 2012) studied the flow resistance and heat transfer characteristics of RWP which were stamped out directly from the fin surface in a channel flow and concluded that punched out winglets performed better in terms of thermohydraulic performance because of the possibility of transverse flow through holes created by punching of the winglet.

(Chen, Fiebig, & Mitra, 1998) found that the form drag of winglet is the main cause for pressure drop and the main source of form drag is the recirculation zone behind the winglet. So, to reduce pressure drop, the recirculation zone should be reduced to as minimum as possible which in turn decreases the form drag and thereby pressure drop can be decreased. **(Zhou & Feng, 2014)** proposed that to reduce the recirculation zone holes can be punched on the surface of the vortex generator and experimentally studied the effect of holes punched on the surface of vortex generator in a channel flow. In their investigations, they had considered plane and curved winglets with and without punched holes on their surface having shapes like rectangular, triangular (delta) and trapezoidal which were mounted in CFD configuration on the lower plate of the channel flow for assessing the thermohydraulic performance. The same has been depicted in figure 2.4. It was reported that the punched holes considerably improves the thermohydraulic performance. Additionally, it was also reported that the curved winglet outperforms the plane winglet. Furthermore, it has been reported in their study that the curved delta winglet exhibits superior performance over the other cases.

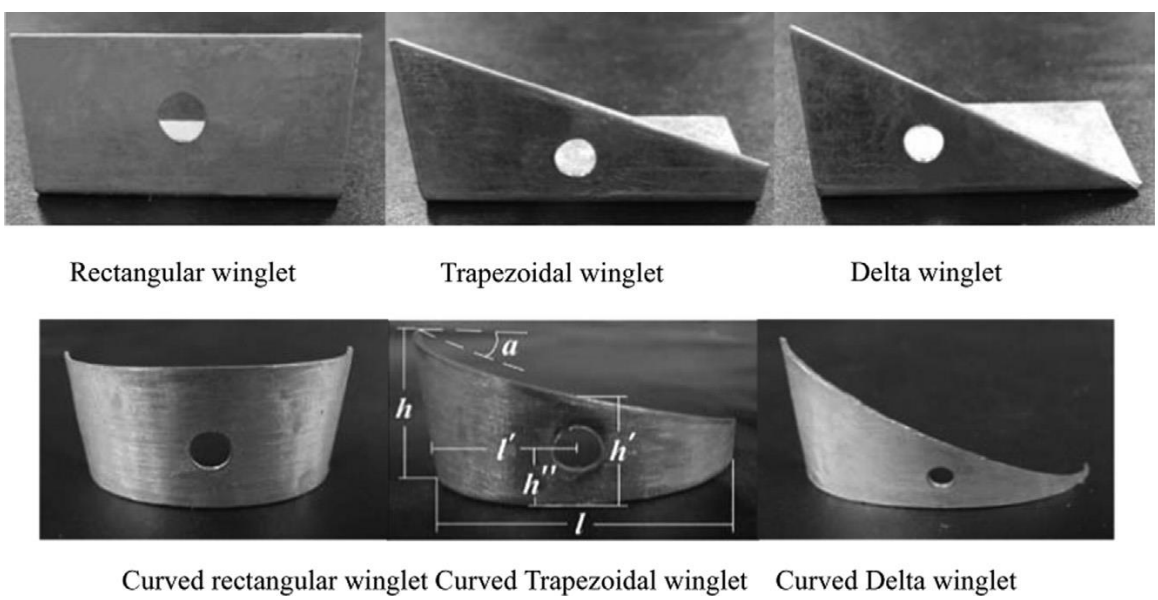

Figure 2.4 Pictorial diagram of vortex generators with punched holes (Zhou & Feng, 2014)

(Naik, Harikrishnan, & Tiwari, 2018) carried out a numerical study to investigate the thermohydraulic behavior of fluid in a channel flow using a curved rectangular winglet as vortex generator in two configurations namely, concave and convex based on the surface facing the fluid flow. They concluded that maximum augmentation achieved is around 22% in heat transfer characteristics for the concave-shaped rectangular winglet vortex generator over the baseline case.

(Song, Tagawa, Chen, & Zhang, 2019) performed a numerical investigation for evaluating the heat transfer characteristics in a channel flow using concave and convex curved delta winglet vortex generator and found that for laminar flow concave curved delta winglet vortex generator exhibits superior heat transfer characteristics than convex curved delta winglet vortex generator with respect to plane delta winglet vortex generator.

(Ke, Chen, Li, Wang, & Chen, 2019) numerically studied the thermohydraulic performance of fluid flow in a channel flow considering a new mixed-up configuration and made a relative comparison with the popularly known common flow down configuration as well as with the common flow up configuration. They concluded that for small channel height new mixed-up configuration presents superior heat transfer characteristics than the traditional CFD and CFU configurations.

(Samadifar & Toghraie, 2018) performs a numerical study for estimating the thermohydraulic behavior of fluid flow in a channel flow using six different kind of winglet as vortex generator namely simple rectangular winglet (SRW), rectangular trapezius winglet (RTW), angular rectangular winglet (ARW), wishbone winglet (WW), intended vortex generator (IVG) and wavy vortex generator (WVG). They reported that a simple rectangular winglet (SRW) gives the maximum augmentation of 7% in heat transfer as compared to the other considered configurations of the winglet. It was also reported that the optimum angle of attack is 45° for maximum enhancement in heat transfer characteristics.

(Esmaeilzadeh, Amanifard, & Deylami, 2017) investigated numerically to study the heat transfer and fluid flow characteristics of fluid flow in a channel flow for the Reynolds no. in the range of 7000-35000 using trapezoidal winglet pair (TWP) as well as

curved trapezoidal winglet pair (CTWP). It was reported that CTWP exhibits better performance as compared to TWP. Moreover, CTWP shows a considerable drop in the pressure drop penalty than the TWP.

(Lu & Zhou, 2016a) made an experimental effort to find the best shape of the winglet from among the considered plane and curved winglet having shapes like rectangular, triangular (delta) and trapezoidal for estimating the thermohydraulic performance of fluid flow in a channel flow with Reynolds number ranging from 700 to 26500. From the study, it was reported that a curved trapezoidal winglet (CTW) exhibits superior performance as compared to the other two shapes of vortex generator with an improvement in the performance up to 14% over the baseline case. They also reported that for CTW optimum value of angle of attack is 45° for maximum heat transfer.

(Lu & Zhou, 2016b) performed a numerical study to find the way for decreasing the pressure drop penalty by punching a hole on the surface of the winglet. In their investigations, they had considered plane and curved winglets with and without punched holes on their surface having shapes like rectangular, triangular (delta) and trapezoidal which were mounted on the lower plate of a channel for assessing the thermohydraulic performance of fluid flow in the heat exchanger. It was reported that the punched holes considerably improves the thermohydraulic performance as high as up to 15% over the non-punched cases. Additionally, it was also reported that the holes should be punched at the lower position and near to the leading edge of the winglet for better performance.

(L. H. Tang, Chu, Ahmed, & Zeng, 2016) proposed a new configuration of winglet to investigate the heat transfer and fluid flow characteristics in a channel flow. They performed 3D numerical simulation considering the rectangular and delta winglet in common flow up configuration combined with an elliptical pole and compared the performance with the rectangular and delta winglet in common flow down and common flow up configuration. It was reported that delta winglet combined with an elliptical pole in common flow up configuration exhibits the superior performance with an improvement of 7.4% in heat transfer over the baseline case.

It has been concluded from the numerous studies **((M. Fiebig, 1998), (Khoshvaght-Aliabadi, Sartipzadeh, & Alizadeh, 2015), (Chomdee & Kiatsiriroat, 2006), (Yanagihara & Torii, 1992), (Allison & Dally, 2007), (Tiwari, Maurya, Biswas, & Eswaran, 2003))** conducted by different researchers that delta winglet as vortex generator exhibits superior performance than the other types of winglets. It was concluded that the maximum improvement in the heat transfer coefficient can be achieved as high as up to 80% on using the delta winglet.

2.3. HEAT TRANSFER AUGMENTATION IN THE FIN-TUBE HEAT EXCHANGERS

Numerous studies **((Shi, Wang, Gen, & Zhang, 2006), (K. Torii et al., 2002)), (C. C. Wang, Lo, Lin, & Wei, 2002), (C. C. Wang et al., 2002), (C. C. Wang et al., 2002), (Allison & Dally, 2007), (Jalil, Abdulla, & Yusuf, 2006), (Joardar & Jacobi, 2008))** both numerical and experimental have also been performed in recent times considering winglet as the vortex generator for investigating the heat transfer and flow resistance characteristics of fluid flow in a fin-tube heat exchangers.

(Jacobi & Shah, 1995) also presented an exhaustive review of thermo-hydraulic characteristics for a fin-tube heat exchanger by using delta and rectangular winglet as VGs.

(Biswas et al., 1994) performed numerical simulations considering delta winglet pair and concluded that thermal performance can be improved by as high as up to 240% behind the tube in the wake region.

(Song, Wang, Fan, Zhang, & Liu, 2008) numerically studied the effectiveness of secondary flow produced by vortex Generators mounted on both the surfaces of the fin and found that secondary flow can greatly enhance the convective heat transfer. The same has been depicted in figure 2.5.

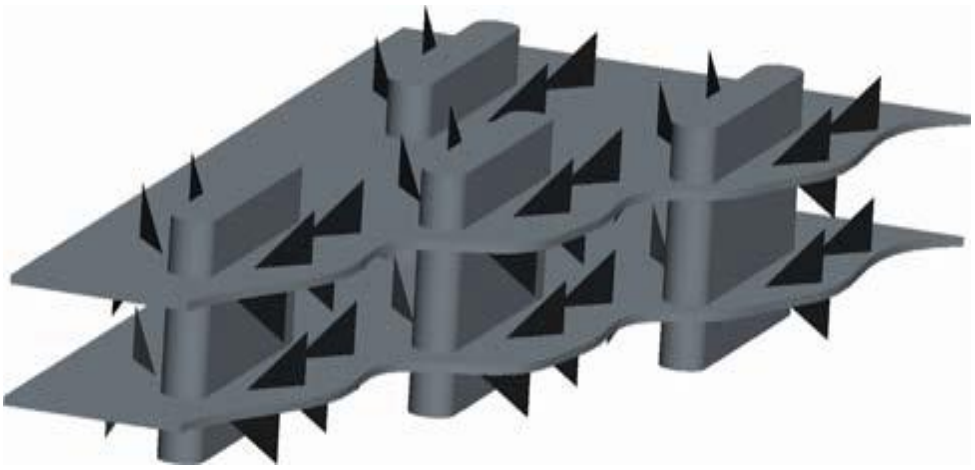

Figure 2.5 Schematic view of a finned flat tube bank with mounted delta winglet vortex generators on both surfaces (Song et al., 2008)

Studies involving numerical investigations have been taken up over the years to examine the effect of different shapes of winglets and to find the best one for a particular application. Earlier studies were focused on rectangular and delta winglet but **(Lotfi, Sundén, & Wang, 2016)** simulated numerically and suggested three novel types of winglets as angle rectangular winglet (ARW), curved angle rectangular winglet (CARW) and rectangular trapezoidal winglet (RTW). They reported that for small attack angles, CARW as VG outperforms the other two types of the winglet.

(W. Wang, Bao, & Wang, 2015) proposed a new configuration called novel combined winglet pair (NCWP) and reported that heat transfer is augmented by up to 24.2% as compared to without VG.

(Gong, Wang, & Lin, 2015) performed numerical investigations to compare the performance of punched out curved rectangular winglet pair (CRWP) with plane rectangular winglet pair in a fin tube heat exchanger and found that curved rectangular winglet pair performed better than plane rectangular winglet pair. The same has been depicted in figure 2.6.

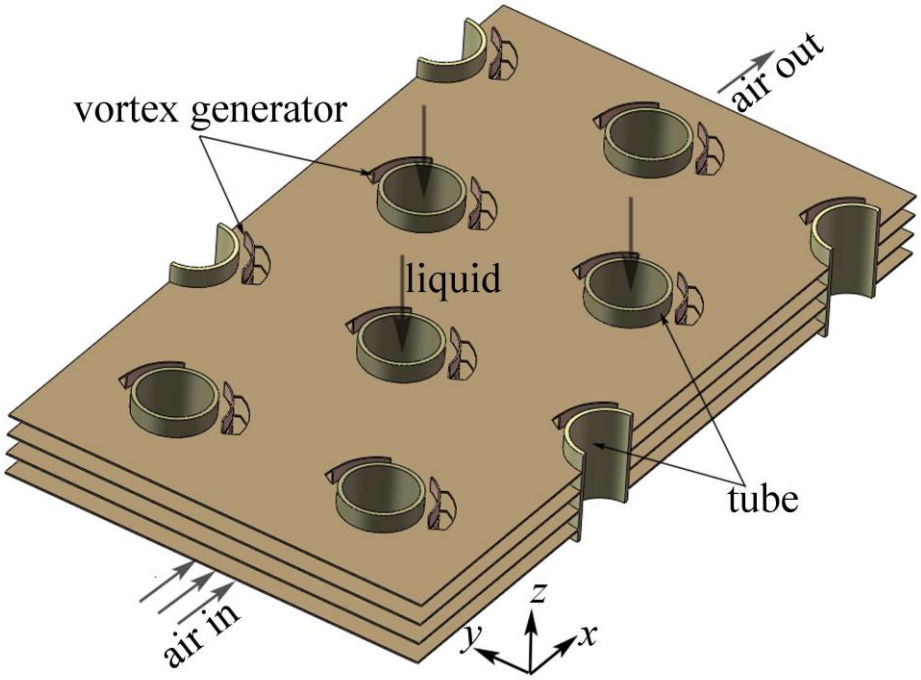

Figure 2.6. Curved Rectangular Winglet Pair (CRWP) punched out from fin surface in fin tube heat exchanger (Gong et al., 2015)

(Song et al., 2017) experimentally investigated the performance of curved delta winglet vortex generator (CDWVG) and found that small size of CDWVG is better when Reynolds number (Re) is less and for a larger value of Re large size of CDWVG is better for superior thermohydraulic performance

(Md Salleh, Gholami, & Wahid, 2018) performed numerical investigations considering rectangular winglet vortex generator (RWVG), delta winglet vortex generator (DWVG) and trapezoidal winglet vortex generator (TWVG) in CFD and CFU configuration placed behind the tube in downstream location. They reported that rectangular winglet mounted in CFD configuration provides maximum augmentation in the heat transfer characteristics for a higher value of Reynolds no. As far as the thermohydraulic performance is concerned, DWVG exhibits the superior performance as compared to RWVG and TWVG over the baseline case with an increase in Reynolds no.

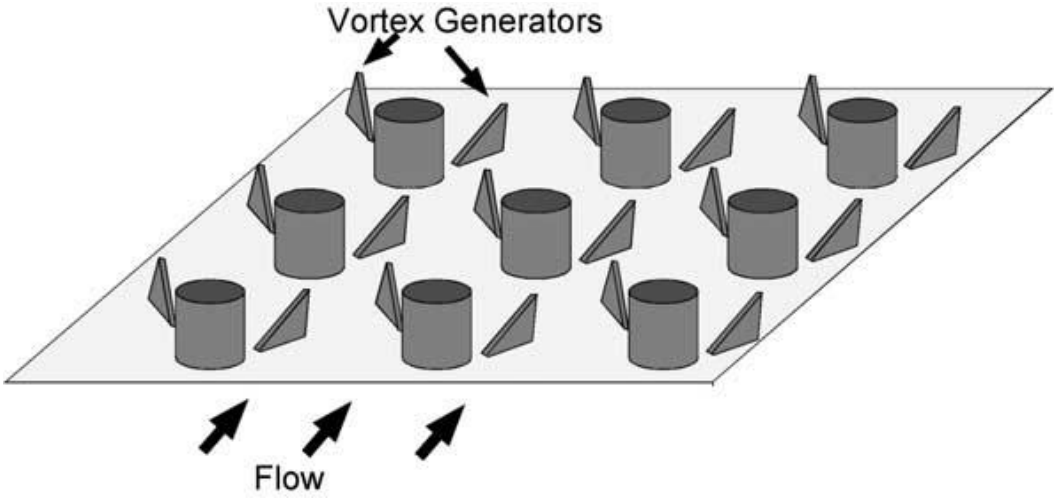

(b) Common Flow Down configuration

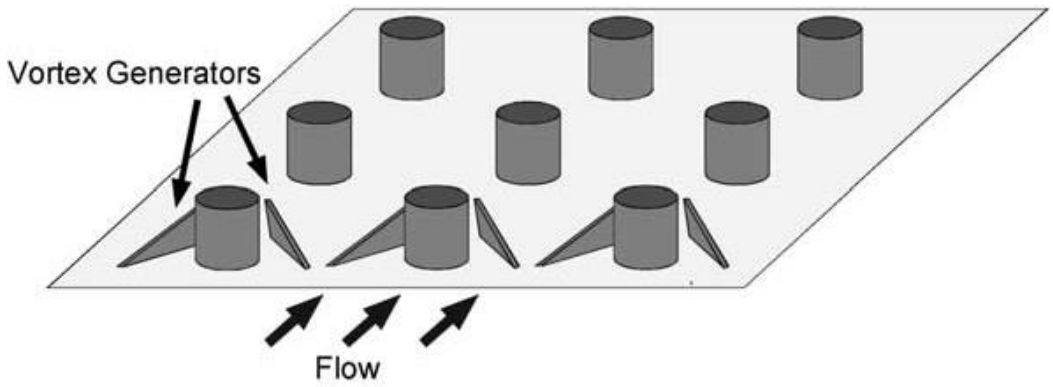

(b) Common Flow Up configuration.

Figure 2.7 Configuration of winglet type vortex generator (K. Torii et al., 2002)

(K. Torii et al., 2002) performed no. of experiments to study common flow up (CFU) configuration for inline as well as staggered tube arrangement and concluded that heat transfer was more in case of staggered tube array than inline tube array. In case of staggered tube banks, the heat transfer was augmented by 30% to 10% ; while in case of in-line tube banks, the same was found to be 20% to 10% for the considered range of Reynolds number (i.e. $350 \leq Re \leq 2100$).

Investigations have also been performed to study the effect of different types of tubes and their arrangements. **(M. Fiebig, Valencia, & Mitra, 1993)** investigated experimentally the comparative performance of staggered and inline tube arrangement with

a pair of delta winglet as VG for a circular and fin tube heat exchanger and found that for inline tube arrangement, augmentation in heat transfer improves by 55-65%, which is higher than staggered tube arrangement.

(Yoo, Park, Chung, & Lee, 2002) investigated experimentally and concluded that flat-tube instead of a circular tube in the fin tube heat exchanger significantly augments the heat transfer.

(Tiwari et al., 2003) simulated numerically and found that the oval tube used in the fin tube heat exchanger presents better thermohydraulic performance than the circular tube.

(J. M. Wu & Tao, 2011) performed numerical simulations considering two rows of circular tubes of different diameters with punched pairs of delta winglet in CFU and CFD configuration. They affirmed that the configuration with smaller size tube in the first row and larger size tube in the second row with punched delta winglet presents better heat transfer augmentation and decrease in pressure drop than fin tube heat exchanger with the same size of tubes.

Considering the factor of the arrangement of winglets, several investigations have been made considering the various arrangement of winglets. **(Chen et al., 1998)** performed numerical simulations on the finned oval tube with an inline arrangement of a pair of punched delta winglet and concluded that performance criterion, PEC = $(j/j_o)/(f/f_o)$ (where j and f are the colburn's factor and friction factor respectively for the heat exchanger using winglet, while j_o and f_o are the same without using winglet i.e. the baseline case) for one, two and three vortex generators inline were 1.04, 1.01, 0.97 respectively.

(Tiwari et al., 2003) simulated numerically for a staggered and inline array of delta winglet pair considering oval tube and found that configuration with four pairs of winglet in the staggered array shows the best thermal performance enhancement as compared to other configurations. Quite a few studies have also been conducted considering more than one row of winglet pairs and they all concluded that a heat exchanger with multiple rows of winglet pairs has better thermohydraulic performance than a single row of winglet pair.

(Pesteei, Subbarao, & Agarwal, 2005) performed no. of experiments in order to find the best location for delta winglet pair w.r.t tube, for the best thermo-hydraulic

performance of fin-tube heat exchanger and reported that the best location is at a horizontal and vertical distance each equal to the radius of the tube and taken from the center of the tube in the downstream location.

(Lemouedda, Breuer, Franz, Botsch, & Delgado, 2010) numerically simulated to optimize the angle of attack for delta winglet pair in a fin-tube heat exchanger having both inline and staggered arrangement of tubes and concluded that staggered arrangement performs better than inline arrangement. They concluded that there is no unique value of optimum angle of attack for delta winglet pair, over the considered range of Reynolds number. With the variation in the Reynolds number, the value of optimum angle of attack also changes. Moreover, it is also different for both i.e. inline and staggered arrangement of tubes.

(Singh, Sørensen, & Condra, 2018) performed numerical investigations to find the optimum angle of attack for rectangular winglet in a double fin and tube heat exchanger and concluded that for -20° attack angle of winglet performance is maximum.

(Arora, Subbarao, & Agarwal, 2015) performed numerical simulation to optimize the location of delta winglet pair w.r.t tube which is attached in CFU configuration in a fin-tube heat exchanger having an inline arrangement of the tubes.

(Naik & Tiwari, 2018) studied numerically for the most promising location of rectangular winglet pair w.r.t tube for a fin-tube heat exchanger having inline arrangements of tubes.

(W. Li, Khan, Tang, & Minkowycz, 2018) performed numerical investigations for optimization of corrugation height of fin and angle of attack of delta winglet type VGs in a wavy fin-and-tube heat exchanger.

(Han, Wang, Sun, Li, & Wang, 2019) performed numerical study to investigate the thermohydraulic behavior of fin-tube heat exchanger using arc winglet type vortex generator and reported a significant average augmentation of up to 35.9% in the Nusselt no. value which is a representative of heat transfer characteristics, over the conventional rectangular winglet vortex generator.

(Lu & Zhai, 2019) investigated numerically the optimal value of angle of attack for a curved vortex generator mounted on the surface of a fin-tube heat exchanger. In the same study, they also performed an investigation for optimizing the curvature of the vortex generator. They concluded that maximum performance was achieved for an attack angle of 15° and curvature (ratio of lateral length to the chord length of a curved vortex generator) value 0.25.

(Chimres, Wang, & Wongwises, 2018b) performed a numerical investigation considering semi dimple pair as vortex generator to study the thermo-hydraulic behavior of fluid flow in a fin tube heat exchanger and reported that there is a 15-20% improvement in the performance of heat exchanger on using the semi dimple pair as vortex generator over the plain fin with no vortex generator.

(Chimres, Wang, & Wongwises, 2018a) carried out a numerical study to investigate the thermohydraulic behavior of fluid flow in a fin-tube heat exchanger using an elliptical winglet as a vortex generator. They concluded that maximum augmentation achieved is around 13% in heat transfer characteristics for elliptical winglet having 1.5mm length over the baseline case.

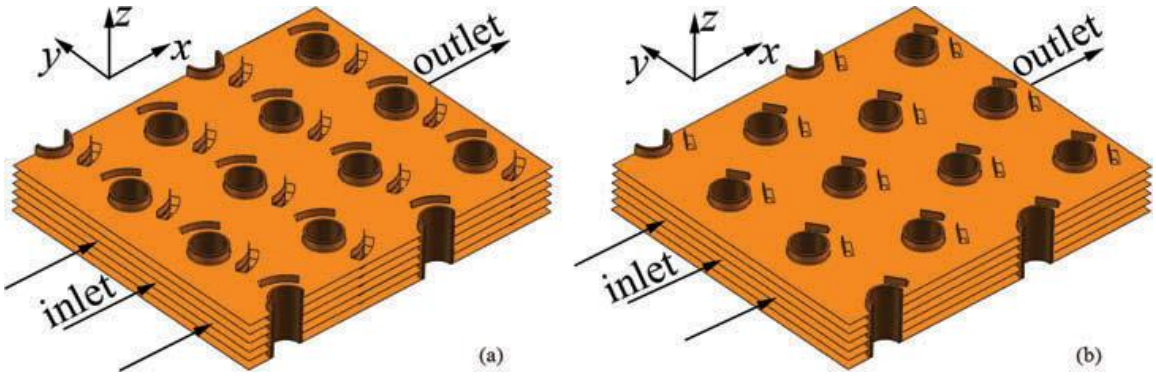

Figure 2.8 Schematic view of a heat exchanger with (a) CRVG (b) PRVG;

(X. L. Tian et al., 2018)

(X. L. Tian et al., 2018) made an experimental study to investigate the effect of fin pitch and tube diameter on thermohydraulic behavior of fin-tube heat exchanger using stamped out plane rectangular vortex generator (PRVG) and curved rectangular vortex

generator (CRVG). The same has been depicted in figure 2.8. They concluded that heat transfer augmentation is more by using a curved rectangular vortex generator than the plane rectangular vortex generator. Additionally, it was also reported that the heat transfer decreases with an increase in the tube diameter. Moreover, the same trend was observed for an increase in the fin pitch. Furthermore, they also found that the difference in heat transfer by using PRVG and CRVG keeps on increasing with an increase in the tube diameter.

(M. J. Li et al., 2018) made an experimental study to investigate the thermohydraulic behavior of fluid flow in a fin-tube heat exchanger using a stamped out delta winglet radially arranged around each tube. The same has been depicted in figure 2.9. They made a comparison of the proposed design of the fin surface with the wavy fin surface and concluded that the plain fin surface with stamped out delta winglet performs better than the wavy fin surface having no winglet. In their study, they also reported that the 5-row tubes of plain fin surface having stamped out delta winglet can replace the 6 rows wavy fin surface with no winglet.

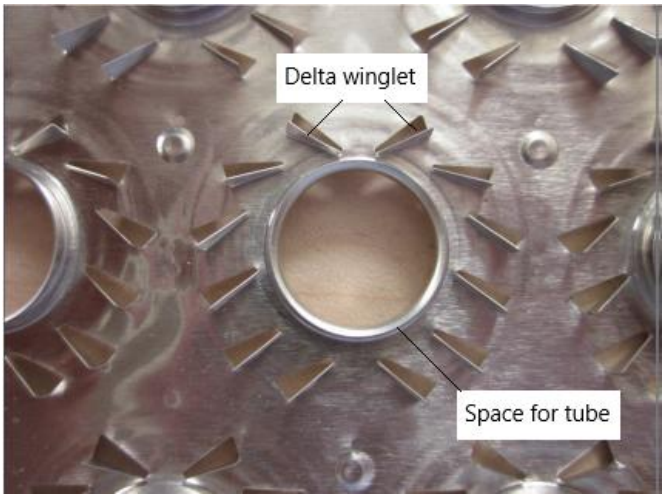

Figure 2.9 Schematic view of the enhanced fin (M. J. Li et al., 2018)

(Sarangi & Mishra, 2017) performed numerical investigations considering rectangular winglet pair as vortex generator to study the thermohydraulic behavior of fluid flow in a fin-tube heat exchanger. VG was placed in a common flow up configuration and the flow was taken as laminar. They reported that the rate of heat transfer increases with

an increase in the no. of winglet pairs. Additionally, it was also reported from the study that the heat transfer increases with an increase in the angle of attack.

(Hu, Wang, Guan, & Hu, 2017) also made an attempt to find the optimum shape of the winglet from among the three considered shapes viz., delta winglet, rectangular winglet and trapezoidal winglet for thermohydraulic performance assessment of the fluid flow in a fin-tube heat exchanger. It was reported that the delta winglet as vortex generator outperforms the other two shapes of winglet for Reynolds no. > 350. Moreover, rectangular winglet as vortex generator reports the least improvement in the overall thermohydraulic performance over the baseline case.

(X. Wu, Liu, Zhao, Lu, & Song, 2016) performed a parametric study using response surface methodology to optimize the fin pitch and tube pitch considering delta winglet as vortex generator for performance augmentation of a fin-tube heat exchanger. It was reported that the overall thermohydraulic performance decreases with an increase in the fin pitch. In addition to that, it was also concluded that performance increases with an increase in the ratio of longitudinal tube pitch to transverse tube pitch.

(Ling Hong Tang, Tan, Gao, & Zeng, 2016) conducted a numerical study considering delta winglet as vortex generator mounted in common flow down and common flow up the configuration on the fin plate in a fin-tube heat exchanger for augmentation of its performance. It had been concluded that winglet mounted in common flow up configuration exhibits superior performance than the winglet located in common flow down configuration. It was reported that as compared to common flow down configuration, the Nusselt numbers of common flow up configuration increased by 2.7-2.9% in the range of studied Reynolds number, while the friction factors reduced by 7.8-10.0%. Moreover, the parameters of the fin-tube heat exchanger with winglet mounted in common flow up configuration had been optimized using Taguchi methodology in the same study. It was reported that the heat transfer increases with an increase in the height of the vortex generator but simultaneously resulting in an increase in the pressure drop penalty also.

(Sinha, Chattopadhyay, Iyengar, & Biswas, 2016) performed a numerical investigation considering rectangular winglet as vortex generator mounted in common flow

up configuration in a fin-tube heat exchanger having three rows of tubes in inline and staggered arrangements. It was concluded that for an inline array of tubes, overall thermo-hydraulic performance increases with an increase in the angle of attack but the same is not true for staggered arrangement. For the staggered arrangement of tubes, performance first increases then decreases with an increase in the angle of attack.

(Salviano, Dezan, & Yanagihara, 2016) made an optimization study (based on the SIMPLEX method) considering rectangular and delta winglet as vortex generator mounted in a fin-tube heat exchanger having two rows of tubes in inline and staggered arrangements. It had been concluded that staggered arrangements of tubes exhibit superior heat transfer characteristics than the inline arrangements. Moreover, it was also reported that the rectangular winglet outperforms the delta winglet for the considered arrangements.

(L. Tian, Liu, Min, Wang, & He, 2015) made a numerical effort to select the best configuration of multi-row delta winglet which were stamped out from fin surface in a fin-tube heat exchanger. In their study, they had arranged stamped out delta winglet in two ways namely leeward and windward stamped out delta winglet which has been depicted in figure 2.10. It was concluded that the windward stamped out delta winglet exhibits superior heat transfer characteristics than the leeward stamped out delta winglet which clearly shows that the punching should be performed on the windward side.

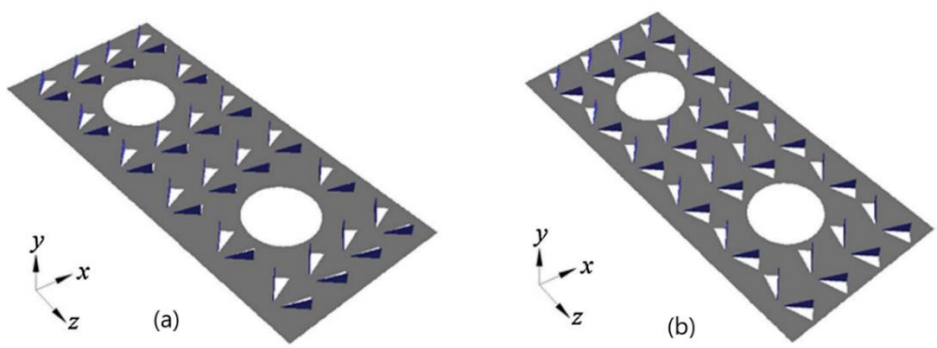

Fig. 2.10 Schematic view of the plain fin with multi-row delta winglets.

(a) Leeward stamped out delta winglet (b) Windward stamped out delta winglet

(L. Tian et al., 2015)

(Jedsadaratanachai & Boonloi, 2015) proposed a new arrangement winglet where two delta winglet were joined together like V-ribs and the V-tip facing upstream known as V-upstream. It has been reported that the improvement in the heat transfer can be as high as 55% over the baseline case for the proposed configuration of the vortex generator.

(L. Li, Du, Zhang, Yang, & Yang, 2015) made an effort to investigate numerically the heat transfer and flow resistance characteristics of fluid flow in a fin-tube heat exchanger considering rectangular and delta winglet which were mounted and stamped out on the fin surface. It was concluded that the rectangular winglet exhibits superior heat transfer characteristics than the delta winglet for the investigated range of Reynolds no. In addition to that, it was also reported that the optimum value of the angle of attack is 45° for delta winglet whereas the same for rectangular winglet is 25°.

Various investigations were performed by the different researchers **((Martin Fiebig, 1995), (Stefan Tiggelbeck et al., 1992), (Datta, Sanyal, & Das, 2016), (Du, Feng, Yang, & Yang, 2013), (Chu, He, Lei, Tian, & Li, 2009))** on wavy fin and flat tube considering longitudinal vortex generator (LVG) as the secondary flow generating device and it was concluded that there is a remarkable augmentation in the heat transfer characteristics on using LVG as compared to the baseline case.

Numerous investigations had been performed by the various researchers **((Kwak, Torii, & Nishino, 2002), (Joardar & Jacobi, 2008), (J. He, Liu, & Jacobi, 2010), (Biswas et al., 1994))** using stamped out delta winglet as vortex generator in a fin-tube heat exchanger and it was concluded that the optimum angle of attack lies in the range of 30° to 45°.

Various studies were performed by the different investigators **((M. Fiebig et al., 1993), (Valencia et al., 1996), (M. Fiebig et al., 1993))** considering flat tube and circular tube in a fin-tube heat exchanger and it had been reported that the circular tube exhibits better heat transfer performance while pressure drop penalty is less for the flat tube.

Table 2.1 gives an overview of the investigations made by various researchers for the channel flow and fin-tube heat exchanger

Table 2.1 A summary of work performed by various researchers

S.No.	Reference	Nature of the work	System Specifications	Results
1.	(Jacobi & Shah, 1995)	Review study	Channel flow Delta winglet Rectangular winglet	Heat transfer enhancement can be up to 100%
2.	(Valencia, Fiebig, & Mitra, 1996)	Experimental Study	Fin tube heat exchanger Flat tube Delta winglet	Heat transfer enhancement by 50% Pressure loss by 30% Flat tube performs better than circular tube
3.	(M. Fiebig, 1998)	Numerical Study	Channel flow Delta wing Rectangular wing Delta winglet Rectangular winglet	Heat transfer performance of winglets is better than wings Global heat transfer enhancement can be 50%
4.	(St. Tiggelbeck, Mitra, & Fiebig, 2008)	Experimental Study	Channel flow Delta wing Rectangular wing Delta winglet Rectangular winglet	Heat transfer performance of winglets is better than wings Local heat transfer enhancement can be up to 120% using delta winglet
5.	(PAULEY & EATON, 2008)	Experimental Study	Channel flow Delta wing (Common flow down, Common flow up)	Common Flow Down (CFD) performs better than Common Flow Up(CFU)
6.	(L. T. Tian, He, Lei, & Tao, 2009)	Numerical Study	Channel flow Delta winglet Rectangular winglet (Common flow down, Common flow up)	Heat transfer performs using rectangular winglet improves by 46% while using delta winglet by 26%
7.	(Min, Qi, Kong, & Dong, 2010)	Experimental Study	Channel flow Rectangular Winglet Pair (RWP) Modified Rectangular Winglet Pair (MRWP)	MRWP performs better than RWP and the heat transfer improvement for MRWP is upto 55% over baseline.
8.	(Oneissi, Habchi, Russeil, Bougeard, & Lemenand, 2016)	Numerical Study	Channel flow Inclined Projected Winglet Pair (IPWP) Delta Winglet Pair (DWP)	Overall thermo-hydraulic performance of IPWP is 6% more than DWP
9.	(J. M. Wu & Tao, 2012)	Experimental Study	Channel flow Delta winglet (punched out)	Nusselt no. of channel with punched out delta winglet improves up to 34% as compared to plain channel.
10.	(Zhou & Feng, 2014)	Experimental study	Channel Flow	Curved winglet performs better than the plane winglet

			Plane & Curved winglet (Rectangular, Delta & Trapezoidal) with punched hole	Curved delta winglet gives the best overall performance Punched hole improves overall performance by upto 20%
11.	(Naik, Harikrishnan, & Tiwari, 2018)	Numerical study	Channel flow Curved rectangular winglet (concave & convex)	Heat transfer enhancement is maximum for the concave-shaped rectangular winglet and is order 22% over the baseline case.
12.	(Song, Tagawa, Chen, & Zhang, 2019)	Numerical study	Channel flow Curved delta winglet (concave & convex)	Surface goodness factor (JF) for the concave curved delta winglet is larger by 11.35% than those for the convex curved delta winglet.
13.	(Ke, Chen, Li, Wang, & Chen, 2019)	Numerical study	Channel flow Common Flow Down (CFD) configuration Common Flow Up (CFU) Mixed-up configuration	For a small channel height i.e. 3mm or 4mm, mixed-up configuration performs better than CFD & CFU configurations
14.	(Samadifar & Toghraie, 2018)	Numerical study	Channel flow Simple rectangular winglet (SRW), Rectangular trapezius winglet (RTW) Angular rectangular winglet (ARW) Wishbone winglet (WW) Intended vortex generator (IVG) Wavy vortex generator (WVG)	Simple rectangular winglet (SRW) gives the maximum augmentation of 7% in heat transfer Optimum angle of attack is 45° for maximum enhancement in heat transfer characteristics.
15.	(Esmaeilzadeh, Amanifard, & Deylami, 2017)	Numerical study	Channel flow $7000 \leq Re \leq 35000$ Trapezoidal winglet pair (TWP) Curved trapezoidal winglet pair (CTWP).	Nusselt number is augmented by 6-8% for CTWP and 9-12% for TWP Friction factor increased by 24-29% and 38-48% with CTWP and TWP
16.	(Lu & Zhou, 2016a)	Experimental study	Channel flow Plane & Curved winglet (Rectangular, Delta & Trapezoidal) $700 \leq Re \leq 26500$	Curved trapezoidal winglet (CTW) exhibits superior performance with an improvement in the performance up to 14% over the baseline case. Optimum value of angle of attack for CTW is 45° for maximum heat transfer.
17.	(Lu & Zhou, 2016b)	Numerical study	Channel flow Plane & Curved winglet (Rectangular, Delta & Trapezoidal) with punched hole at the centre	Punched holes improves thermo-hydraulic performance up to 15% over the non-punched cases.

18.	(L. H. Tang, Chu, Ahmed, & Zeng, 2016)	Numerical study	Channel flow Rectangular and delta winglet in CFU configuration combined with an elliptical pole Common Flow Down (CFD) Common Flow Up (CFU)	Delta winglet combined with an elliptical pole in CFU configuration exhibits the superior performance with an improvement of 7.4% in heat transfer over the baseline case.
19.	(Biswas et al., 1994)	Numerical study	Fin-tube heat exchanger Delta Winglet Pair (DWP)	Thermal performance improvement up to 240% behind the tube in the wake region.
20.	(Song, Wang, Fan, Zhang, & Liu, 2008)	Numerical study	Fin-tube heat exchanger VG mounted on both surface of fin	Significant improvement in heat transfer
21.	(Lotfi, Sundén, & Wang, 2016)	Numerical study	Smooth wavy fin-and-elliptical tube heat exchanger Angle rectangular winglet (ARW), Curved angle rectangular winglet (CARW) Rectangular trapezoidal winglet (RTW)	For small attack angles, CARW outperforms the other two types of the winglet because of low friction factor which is 20% less than RTW having highest friction factor
22.	(W. Wang, Bao, & Wang, 2015)	Numerical study	Fin-tube heat exchanger novel combined winglet pair (NCWP)	Heat transfer augmentation up to 24.2% as compared to without VG.
23.	(Gong, Wang, & Lin, 2015)	Numerical study	Fin-tube heat exchanger (CRWP) Curved rectangular winglet pair (punched out) (PRWP) Plane rectangular winglet pair (punched out)	Area goodness factor for CRWP is highest and its value is 1.38
24.	(Song et al., 2017)	Experimental study	Fin-tube heat exchanger Curved delta winglet vortex generator (CDWVG)	For small *Re*, small size of CDWVG is better For large *Re*, large size of CDWVG is better
25.	(Md Salleh, Gholami, & Wahid, 2018)	Numerical study	Fin-tube heat exchanger Rectangular winglet vortex generator (RWVG) Delta winglet vortex generator (DWVG) Trapezoidal winglet vortex generator (TWVG)	For DWVG exhibits the superior performance as compared to RWVG and TWVG over the baseline case with increase in Nusselt no. by 55.4%
26.	(K. Torii et al., 2002)	Experimental study	Fin-tube heat exchanger Common Flow Up (CFU) configuration Inline & staggered tube arrangement $350 \leq Re \leq 2100$	For staggered tube banks, the heat transfer enhancement by 30% to 10% ; For in-line tube banks, the heat transfer enhancement by 20% to 10%
27.	(M. Fiebig, Valencia, & Mitra, 1993)	Experimental study	Fin-tube heat exchanger Inline & staggered tube arrangement Delta winglet pair	For in-line tube banks, the heat transfer enhancement is highest and is upto 65%

28.	(Yoo, Park, Chung, & Lee, 2002)	Experimental study	Fin-tube heat exchanger Flat tube Circular tube	Flat-tube performs better and overall improvement of 75% over baseline case
29.	(Tiwari et al., 2003)	Numerical study	Fin-tube heat exchanger Oval tube Circular tube	Oval tube performs better and overall improvement of 43.86% over baseline case
30.	(J. M. Wu & Tao, 2011)	Numerical study	Fin-tube heat exchanger Circular tubes of different diameters Delta winglet pair (punched out) CFD & CFU configuration	Nusselt no. for CFU arrangement improves by 18% Nusselt no. for CFD arrangement improves by 21%
31.	(Chen et al., 1998)	Numerical study	Fin-tube heat exchanger Oval tube Delta winglet pair (punched out) Inline array of winglet	PEC = 1.04, 1.01, 0.97 (for one, two & three vortex generators)
32.	(Tiwari et al., 2003)	Numerical study	Fin-tube heat exchanger Oval tube Delta winglet pair Inline & staggered array of winglet	Configuration with four pairs of winglet in the staggered array shows the best thermal performance with an improvement of about 100% in Nusselt no.
33.	(Pesteei, Subbarao, & Agarwal, 2005)	Experimental study	Fin-tube heat exchanger Delta winglet pair	Optimum location of winglet; x=D/2, y=D/2 (D, diameter of tube)
34.	(Lemouedda, Breuer, Franz, Botsch, & Delgado, 2010)	Numerical study	Fin-tube heat exchanger Delta winglet pair Inline & staggered array of tube	For inline array, improvement in heat transfer is 24% For staggered array, improvement in heat transfer is 15.7%
35.	(Singh, Sørensen, & Condra, 2018)	Numerical study	Fin-tube heat exchanger Rectangular winglet	Optimum angle of attack(α) = -20° PEC = 1.91 (for *Re* =11000)
36.	(Arora, Subbarao, & Agarwal, 2015)	Numerical study	Fin-tube heat exchanger Delta winglet pair CFU configuration Inline array of tube	For optimum location, improvement in Nusselt number by 60.4% (for *Re* = 4245)
37.	(Naik & Tiwari, 2018)	Numerical study	Fin-tube heat exchanger Rectangular winglet pair Inline array of tube	Optimum angle of attack(α) = 45° (for downstream region) PEC = 1.1 (for α = 45°)
38.	(W. Li, Khan, Tang, & Minkowycz, 2018)	Numerical study	Wavy fin and tube heat exchanger Delta winglet pair	PEC = 1.3237 (for optimal design)
39.	(Han, Wang, Sun, Li, & Wang, 2019)	Numerical study	Fin-tube heat exchanger Arc Winglet Vortex Generator (AWVG) Rectangular Winglet Vortex Generator(RWVG)	Nusselt no. for AWVG improves by 35.9% over RWVG

40.	(Lu & Zhai, 2019)	Numerical study	Fin-tube heat exchanger Curved vortex generator	Optimum angle of attack(α) = 15°
41.	(Chimres, Wang, & Wongwises, 2018b)	Numerical study	Fin-tube heat exchanger Semi dimple winglet pair	1.15 ≤ PEC ≤ 1.20 (w.r.t . baseline case)
42.	(Chimres, Wang, & Wongwises, 2018a)	Numerical study	Fin-tube heat exchanger Elliptical winglet pair	j/j_o = 1.13 (for elliptical winglet pair over baseline case)
43.	(X. L. Tian et al., 2018)	Experimental study	Fin-tube heat exchanger Plane rectangular vortex generator (PRVG) Curved rectangular vortex generator (CRVG).	PEC, for CRVG is 12.6% more than that of PRVG
44.	(M. J. Li et al., 2018)	Experimental study	Fin-tube heat exchanger Stamped out delta winglet radially arranged around each tube.	5-row tubes of plain fin surface having stamped out delta winglet can replace the 6 rows wavy fin surface with no winglet.
45.	(Sarangi & Mishra, 2017)	Numerical study	Fin-tube heat exchanger Rectangular Winglet Pair Common Flow Up(CFU) configuration	Heat transfer improvement = 12%, 37%, 47% (for single, double and triple rectangular winglet pair)
46.	(Hu, Wang, Guan, & Hu, 2017)	Numerical study	Fin-tube heat exchanger Delta winglet Rectangular winglet Trapezoidal winglet	Delta winglet has highest PEC = 1.08 (for *Re* = 1450)
47.	(X. Wu, Liu, Zhao, Lu, & Song, 2016)	Numerical study	Fin-tube heat exchanger Delta winglet	Overall performance decreases with an increase in the fin pitch.
48.	(Ling Hong Tang, Tan, Gao, & Zeng, 2016)	Numerical study	Fin-tube heat exchanger Delta winglet Common Flow Down (CFD) configuration Common Flow Up (CFU) configuration	Nusselt numbers of CFU configuration increases by 2.7-2.9% over CFD configuration Friction factors of CFU configuration reduces by 7.8-10.0%.over CFD configuration
49.	(Sinha, Chattopadhyay, Iyengar, & Biswas, 2016)	Numerical study	Fin-tube heat exchanger Rectangular Winglet Common Flow Up (CFU) configuration Inline & staggered array of tube	For an inline array of tubes, overall performance increases with an increase in the angle of attack For the staggered array of tubes, performance first increases then decreases with an increase in the angle of attack.
50.	(Salviano, Dezan, & Yanagihara, 2016)	Numerical study	Fin-tube heat exchanger Delta winglet Rectangular winglet Inline & staggered array of tube	Staggered array of performs better than the inline array Rectangular winglet outperforms the delta winglet

51.	(Jedsadaratanachai & Boonloi, 2015)	Numerical study	Fin-tube heat exchanger V-upstream (delta winglets joined together like V-ribs and V-tip facing upstream)	j/j_o = 1.55 (for V-upstream over baseline case)
52.	(L. Li, Du, Zhang, Yang, & Yang, 2015)	Numerical study	Fin-tube heat exchanger Delta winglet (mounted & punched out) Rectangular winglet (mounted & punched out)	Rectangular winglet transfers more heat than delta winglet Optimum angle of attack (α) = 45° (for delta winglet) Optimum angle of attack (α) = 25° (for rectangular winglet)

2.4. GAPS IN THE LITERATURE

1) Investigations are required for studying the effect of using rectangular winglet with punched hole, which is mounted/punched out on the fin surface in a fin-tube heat exchanger.
2) Investigations are required to be made for studying the effect of using delta winglet with punched hole, which is mounted/punched out on the fin surface in a fin-tube heat exchanger.
3) Investigations are also required for studying the effect of using winglet (Delta/Rectangular) with punched hole, in a fin-tube heat exchanger having different arrangements of tubes i.e. inline and staggered.
4) Further investigations are required for studying the effect of using curved winglet (Delta/Rectangular) with punched hole, in a fin-tube heat exchanger.
5) The optimum configuration and size needs to be worked out for the winglet (Delta/Rectangular) with punched hole, which is mounted/punched out on the fin surface in a fin-tube heat exchanger.

2.5. CONCLUDING REMARKS

The topic concerning the influence of longitudinal vortices embedded by vortex generators, on the heat transfer and flow loss is very interesting and in the beginning relatively little explored. But, a large number of research works appeared in the recent

years (last decade). The present literature survey shows that the use of vortex generators in order to increase the gas side heat transfer coefficient, in a gas-liquid heat exchanger is a promising technique. Though, there are numerous publications available in this area. The following are the major conclusions based on the available literature.

1) The vortex generators are useful devices for improving the heat transfer coefficient in the laminar boundary layer, turbulent boundary layer, and channel flow. Their effectiveness is more significant when they are used in the gas side of a cross-flow heat exchanger.
2) The fewer number of small vortex generators whose surface areas are very small compared to the convective heat transfer area can significantly increase the heat transfer coefficient with little increase in pressure drop.
3) Delta winglets exhibit the best performance of all shapes. Heat transfer increases with an increase in the angle of attack. In the case of the fin tube arrangement, the optimum angle of attack is $\beta = 45^{\circ}$.
5) Fin-tube heat exchanger of inline arrangement with vortex generators gives higher heat transfer and pressure drop than the staggered arrangement and hence inline arrangement with vortex generator is possibly the best choice.
6) In the case of finned oval heat exchangers, the staggered arrangement of the winglets is more effective than the inline arrangement for heat transfer enhancement.
7) Fin-flat tubes with vortex generators give superior performance to the round tube with or without vortex generators.
8) In comparison to the plain fin surface with a rectangular cross-section, the vortex generator surface could reduce the heat transfer area of 76% for fixed heat duty and for fixed pumping power.
9) A thorough study of various publications in this area shows that the use of longitudinal vortex generators in fin-tube heat exchangers will increase the rate of heat transfer at all Reynolds numbers.

CHAPTER - 3

(RESEARCH METHODOLOGY)

3.1 INTRODUCTION

The present investigations have been performed to improve the overall performance of the fin-tube heat exchanger. To achieve this, winglet as the vortex generators have been mounted as well as punched-out from the fin plate surface. This chapter describes the problem statement in detail. The experimental test-rig used and the procedure followed have been explained clearly. Various elements of the numerical simulation viz., selection of turbulence model, grid independence and validation of simulation with the experimentation have also been presented. Various performance parameters used have been explained clearly including a note on uncertainty analysis. Additionally, a section on the sample calculation has also been added to clearly explain the various performance parameters calculated during the entire investigations. The main aim is to have a clear understanding of the problem in hand, the methodology adopted for the solution of the problem including experimentation and numerical simulation.

3.2 STATEMENT OF THE PROBLEM

In the present investigations I have examined the effects of using Rectangular winglet with a circular hole at the center which is mounted/punched out on fin plate surface in Common Flow Down (CFD) and Common Flow Up (CFU) configuration at downstream as well as upstream location of flow in a fin -tube heat exchanger. Investigations have been performed considering Reynolds number in the range of 1400 to 9000 (calculated on the basis of hydraulic diameter and variation in the velocity from 1m/s to 6m/s) and keeping an angle of attack at 45° as suggested by (Martin Fiebig, Mitra, & Dong, 1990). I have explained the improvement in the performance of the fin-tube heat exchanger using a winglet, over the baseline case having no vortex generator. The present work also examines the effects of punched holes on the surface of the rectangular winglet.

Firstly, my focus was on studying localized heat transfer augmentation, especially in the wake region. For this purpose, two points have been taken. One point (Point A) was 32 mm away from the tube center radially and located at the intersection of winglet center and tube center, and the second point (Point B) was a random point taken downstream of

the tube. The same has been depicted in the figure 3.1. This point happened to lie after the winglets in all of the four cases (Common Flow Down (CFD) and Common Flow Up (CFU) configuration at downstream as well as upstream location i.e. CFD_D, CFU_D, CFD_U, CFU_U configurations). In the case of the common flow down orientation of the winglet located at a downstream position, the point was right near the region where the formation of vortices was most pronounced. The reason behind making such a selection of point location was to study the effect of vortex formation on temperature values over the plate. In other words, the motive was to study the effect of winglets on heat transfer from the fin plate in the wake region. Besides representing probe points A and B, figure 3.1 also represents the computational domain selected for fin plate, tube and winglet, during the numerical analysis.

Heat transfer, as well as flow resistance characteristics, have been compared for all the four configurations of winglet viz., CFD and CFU configurations in downstream as well as upstream location using Colburn's factor (j) and friction factor (f) respectively. Overall thermohydraulic performance is the cumulative effect of thermal characteristics and flow resistance characteristics which have been assessed by Performance Evaluation Criterion, (PEC) = $((j/j_0)/(f/f_0)^{1/3})$ also known as JF factor (where j and f are the colburn's factor and friction factor respectively for the heat exchanger using winglet, while j_o and f_o are the same without using winglet i.e. the baseline case)

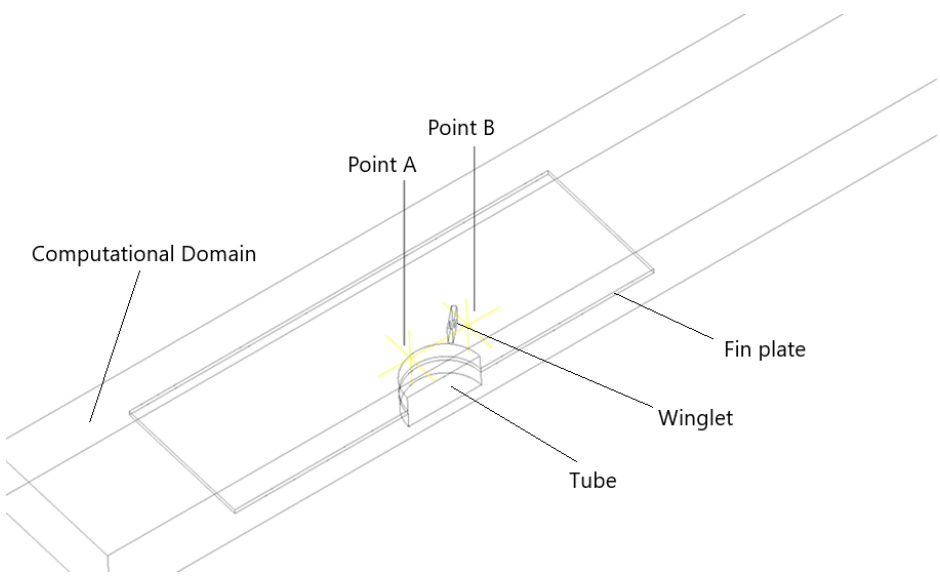

Figure 3.1 Depiction of probe points A and B

Secondly, I move on to find the globalized effect of employing a rectangular winglet having a punched hole at its center. In these investigations also, studies have been performed on all the four configurations viz., CFD and CFU configurations in downstream as well as upstream location. The same has been depicted in the figure 3.2. Heat transfer, as well as flow resistance characteristics, have been compared using Colburn's factor (j) and friction factor (f) respectively. The cumulative effect of thermal characteristics and flow resistance characteristics was observed with the help of area goodness factor, termed as Performance Evaluation Criterion (PEC) = (j/f).

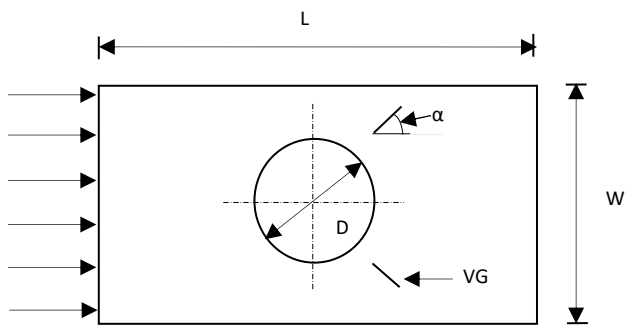

Figure 3.2(a) Common Flow Down (CFD), Downstream

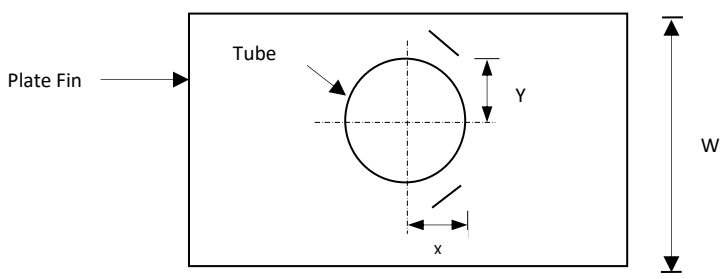

Figure 3.2(b) Common Flow Up (CFU), Downstream

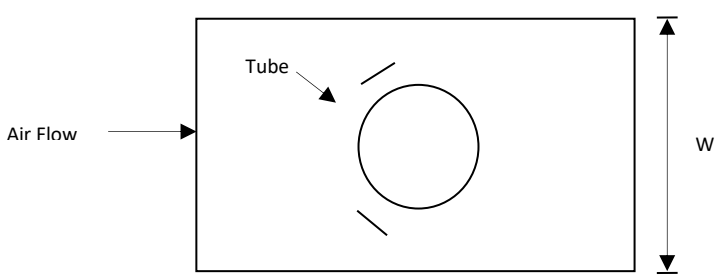

Figure 3.2(c) Common Flow Down (CFD), Upstream

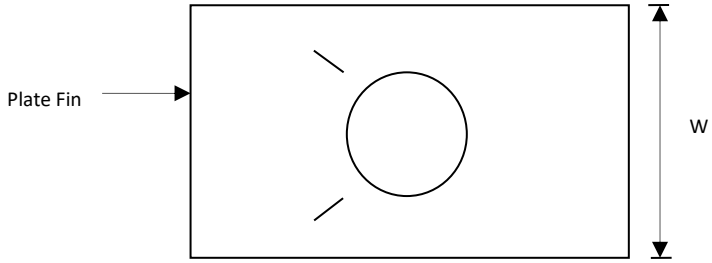

Figure 3.2(d) Common Flow Up (CFU), Upstream

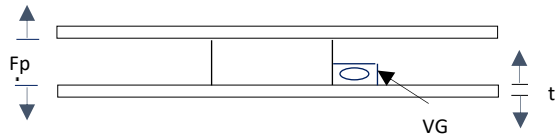

Figure 3.2(e) Geometrical configuration of the test plate (Front View)

Figure 3.2 Different configurations of the test plate

The present study goes on further to investigate the effects of punching out a rectangular winglet with a hole, on flow resistance and heat transfer characteristics in a fin-and-tube heat exchanger. Three cases have been studied numerically in case of RWPH with plate-punching viz., common flow up at an upstream location, common flow down at an upstream location and common flow down at the downstream location. The location of the winglet and its angle of attack in the punched-out case has been kept identical to that in the non-punched case in order to draw coherent comparisons between the performance characteristics of the two. Due to placement of the winglet at the determined location and selected angle of attack, plate punching interferes with the tube placement for the fourth case that is, common flow up at a downstream location. This could also be made out of the schematic diagrams of fin-plates shown in figure 3.3. Nevertheless, the investigated configurations of punched-out cases present a good basis for commenting on relative differences between the effect of punching based on location and orientation, as have been explained in the coming chapters.

Flow resistance and heat transfer characteristics have been compared for all the cases using friction factor (*f*) and Colburn's factor (*j*) respectively. Overall thermohydraulic performance is the cumulative effect of thermal characteristics and flow resistance characteristics which have been assessed by Performance Evaluation Criterions, (PEC (2) = $(j/j_0)/ (f/f_0)^{1/3}$) also known as JF factor which is used to evaluate the improvement over

baseline case and (PEC (1) = (j/f)) termed as area goodness factor, used for the relative comparisons between the four considered configurations. Investigations have been performed keeping the same Reynolds number i.e. 1400 to 9000 and the same angle of attack i.e. 45°.

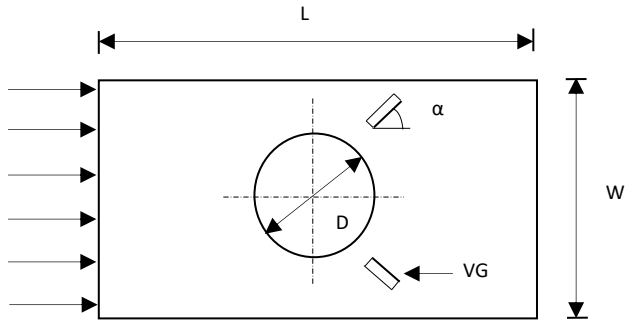

Figure 3.3(a) Common Flow Down (CFD), Downstream

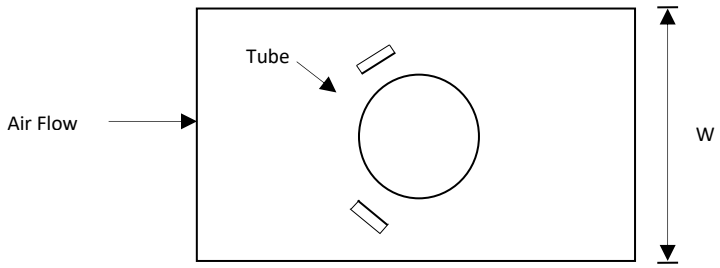

Figure 3.3(b) Common Flow Down (CFD), Upstream

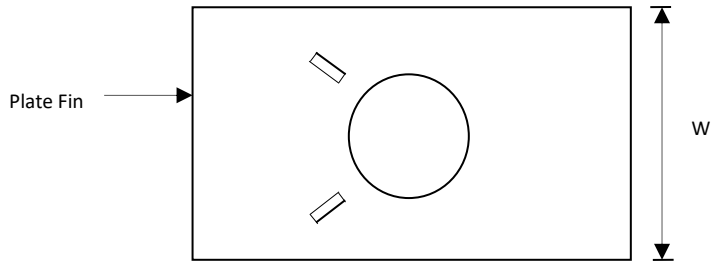

Figure 3.3(c) Common Flow Up (CFU), Upstream

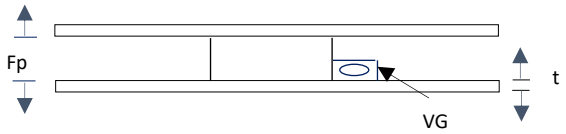

Figure 3.3(d) Geometrical configuration of Test plate (Front View)

Figure 3.3 Different configurations of the test plate (punched out winglet)

3.3 SCHEME OF INVESTIGATION

The scheme of the investigations to be performed is presented in the block diagram shown in figure 3.4.

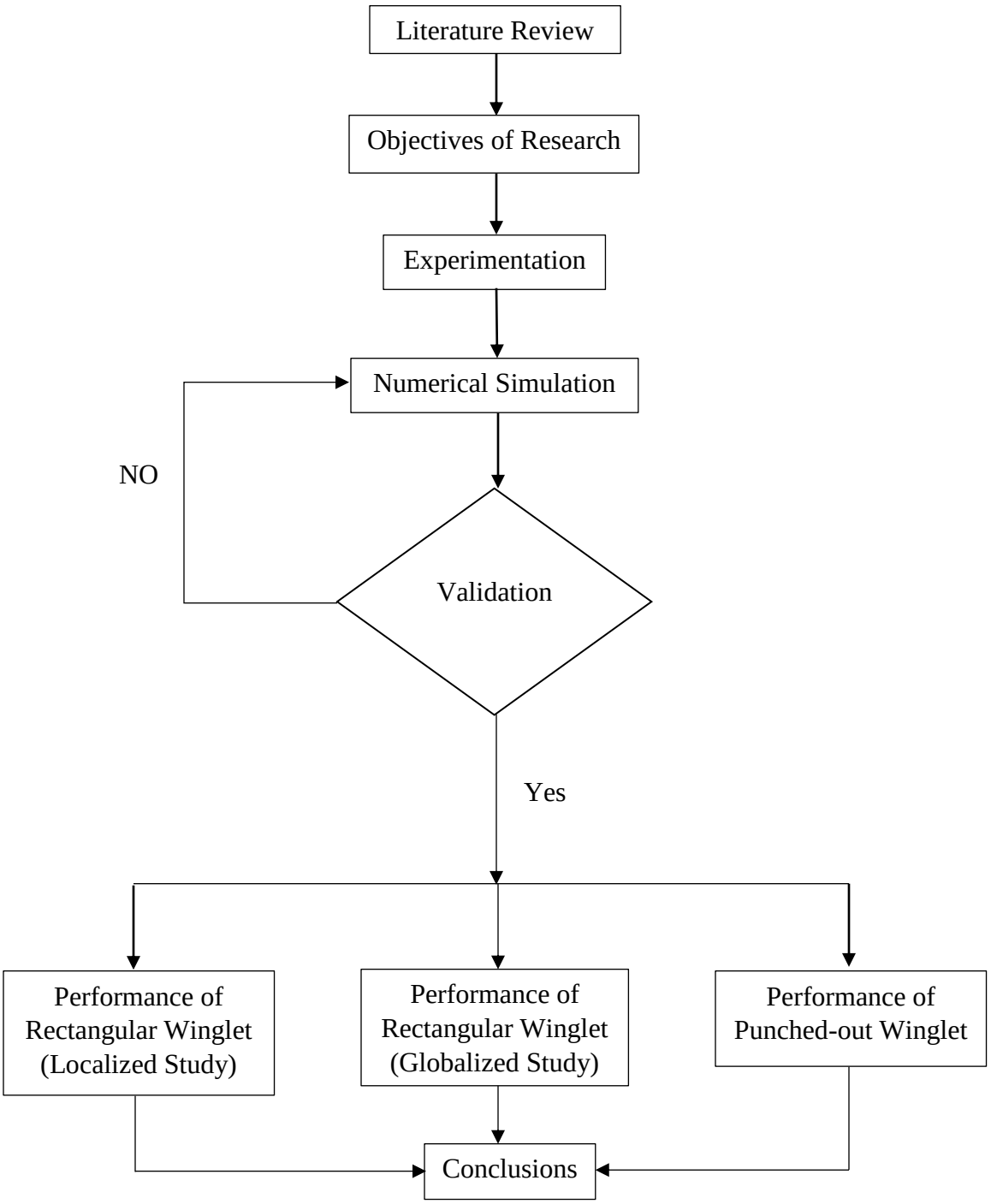

Figure 3.4 Scheme of investigation

3.4 EXPERIMENTATION

In the present investigation, experiments were performed on a fin-and-tube heat exchanger installed in a wind tunnel test rig. Fig. 3.7 & 3.8 shows an experimental setup with a test prototype. Optimum location and size of vortex generator have been taken as suggested by (Pesteei et al., 2005), so in order to justify the selection of same, all the other parameters related to experimental set-up and test model have also been taken as per the design concluded by (Pesteei et al., 2005). The experimental setup used comprises of a wind tunnel test rig having dimensions as 200 × 300 × 600 mm^3 (height × width × length). Numerous tests have been performed for ensuring high quality of distribution of parallel velocity at the measuring section. The test section used and close-up images of the winglet with hole have been shown in figure 3.6 and figure 3.9 & figure 3.10 respectively. Air was suctioned with the help of a fan having the provision of variable speeds that flowed air through the wind tunnel test rig section. For maintaining smooth and streamlined airflow, honeycombs have been used. The test model has been made up of 25 parallel aluminum fin plates having dimensions as 300×200 mm^2 and fin pitch as 12 mm. A circular tube made up of copper with an outer diameter as 52 mm and effective length as 300 mm has been fitted through the center of the series of parallel aluminum fin plates. In addition to circulating hot water inside the copper tube, an electric heater element (of power 300W) has been used for heat generation and kept inside the copper tube.

Fin plate number 13 with 3 mm thickness in the middle has been chosen for the experimentation work among all the fin plates and fitted with winglets. The reason for making such a selection was that the same has been located centrally, and due to which there will be minimum leakage of the heat to the surroundings, so, the whole amount of heat will be taken away by the air flowing over the fin plate surface. The rest of the fin plates have been fitted only to maintain the periodicity of the heat exchanger. The fin plate at the middle has been divided into small zones which are fitted with T-type thermocouples at predefined points. A total of 23 thermocouples have been attached on half part of the fin surface for finding the distribution of local temperature and convective heat transfer coefficient on the fin plate surface. Thermocouples have been attached at the center of the fin plate surface for preventing them from interfering with the thermo-hydraulic behavior

of air. In order to fulfill this motive, the middle fin plate has been made up of two thin plates of aluminum that have been sandwiched together with the thermocouple junctions being placed in grooves inside the fin plates. The span-wise and stream-wise pitch of the thermocouples have been taken as 20 mm. Figure 3.5 represents the location of thermocouples on central fin plate in detail.

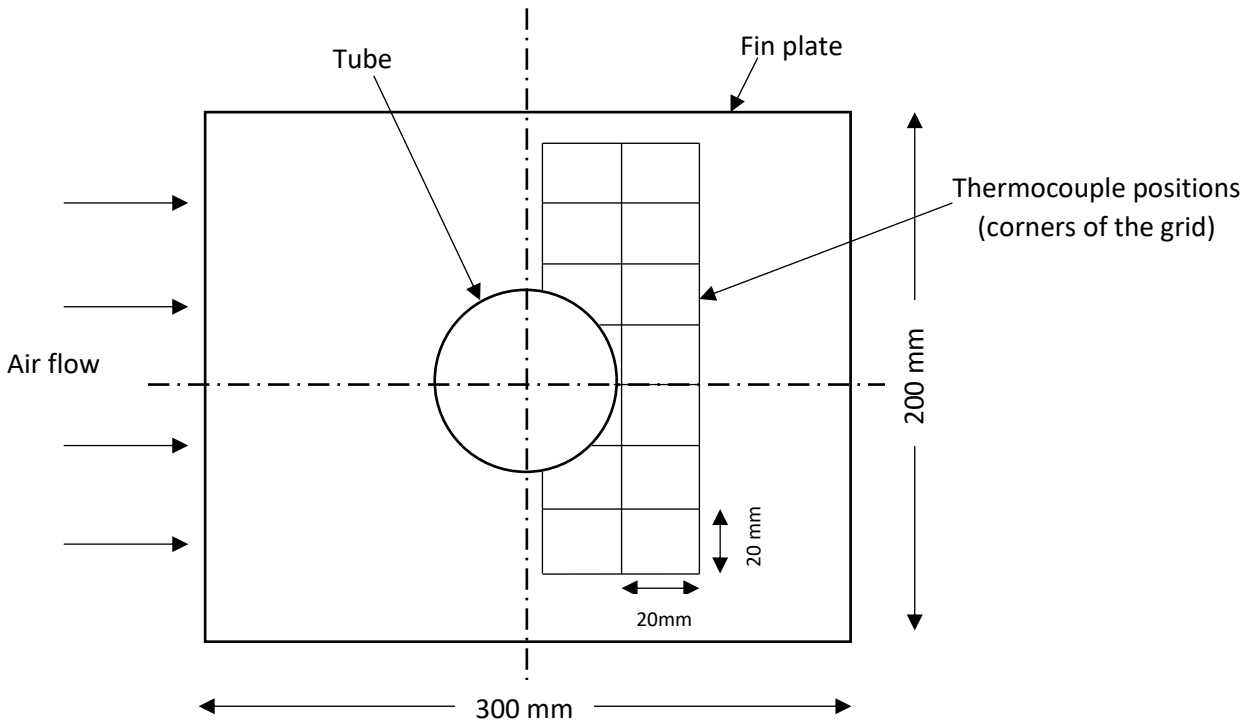

Figure 3.5 Location of thermocouples on the fin plate

Size of VGs, also represented by a measure of aspect ratio has been taken as 1.33 and positions of winglets have been taken as suggested by (Pesteei et al., 2005). As reported by (Zhou & Feng, 2014) the diameter of the hole has been considered as 4 mm. Reynolds number was varied from 1400 to 9000 and the angle of attack was taken as 45°for optimum thermal performance enhancement as concluded by (Martin Fiebig, Mitra, & Dong, 1990). It is to be noted that experiments were performed on fin plates having RWPH as vortex generators, for which test plates were made. Table 3.1 represents the different parameters

pertaining to fin-tube heat exchanger as well as vortex generator and the justification for the same has already been given.

Figure 3.6 Fin-and-tube heat exchanger

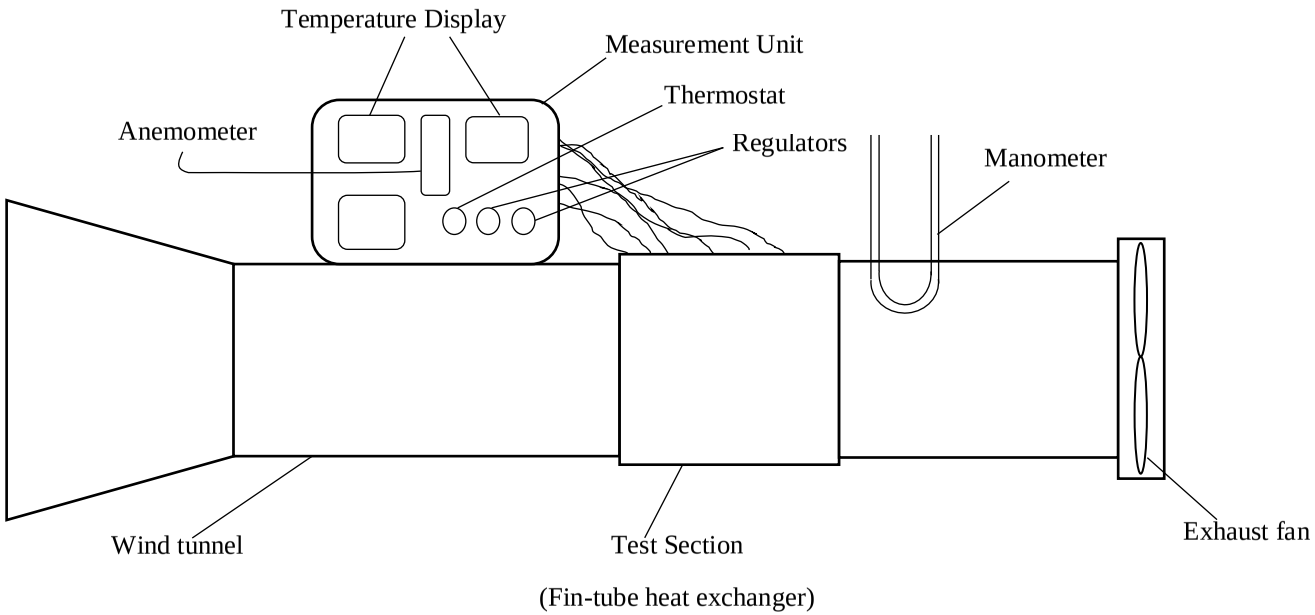

Figure 3.7 Schematic of Experimental Setup

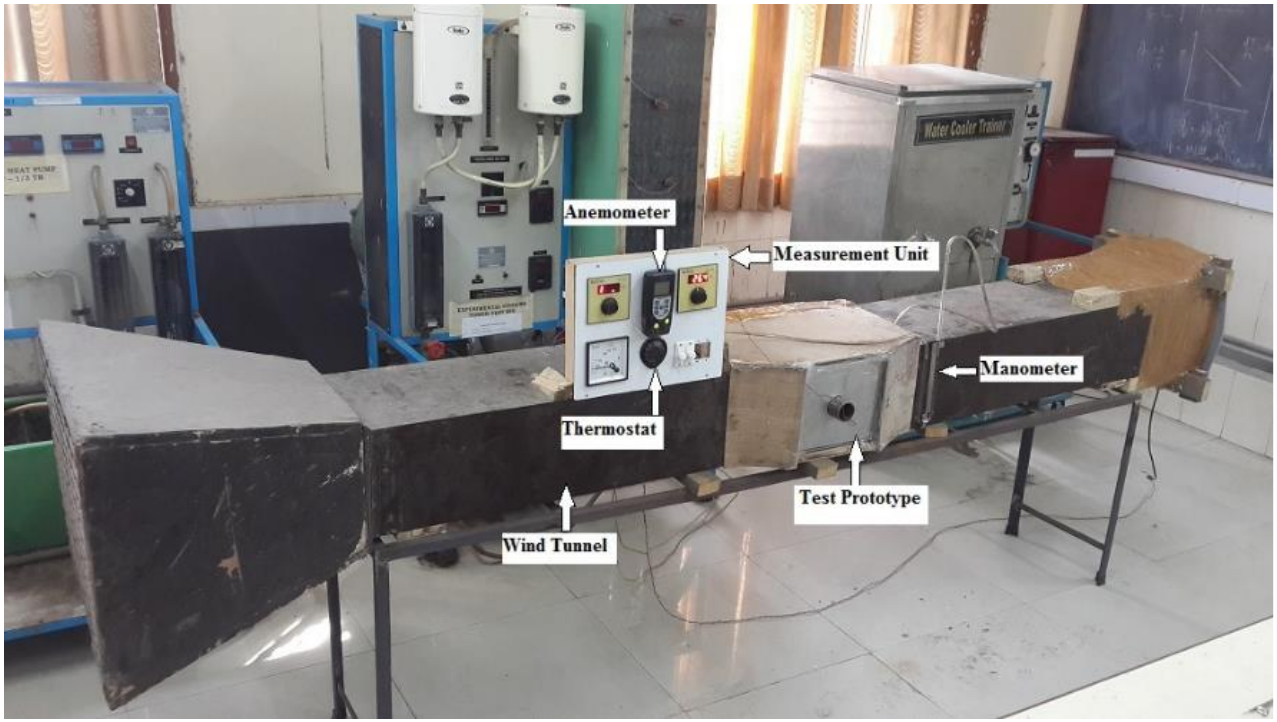

Figure 3.8 Experimental Setup

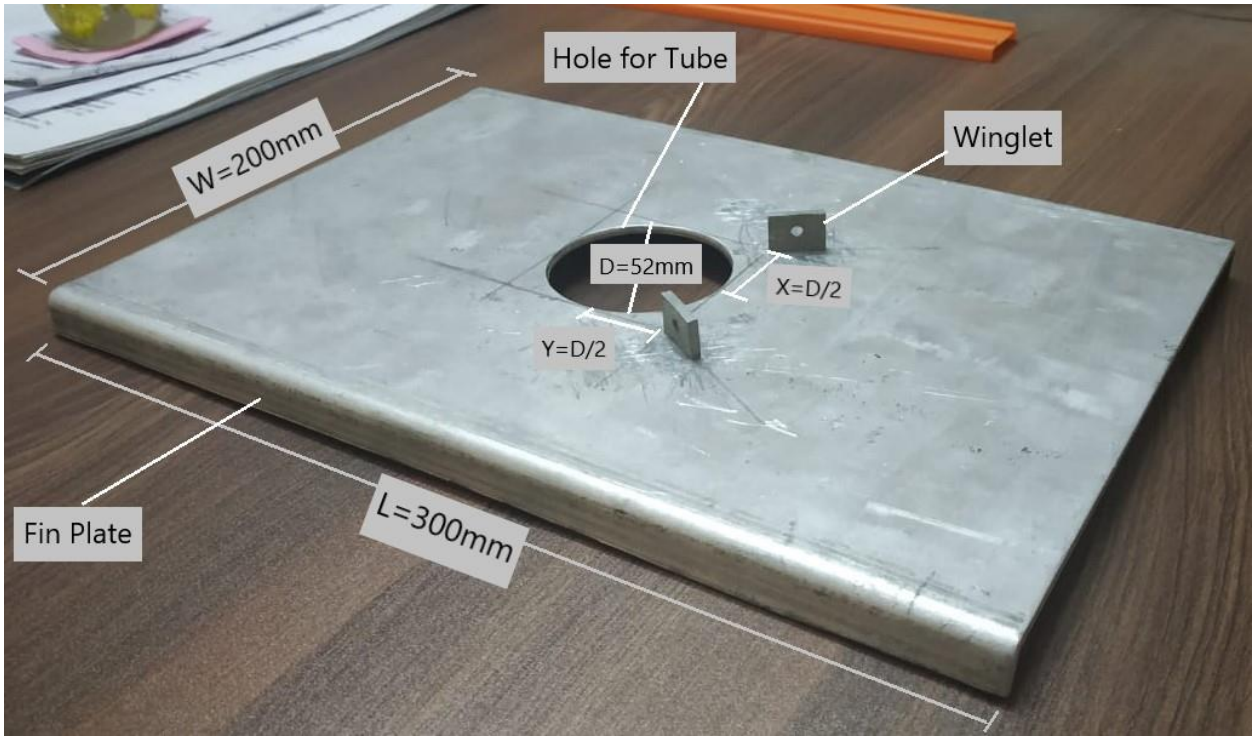

Figure 3.9 Fin plate with winglet attached

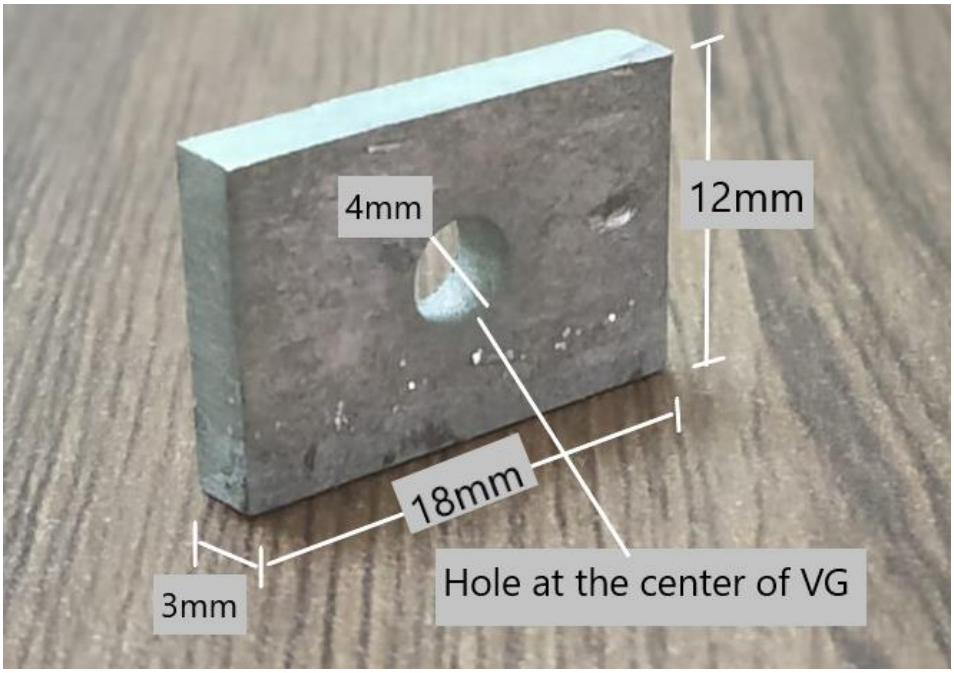

Figure 3.10 Winglet with a hole

Table 3.1 Parameters of fin-tube heat exchangers under consideration

Parameters	**Without VG**	**With VG**
Tube outside diameter(D)	52mm	52mm
Fin plate length(L)	300mm	300mm
Fin plate width(W)	200mm	200mm
Fin plate thickness(t)	3mm	3mm
Fin pitch(F_p)	12mm	12mm
Longitudinal vortex generator position(X)	-----	26mm(0.5D)
Transverse vortex generator position(Y)	-----	26mm(0.5D)
Vortex generator attack angle(α)	-----	45°
Vortex generator length (L_g)	-----	18mm
Vortex generator height (H_g)	-----	12mm
Vortex generator thickness (t_g)	-----	3mm
Hole diameter(d)	-----	4mm
Longitudinal hole position(x)	-----	9mm
Transverse hole position(y)	-----	6mm

3.4.1. Uniform Flow Condition At Inlet

A pitot-static tube has been used for measuring air flow velocity in the present experimentation. Additionally, the calibration of the pitot-static tube has been carried out using a standard calibrated thermal probe in the wind-tunnel. During calibration, both the probes were subjected to similar flow conditions. This demanded simultaneous measurements of flow velocity at a given point in the wind tunnel. Placement of two probes at a point simultaneously was not possible hence the probes were placed closed to each other during calibration.

Experiments were carried out to find the optimum separation distance between the thermal probe and the pitot-static tube for accurate calibration. It has been found that the least deviation of 4.65% between the airflow velocity measured by the thermal probe with and without pitot static tube was at 5mm of separation distance. Moreover, the presence of the thermal probe showed negligible interference effects (maximum deviation of 0.86%) on pitot-static tube measurements.

On the other hand, a pitot-static tube has a small interference effect (maximum deviation of 1.94%) on thermal probe readings. Because of this, the thermal probe was removed and deviations in air velocity measurements using only a pitot-static tube at its original position as well as at the position of the thermal probe i.e. 5mm above the initial position of the pitot-static tube were studied. A maximum deviation of 0.54% was observed (Refer Appendix A) as compared to 0.43% reported by (Pesteei et al., 2005) following the same procedure, which indicates that shifting of the pitot-static tube to 5mm above its initial position had a negligible effect on pitot-static tube measurements.

For analysis in the present experimentation, only one fin plate i.e. central plate was considered and the airflow velocity has been measured (at a temp. of 26.5°C) between the space with the adjoining fin plate. The distance between the two plates was considered to be 12 mm. As we stated earlier, the maximum deviation was 0.54% (in mean velocity of airflow) in pitot-static tube measurements on account of shifting of probe points by 5mm, which could be neglected. This ultimately leads to the fact that the average wind speed distribution in the test section can be considered uniform.

3.5 NUMERICAL SIMULATION

In order to draw validations with the experiment results, numerical simulations were carried out by employing the concepts of computational fluid dynamics. Geometry for representing the cases was built on Solidworks while computational fluid dynamics simulations were performed on ANSYS Fluent. For meshing the problem in hand, the ICEM computational fluid dynamics module built within ANSYS Meshing was used.

Whenever numerical simulations are dealt with, we are presented with a limitation of computational power and resources. In this case, computational fluid dynamics studies were carried out on a single fin of a heat exchanger with a vortex generator. The tube was accordingly sized within the computational domain. Experimentation was performed on common flow down and common flow up cases at downstream positions but simulation studies were performed on all of the four possible cases viz., common flow up at the upstream position, common flow up at the downstream position, common flow down at upstream position and common flow down at downstream position.

The current section deals with the case setup of the problem for performing computational fluid dynamics analysis which pertains to making the computational domain, meshing the cases and problem setup by defining flow parameters and boundary conditions. A note on grid independence study has also been presented.

3.5.1. Governing Partial Differential Equations And Boundary Conditions

3.5.1.1. Governing Partial Differential Equations

The following governing equations in Cartesian coordinates have been used for numerical investigations as suggested by (Ya Ling He, Chu, Tao, Zhang, & Xie, 2013)

Continuity equation:

$$\frac{\partial}{\partial x_i}(\rho u_i) = 0 \qquad (1)$$

Momentum equation:

$$\frac{\partial}{\partial x_i}(\rho u_i u_k) = \frac{\partial}{\partial x_i}\left(\mu \frac{\partial u_k}{\partial x_i}\right) - \frac{\partial p}{\partial x_k} \tag{2}$$

Energy equation:

$$\frac{\partial}{\partial x_i}(\rho u_i T) = \frac{\partial}{\partial x_i}\left(\frac{\lambda}{C_p}\frac{\partial T}{\partial x_i}\right) \tag{3}$$

In addition to the momentum, continuity and energy equations, two equations represented by Equation (4) for turbulent kinetic energy (k) and Equation (5) for specific dissipation rate (ω) were solved as shown below.

$$\frac{\partial}{\partial t}(\rho k) + \frac{\partial}{\partial x_i}(\rho k u_i) = \frac{\partial}{\partial x_j}\left[\left(\mu + \frac{\mu_t}{\sigma_k}\right)\frac{\partial k}{\partial x_j}\right] + G_k + Y_k \tag{4}$$

$$\frac{\partial}{\partial t}(\rho \omega) + \frac{\partial}{\partial x_i}(\rho \omega u_i) = \frac{\partial}{\partial x_j}\left[\left(\mu + \frac{\mu_t}{\sigma_\omega}\right)\frac{\partial \omega}{\partial x_j}\right] + G_\omega + Y_\omega \tag{5}$$

In the above equations, μ_t in the effective diffusivity, the term denotes turbulent viscosity while σ_k and σ_ω denote turbulent Prandtl numbers for k and ω respectively. G_k and G_ω represent generation terms for k and ω due to mean velocity gradients. The dissipation of k and ω is denoted by Y_k and Y_ω.

3.5.1.2. Boundary Conditions

For analysis purposes, boundary conditions as suggested by (Ya Ling He et al., 2013), corresponding to the different computational domains (Zeeshan, Nath, Bhanja, & Das, 2018) shown in fig. 3.11 & fig. 3.12, are described as under:

Upstream extended region:

- At inlet boundary,
$$u = u_{in} = constant, v = w = 0, T = T_{in} = constant$$
- At side boundaries,
$$\frac{\partial u}{\partial y} = \frac{\partial w}{\partial y} = 0, v = 0, \frac{\partial T}{\partial y} = 0$$
- At the top and bottom boundaries,

  Periodic condition for velocity $u_{up} = u_{down}$

  Periodic condition for temperature $T_{up} = T_{down}$

Fin coil region:

- At side boundaries,

  Fluid region $\frac{\partial u}{\partial y} = \frac{\partial w}{\partial y} = 0, v = 0, \frac{\partial T}{\partial y} = 0$

  Fin region $u = v = w = 0, \quad \frac{\partial T}{\partial y} = 0$

  Tube region $u = v = w = 0, \quad T = T_w = constant$

- At top and bottom boundaries,

  Periodic condition for velocity $u_{up} = u_{down}$

Periodic condition for temperature $T_{up} = T_{down}$

Downstream extended region:

- At the outlet boundary,

$$\frac{\partial u}{\partial x} = \frac{\partial v}{\partial x} = \frac{\partial w}{\partial x} = \frac{\partial T}{\partial x} = 0$$

- At side boundaries,

$$\frac{\partial u}{\partial y} = \frac{\partial w}{\partial y} = 0, \mathrm{v} = 0, \frac{\partial T}{\partial y} = 0$$

- At the top and bottom boundaries

Periodic condition for velocity $u_{up} = u_{down}$

Periodic condition for temperature $T_{up} = T_{down}$

Periodic computational domain has been selected as we have considered only one fin plate for the analysis rather than considering the complete heat exchanger. Conditions at the domain upper surface are similar to that at the domain lower surface, meaning that the flow exactly repeats itself at a certain pitch.

Furthermore, the adiabatic condition has been chosen for sidewalls and outlet of the computational domain because it has been assumed that entire heat transfer is to the air entering from the inlet of the computational domain by tube, plate, and winglet. There is no air entering from the sidewalls and outlet extended region. Due to this reason we have isolated side walls and outlets of the computational domain.

Moreover, the Conjugate Heat Transfer model has been used in the Fluent by making use of the coupled boundary conditions on wall zones which defines fluid / solid interface. The conjugate heat transfer model considers resistance of both i.e. solid as well as fluid. The numerical values of different boundary conditions pertaining to the computational domain have been represented in Table 3.2.

Table 3.2 Numerical values of boundary conditions

Parameters	**Values**
Inlet velocity boundary condition	1 to 6 m/s
Outlet pressure boundary condition	0 Pa (gauge)
Turbulent intensity (Inlet/Outlet) %	1 / 5
Turbulent viscosity ratio	10
The ratio of specific heats	1.4
Air density (at 20°C)	1.225 kg/m^3
Viscosity (at 20°C)	1.7894e-05 kg/m-s
Pressure-velocity coupling scheme	Coupled
Flow courant number	50
Momentum explicit relaxation factor	0.25
Pressure explicit relaxation factor	0.25
Gradient	Least square cells based
Pressure	Standard
Momentum	Second-order upwind
Turbulent kinetic energy	Second-order upwind
Turbulent dissipation rate	Second-order upwind
Energy equation	Second-order upwind
Turbulent viscosity under-relaxation factor	0.80

3.5.2. Computational Domain

The first and foremost stage of any numerical simulation study deals with the creation and definition of a domain. It is important to note that setting up the computational domain has direct links with the accuracy of results whenever we start dealing with transitional and turbulent flow problems. A simple cuboidal domain was defined in order to replicate the flow taking place inside a wind tunnel with unequal domain extensions in order to avoid the effect of reversed flow, as encountered by the solver and widely prescribed in literature. The domain was extended by 45 times the fin pitch ($45F_p$) towards the outlet and 7.5 times the fin pitch ($7.5F_p$) towards the inlet. Investigations were performed on a symmetric domain with fin-plate and tube assembly being cut into half by an XY plane passing through the centroid of the assembly. Uniform cushioning of 10mm was provided in the domain towards the top of the tube and side of the plate. It is also to be noted that only one fin-plate was considered inside the domain due to the periodicity of the actual setup.

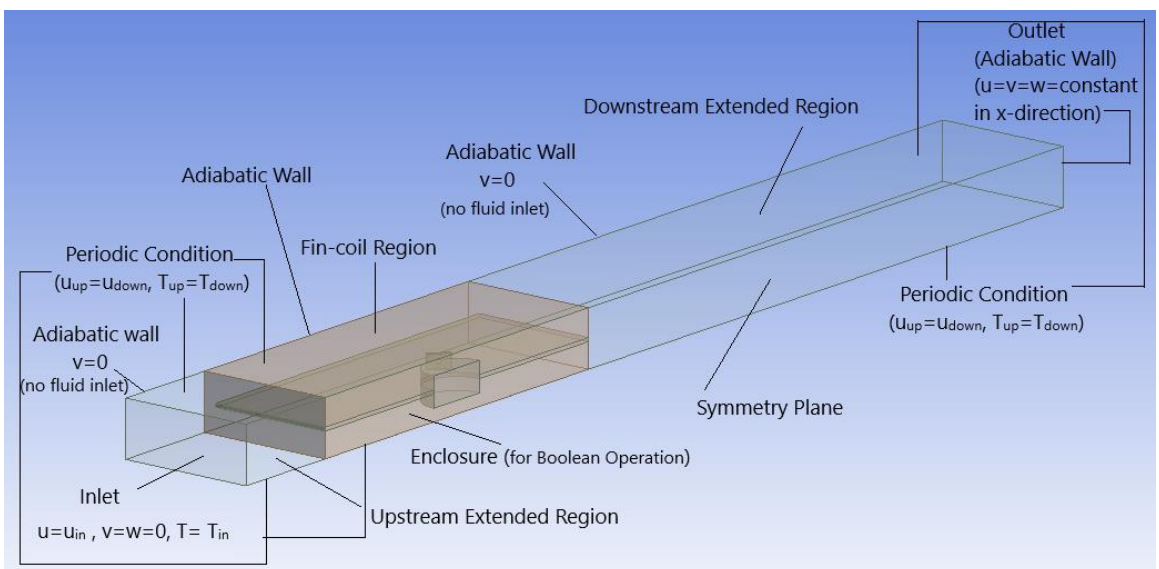

Figure 3.11 Computational Domain (for winglet mounted over the fin plate)

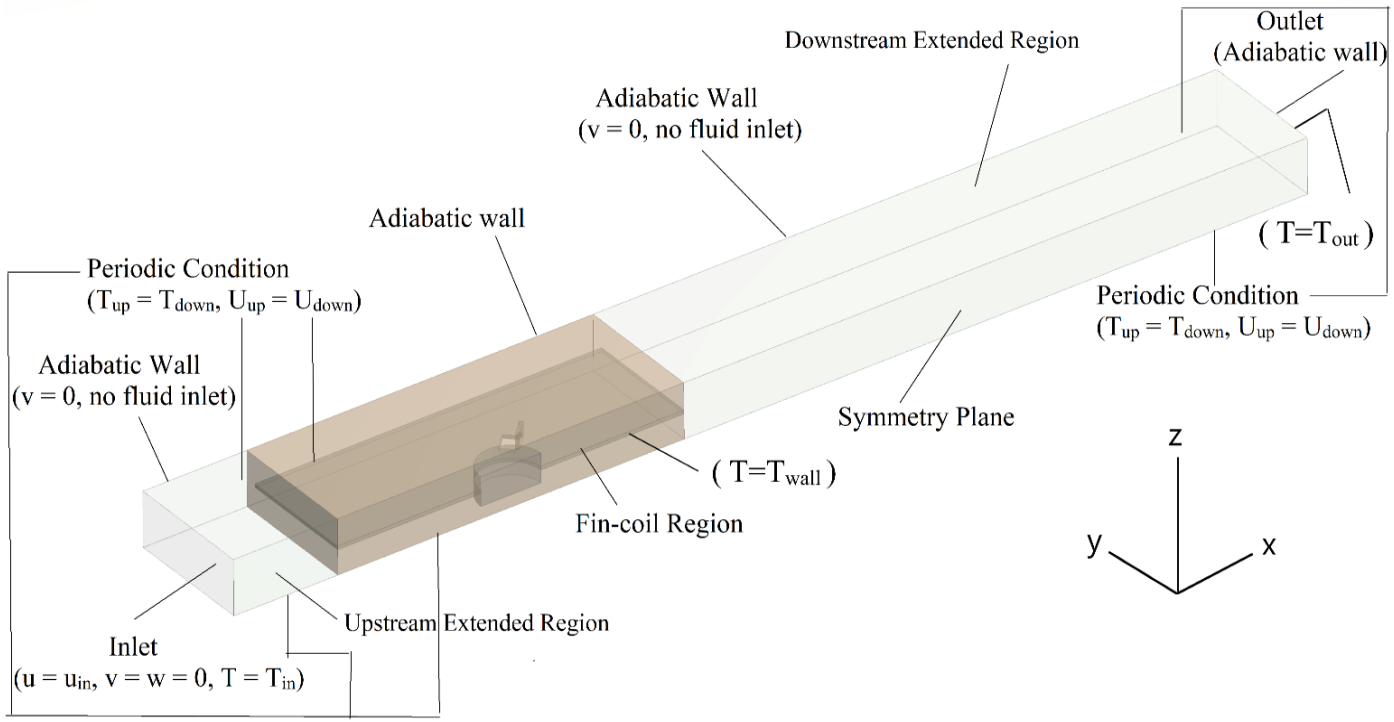

Figure 3.12 Computational Domain (for winglet punched out from the fin plate)

3.5.3. Grid Discretization

After defining the domain, the tube and plate along with winglet were defined as tool bodies whereas the domain was defined as the target body in ANSYS Design Modeler. This was done solely for performing a Boolean operation (subtraction) wherein, tool bodies were subtracted from the target body. Tool bodies were preserved, as is customary in heat transfer simulations for investigating the heat flow due to conduction and convection from tool body surfaces.

Moving on to meshing, the sizing function for each of the cases was set to Curvature. Relevance center was set to Coarse, a justification of which would be evident in the upcoming section on grid independence study. Span angle center was set to fine and curvature normal angle was kept as default that is, 18 degrees. Hexahedral elements, both structured and unstructured, have been made use of for dividing the domain into small discrete cells for solving the governing equations. Figure 3.13 to 3.15 can be referred for the same.

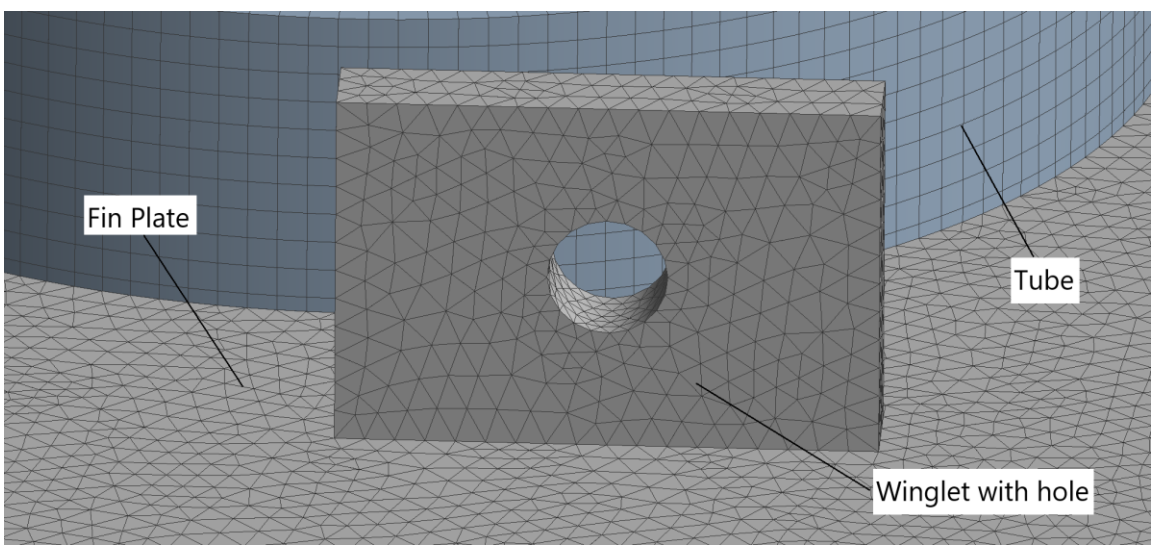

Figure 3.13 Discretization of the plate with winglet

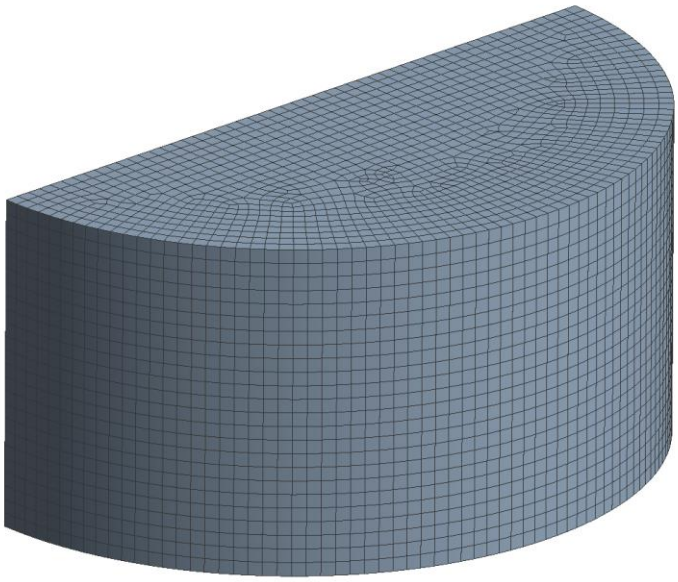

Figure 3.14 Tube discretization

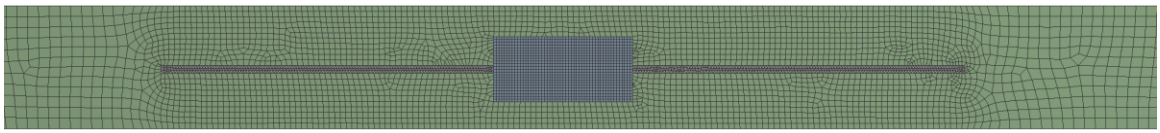

Figure 3.15 Domain discretization

Fig. 3.16 shows how a multizone method has been used to create blocks on the fin-plate and divide it into two zones of structured and unstructured elements. While face sizing functions were implemented on the plate and tube surface for generating a mesh of very fine resolution, the concept of the body of influence was employed for defining preferential element sizing on the part of the domain in the vicinity of the fin-plate and tube. A cuboidal body aligned with the domain was built surrounding the plate and winglet region and defined as the body of influence in order to govern the element size within that region. The motive was to have a finer discretization within our region of interest as a result of which, an element size of 2mm was chosen for the body of influence. Preserving the tool bodies

in Boolean operation ensured that the body of influence played no role in defining the element sizes of plate, tube, and winglet. It was only the part of the domain being covered by a body of influence which was refined by using the same. In order to make the plate and winglet elements more refined, independent body sizing was used and the element sizes for plate and winglet were set to 1 mm. The wall y+ value used in this study, which is one of the imperative parameters that govern mesh quality having a direct impact on the accuracy of the numerical solution, was kept below 5, which was well within the viscous sublayer. This would also be discussed in the next section.

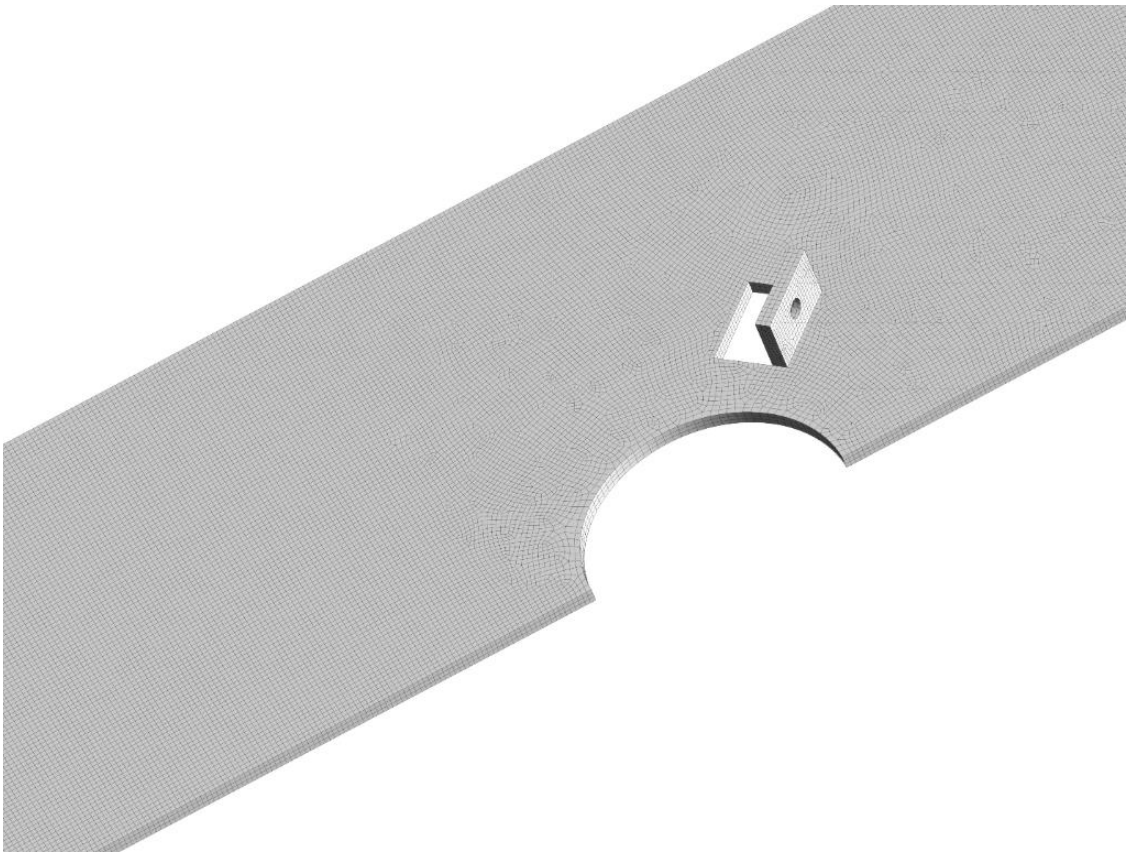

Figure 3.16 Representation of multizone method for meshed plate and punched-out winglet

3.5.4. Numerical Modeling

The range of Reynolds number being studied in this work lies between 1400 and 9000. Some portion of the range falls under the transitional regime while some of it falls in the turbulent regime which makes it customary to employ turbulence modeling techniques. (Sahiti, Lemouedda, Stojkovic, Durst, & Franz, 2006) suggested that laminar models are not proficient in predicting flow phenomena at $Re > 500$.

Moreover, it has been observed from the literature review that the k-ε turbulence model along with the energy conservation equation is fairly well equipped at predicting thermal performance parameters but numerical pressure drop values have some disagreement with experimental values to a significant extent. The reason behind the same could be that the k-ε model fails to accurately capture separated flows caused due to the addition of vortex generators. As a result, the Shear Stress Transport (from now on referred to as SST) k-ω turbulence model, as proposed by (Menter, 1994) has been used in the present study for modeling all the configurations viz., common flow up and common flow down at upstream as well as downstream locations i.e CFU_U, CFD_U, CFU_D, and CFD_D configuration.

The SST formulation uses a k-ω model near the wall boundaries and k-ε model elsewhere. In addition, (Menter, 1994) proposed a new wall treatment approach that switches between the methods of integration to the surface and log-law layer wall functions with the help of a blending function. Results produced by the SST model with proposed wall treatment were closest to experimental data when compared with other eddy viscosity formulations for various problem cases, including heat transfer applications.

In order to test the accuracy of results of our case predicted by SST model, I ran test case simulations on CFD_D non-punched case using both, the standard k-ω model proposed by (Wilcox, 1993) and Menter's SST formulation of the k-ω model and found out that keeping wall y+ value below 1 was a mandatory requirement in the standard model whereas comparable results of high conformation with experimental data could be attained at wall $y+ \approx 5$ with SST formulation. This significantly reduced our mesh requirements and computational power as a result of which, choice of using the SST k-ω model was finalized.

Furthermore, motivation was sought from the recent work of (Chimres et al., 2018b) who used the SST k-ω model in their investigation of heat transfer augmentation using semi-dimple vortex generators.

The material of fin-plate and winglet was aluminum and heat was being generated by a copper tube situated at the centre of the plate. Different thermal boundary conditions pertaining to heat exchanger have been represented in Table 3.3.

Instead of solving the pressure and momentum equations separately, as is done in the segregated algorithm, pressure-velocity coupling was achieved by performing a full discretization of the Rhie Chow pressure dissipation and gradient terms in the governing equations. The selection of the pressure-based coupled algorithm led to superior performance and faster convergence. Second-order discretization was used for all the governing equations and convergence criterion was satisfied once the values of scaled residuals of continuity, momentum and energy equations reached 10^{-4}, 10^{-4} and 10^{-6} respectively.

Table 3.3 Thermal boundary conditions

Parameters	**Values**
Heat generation rate from copper tube per unit volume (of copper tube)	379740 W/m^3
Convective heat transfer coefficient	32 W/m^{2}K
Free stream temperature	293 K
Specific heat of fin material (Aluminum)	1.047 x 10^3 J/kg-K
Thermal Conductivity of fin material (Aluminum)	130 W/m-K

3.5.5. Grid Independence Study

Cell sizes were varied along with the domain in order to study the dependence of the number of grid elements on numerical results. An investigation of the effect of the number of grid elements on the Nusselt number, as shown in fig. 3.17 was made in order to conduct the grid dependence study, wherein four types of grids were made. The extra-coarse, coarse, medium and fine grids consisted of 4.1 lakh, 7.58 lakh, 11.54 lakh, and 20 lakh elements respectively. Error percentage between extra coarse and coarse grids was 1.972%, that between coarse and medium grids was 1.155% whereas the error reduced to an insignificant percentage of 0.014% between medium and fine grids. In order to save on computational resources and allied costs without compromising on the accuracy of results, the medium grid was chosen for our simulations. Results of grid dependence shown in fig. 3.16 are for CFD_D non-punched case but a similar study was performed for the other cases.

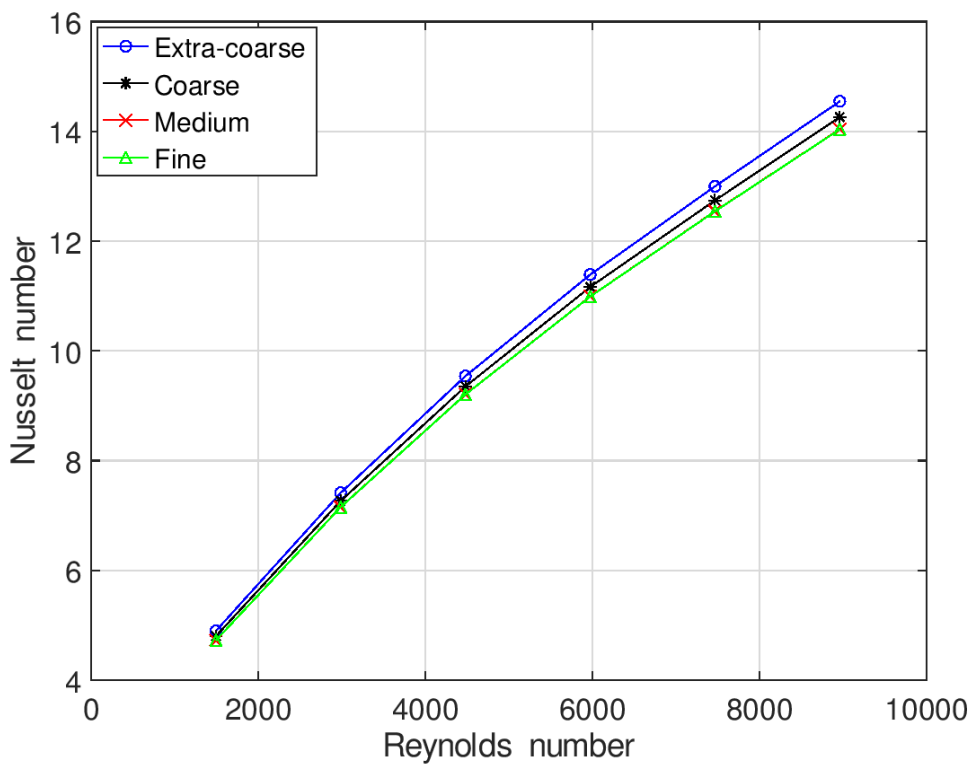

Figure 3.17 Grid Independence Study

3.5.6. Verification

Verification is the process of determining the accuracy of the computational model. The main error associated with verification is the discretization error. Lesser is the discretization error, more will be the accuracy of the computational model. So to achieve this I have used a coupled scheme rather than a SIMPLE scheme for pressure-velocity coupling which increases convergence speed drastically and thereby reduces discretization error. Coupled solver simultaneously solve all the governing differential equations at each cell center as compare to the SIMPLE solver in which governing differential equations are solved one by one. Hence, convergence is achieved with lesser no. of iterations.

3.5.7. Validation

Fig. 3.18 & 3.19 shows a comparison of the convective heat transfer coefficient (*h*) and pressure drop (*dP*) values obtained from numerical simulations and experimentation. Results of experimental validation shown in fig. 3.18 & 3.19 are for CFD_D and CFU_U non-punched cases respectively because of experimentation being performed on these two cases. For CFD_D configuration average error between experimental and numerical pressure drop values is 10.6% whereas the same between experimental and numerical convective heat transfer coefficients is 8.1%. The same has been depicted in the figure 3.18(a) and (b) respectively. Similarly, for CFU_U configuration average error between experimental and numerical pressure drop values is 9.1% whereas the same between experimental and numerical convective heat transfer coefficients is 7.7%. The same has been shown in the figure 3.19(a) and (b) respectively. It is evident from fig. 3.18 that numerically obtained results are in close proximity with the experimentally obtained results for CFD_D configuration. Initially, when the Reynolds number has been varied from 1490 to 3600 we noticed that numerically obtained value of convective heat transfer coefficients was very close to experimentally obtained value. This may be attributed to the fact that at small velocity turbulence is small so the heat transfer losses are less. As Reynolds number increases, heat transfer losses become more pronounced. The minor deviation of the numerical curve from the experimental curve could be attributed to the fact that at higher values of Reynolds number, flow characteristics induced by the formation of the boundary

layer over the plate comes into the picture. In this regard, the flow could be better captured by employing inflation layers on the plate surface during discretization at high Reynolds numbers but this was not done and mesh parameters were kept identical for all the cases. Dissimilarities between datasets may also be due to the unavoidable circumstances of leakage of fluid and contact resistances during experimentation. On the contrary, ideal condition scenarios are assumed while performing numerical simulations. Nevertheless, results were comparable to experimentally obtained values. After making a comparison with the available literature also, it was realized that error percentages were well within the acceptable limits and the selected turbulence modeling strategy faired adequately well in predicting the performance parameters and associated flow phenomena. k-ω turbulence model has been taken as the standard for the rest of the analysis part considering common flow down and common flow up configuration in downstream and upstream locations.

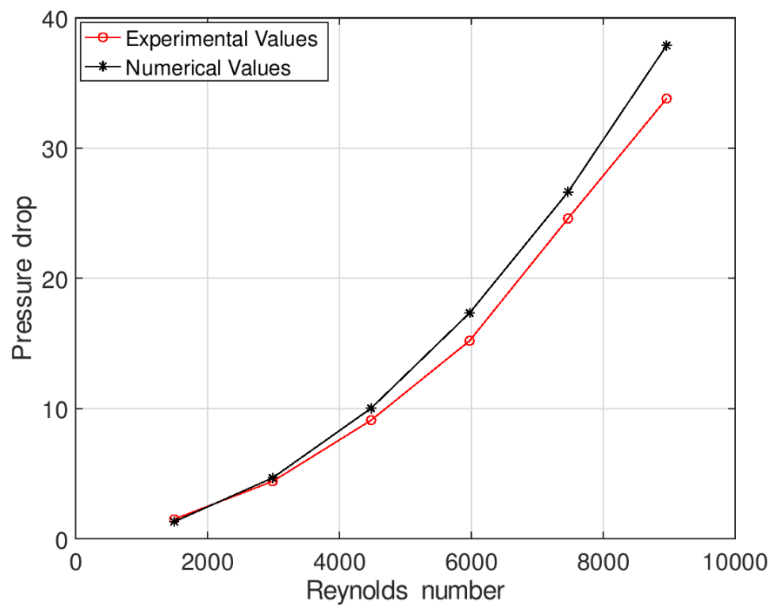

Figure 3.18(a) Comparison of experimental and numerical results for CFD_D configuration

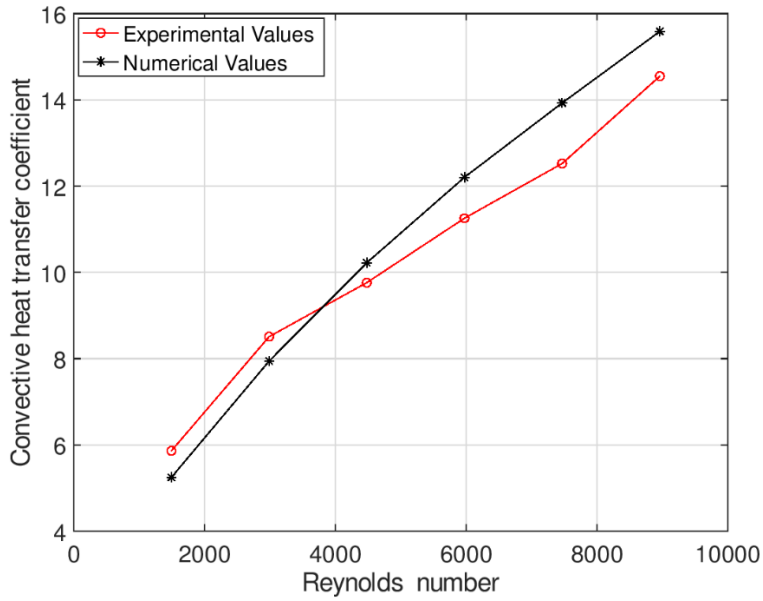

Figure 3.18(b) Comparison of experimental and numerical result for CFD_D configuration

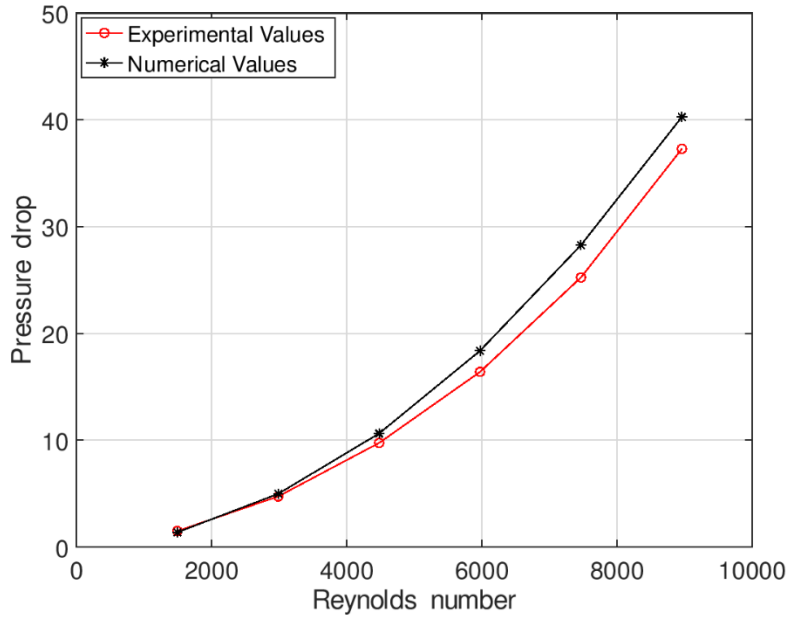

Figure 3.19(a) Comparison of experimental and numerical result for CFU_U configuration

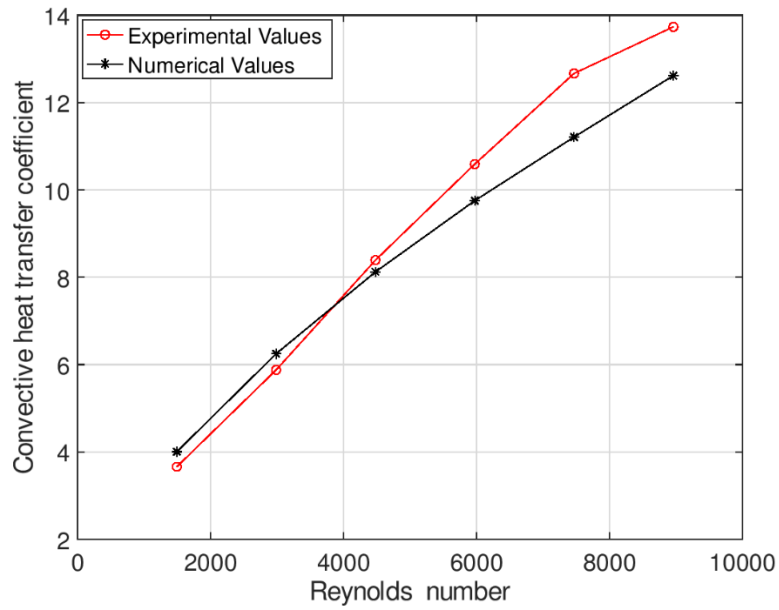

Figure 3.19(b) Comparison of experimental and numerical result for CFU_U configuration

3.5.8. Transient Simulation

Von Karman Street may exist and can create instabilities in fluid flow. To check this, at the beginning of the CFD analyses, a preliminary calculation has been made to determine whether the airflow shows any transient behavior. A fluid flowing around a tube may cause vortex shedding, which can be expressed in terms of the Strouhal number, defined by the following equation

$$S = \frac{f_v D}{u} \tag{6}$$

to be 0.2, where S, f_v, and D represent the Strouhal number, vortex shedding frequency, and tube diameter, respectively. The vortex shedding frequency may then be obtained by substituting the values of S, u, and D. The transient simulation has been performed for 102 sec in ANSYS but did not find any vortex shedding for the considered range of Reynolds no. when analyzed the flow in CFD-Post. In order to be ensured about the vortex shedding, the transient simulation has also been performed using the SST k-ω turbulence model

which captures boundary layer separation more accurately but found the same result as with the k-ε turbulence model used in the present study. This could be attributed to the presence of winglet over fin plate because as we know that Von Karman Vortex Street is a direct result of boundary layer separation over bluff bodies and due to the presence of winglet, boundary layer separation from tube surface is delayed.

3.6 DATA REDUCTION AND UNCERTAINTY ANALYSIS

3.6.1. Data Reduction

The mean temperature (T_m) and mean pressure (P_m) for a cross-section are defined as follows:

$$T_m = \frac{\iint_A uTdA}{\iint_A udA} \tag{7}$$

$$P_m = \frac{\iint_A PdA}{\iint_A dA} \tag{8}$$

The equations shown below have been made use of for determining the required thermo-hydraulic performance characteristics. Q represents the total heat transfer rate and ΔT_M denotes temperature difference.

$$Q = \dot{m}.C_p.(T_{m,out} - T_{m,in}) \tag{9}$$

$$\Delta T_M = \frac{(T_{m,wall} - T_{m,in}) - (T_{m,wall} - T_{m,out})}{\ln\frac{(T_{m,wall} - T_{m,in})}{(T_{m,wall} - T_{m,out})}} \tag{10}$$

Heat transfer coefficient due to convection (h) becomes

$$h = \frac{Q}{A_S . \Delta T_M} \tag{11}$$

Where, $\dot{m}$(kg/s) is the mass flow rate of the working fluid, $T_{m,out}$(K) is the fluid temperature at the outlet, $T_{m,in}$(K) is the fluid temperature at the inlet, $T_{m,wall}$(K) is the wall temperature. Specific heat capacity of working fluid is represented by C_p(J/kg K) and A_S(m^2) denotes the total surface area of heat transfer.

The hydraulic diameter (D_h) is given by,

$$D_h \ = 4. A_c / P_w \tag{12}$$

The kinematic viscosity (ν) is given by,

$$\nu = \mu / \rho \tag{13}$$

The hydraulic diameter-based Reynolds number (Re) is given by

$$Re = u D_h / \nu \tag{14}$$

In the above equations, u, A_c and P_w denote the air inlet velocity, cross-sectional area of fluid flow and perimeter of wetted surface, respectively. μ and ρ are dynamic viscosity and density of air respectively.

The Nusselt number (Nu) is defined by,

$$Nu = \frac{h. D_h}{k} \tag{15}$$

The Prandtl number (Pr) is defined by,

$$Pr = \mu . C_p \ / k \tag{16}$$

Darcy Friction factor (f) which determines the friction characteristics is defined by,

$$f = \Delta P_m . D_e / (2L.\rho.u^2) \tag{17}$$

Heat transfer capacity represented by Colburn's factor (j) is defined by,

$$j = \frac{Nu}{Re.Pr^{1/3}} \tag{18}$$

Here, ΔP_m and L denote the pressure drop between the inlet and outlet section of the test section and length of the plate along the direction of flow, respectively. Performance evaluation criterion (PEC) as suggested by (Yun & Lee, 2000) mentioned below has been used for estimating the thermal performance and pressure drop or flow resistance characteristics of the fin-and-tube heat exchanger.

$$PEC(1) = j/f \tag{19}$$

$$PEC(2) = \frac{\frac{j_1}{j_0}}{(\frac{f_1}{f_0})^{1/3}} \tag{20}$$

3.6.2. Uncertainty Analysis

The total uncertainty of the investigation was checked by calculating the accuracy of various measuring instruments attached in the setup. Table 3.4 gives the details related to various measuring instruments used. It is obvious that the larger the measured value, the smaller the related uncertainty. All the geometric parameters were offered by the heat exchanger manufacturer; thus, we ignore the uncertainty of these parameters. Based on the uncertainty of these devices, the total uncertainty of the experiment was calculated using the method of propagation of errors, as defined by (Holman, 2001). The total uncertainty of the experiment was calculated as mentioned below.

Table 3.4 Operating range and accuracy of various measuring instruments

Measuring Instruments	Operating Range	Accuracy
Copper-constantan(T-type) thermocouple	-200 to 100°C	0.1 °C
U-tube manometer		0.1mm
Anemometer	0.1 to 20 m/s	0.1m/s

Total uncertainty of the experiment

$= \text{ square root of } \{(\text{uncertainty in measuring ambient temperature}, T_\infty)^2$

$+ \ ((\text{uncertainty in measuring temperature at selected probe points}, T_{ij})^2$

$\times \ \text{No. of probe points}(23)) \ + \ (\text{uncertainty in measuring Pressure}, P_m)^2$

$+ \ (\text{uncertainty in measuring Velocity at inlet}, V_{in})^2$

$+ \ (\text{uncertainty in measuring Thermal Conductivity}, k)^2\}$

$$= \text{ square root of } \{0.5^2 + (0.5^2 \times 23) \ + \ 3^2 + \ 4^2 + \ 2^2\}$$

$$= \text{ square root of } (35) = \pm 5.916\%$$

Thus, the total uncertainty for the experiment was obtained to be ± 5.916%. Table 3.5 shows all the relevant data.

Table 3.5 Data of experimental measurement accuracy and uncertainty

Measured Parameter	Measurement Accuracy	Uncertainty (%)
Ambient temperature (T_∞)	± 0.1 °C	± 0.5
Temp. at selected probe points (T_{ij})	± 0.1 °C	± 0.5
Pressure (P_m)	± 1 Pa	± 3
Velocity at inlet (V_{in})	± 0.1 m/s	± 4
Thermal Conductivity (k)	± 0.0001 W/m-K	± 2

3.7. SAMPLE CALCULATIONS

In order to calculate convective heat transfer rate and j factor following calculations have been made: (For baseline case)

The hydraulic diameter is given by

$$D_h = \frac{4A_c}{P_w} \qquad (i)$$

Where A_c represents the cross-sectional area for fluid flow and P_w represents the wetted surface perimeter

So,

$$D_h = \frac{4 \times (width\ of\ fin\ plate \times fin\ pitch)}{2 \times (width\ of\ fin\ plate + fin\ pitch)}$$

$$D_h = \frac{4 \times (200 \times 12)}{2 \times (200 + 12)} = 22.64\ mm$$

The kinematic viscosity is given by

$$\nu = \frac{\mu}{\rho} \qquad (ii)$$

and Reynolds number based on hydraulic diameter is given by

$$Re = \frac{uD_h}{\nu} \qquad (iii)$$

Where u represents the inlet velocity of air, ν represents kinematic viscosity of air, μ and ρ were dynamic viscosity and density of air respectively.

So, for u = 4m/s & $\nu = 1.516 \times 10^{-5}$ m^2/s (at 20°C air temp.), equation (iii) yields

$$Re = \frac{4 \times 22.64 \times 10^{-3}}{1.516 \times 10^{-5}} = 5974$$

Now, Q represents the total heat transfer rate to the air, m is mass flow rate of working fluid, $T_{,m,out}$ is the temperature of the fluid at the outlet, $T_{,m,in}$ is the temperature of the fluid at the inlet, T_{wall} is the temperature of the wall, c_p is specific heat of working fluid

$$Q = \dot{m}.c_p.\left(T_{m,out} - T_{m,in}\right) \qquad (iv)$$

$$Q = \left(\rho \times \dot{V}\right).c_p.(T_{m,out} - T_{m,in})$$

$$Q = (\rho \times A_c \times u).c_p.\left(T_{m,out} - T_{m,in}\right) \qquad (v)$$

Using $T_{m,in}$ = 293 K, $T_{m,out}$ = 293.401 K and c_p=1007 J/kg-K, ρ = 1.204 kg/m^3 (for air at 20°C), equation (v) yields

$$Q = (1.204 \times (200 \times 10^{-3} \times 12 \times 10^{-3}) \times 4) \times 1007 \times (293.401 - 293)$$
$$= 4.668\ W$$

And the temperature difference has been defined according to the Equation (12) as

$$\Delta T_M = \frac{(T_{m,wall} - T_{m,in}) - (T_{m,wall} - T_{m,out})}{\ln \frac{(T_{m,wall} - T_{m,in})}{(T_{m,wall} - T_{m,out})}} \qquad (vi)$$

Using $T_{m,wall}$ = 298.255 K, $T_{m,in}$ = 293 K, $T_{m,out}$ = 293.401 K, equation (vi) yields

$$\Delta T_M = \frac{(298.255 - 293\ ) - (298.255 - 293.401)}{\ln \frac{(298.255 - 293)}{(298.255 - 293.401)}} = 5.05\ K$$

So, the convective heat transfer coefficient

$$h = \frac{Q}{A_S.\Delta T_M} \qquad (vii)$$

Where Q is the total rate of heat transfer to the air, and A_s is the total surface area of heat transfer.

Now,

$$A_s = 2 \times \{(Length\ of\ fin\ plate \times width\ of\ fin\ plate) + (Length\ of\ fin\ plate \times fin\ thickness) + (Width\ of\ fin\ plate \times fin\ thickness)\}$$

$$A_s = 2 \times \{(300 \times 200) + (300 \times 12) + (200 \times 3)\}$$

$$A_s = 123000\ mm^2$$

So, using A_s = 123000 mm^2, Q = 4.668 W and ΔT_M = 5.05 K, equation (vii) yields

$$h = \frac{4.668}{(123000 \times 10^{-6}) \times 5.05} = 7.51 W/m^2K$$

The Nusselt number has been defined as follows:

$$Nu = \frac{h.D_h}{k} \qquad (viii)$$

Using k = 0.02514 W/m.K (for air at 20°C), h = 7.51 W/m^2K and D_h = 22.64 mm, equation (viii) yields

$$Nu = \frac{7.51 \times (22.64 \times 10^{-3})}{0.02514} = 6.76$$

The Prandtl number has been defined as follows:

$$Pr = \mu.C_p/k$$

For air at 20°C, Pr = 0.7309

Besides, Colburn's factor 'j' represented the heat transfer capacity, has been defined as follows:

$$j = \frac{Nu}{Re.Pr^{1/3}} \qquad (ix)$$

Using Nu = 6.76, Re = 5974 and Pr = 0.7309 equation (ix) yields

$$j = \frac{6.76}{5974 \times 0.7309^{1/3}} = 0.00126$$

CHAPTER - 4

(PERFORMANCE OF RECTANGULAR WINGLET (LOCALIZED STUDY))

4.1. INTRODUCTION

The present investigations have been carried out in the three phases. In the very first phase, I focused my attention on studying the localized heat transfer augmentation, especially in the wake region. The present chapter discusses the improvement in the performance of the fin-tube heat exchanger in the wake region, using a rectangular winglet having a circular hole at its center, over the baseline case having no vortex generator. This chapter also explains the effects of punched holes on the surface of the rectangular winglet over the winglet having no punched hole. Finally, at the end of the chapter, a section has been added which compares the performance of the considered vortex generator in various configurations and suggests the optimum configuration of the vortex generator for maximum heat transfer augmentation and minimum flow resistance using various performance parameters.

4.2. EFFECT OF PUNCHED HOLE ON THE SURFACE OF THE WINGLET

In the present investigations a rectangular winglet with hole punched at the center has been considered as we can create hole of very small diameter only at the center of delta winglet while rectangular winglet does not have such limitation. It has been found that the form drag of winglet is mainly responsible for pressure drop and the main source of form drag is the recirculation zone that exists behind the winglet. Therefore, in order to reduce pressure drop, the recirculation zone should be reduced to as minimum as possible. This can be attained by punching a hole on the surface of the winglet. The presence of a hole in the winglet allows a path for the air stream to flow through it. When comparing with winglets without holes, the present case offers less resistance to airflow. This means that pressure drop in winglets with holes is lesser as compared to those without holes.

Figure 4.1 shows an enlarged view of the winglet with velocity contours embedded on the same. An arbitrary plane passing from the center of the hole has been taken and flow streamlines have been plotted. Considering the CFD case at a downstream position, some inferences could be drawn. It can be observed from figure 4.2 that Performance Evaluation Criterion, PEC (1) = (j/ f) (where j and f are the colburn's factor and friction factor) for CFD_D case with winglet having punched hole at the center, is higher up to 65% as compared

to the winglet without any hole. It is because the previous case offers less resistance to airflow than the later and thus is a better choice for use in the heat exchangers.

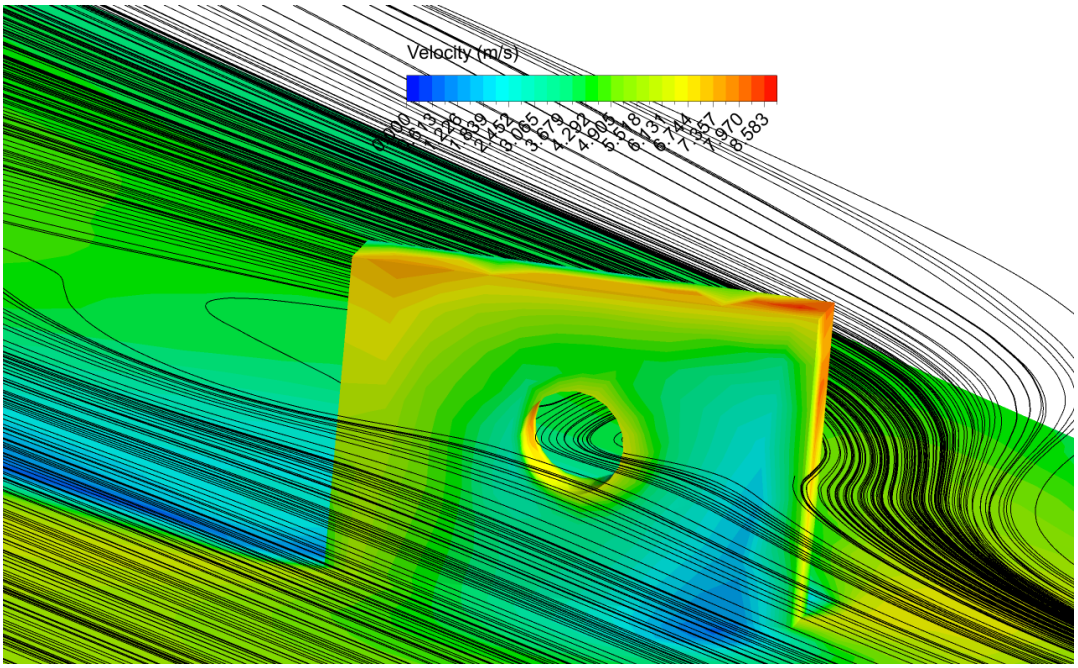

Figure 4.1 Airstreams passing through punched hole depicted on velocity contour for CFD down case at 6 m/s velocity (flow R-L)

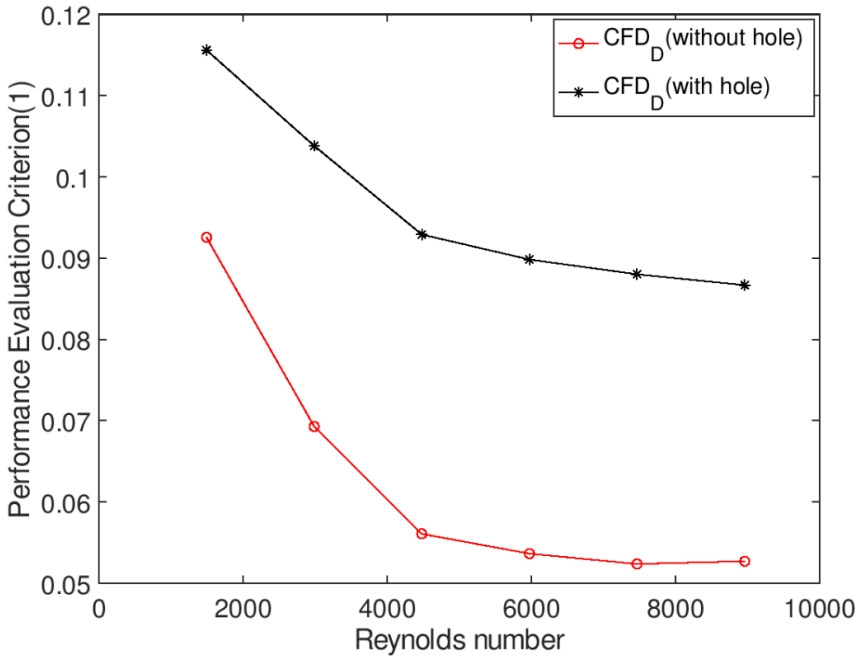

Figure 4.2 Variation of Performance Evaluation Criterion with Reynolds no.

4.3. EFFECT OF USING WINGLET, ON THE WAKE REGION OF TUBE

Simulations were performed on all of the four cases (i.e. Common Flow Down (CFD) and Common Flow Up (CFU) configuration at downstream as well as upstream location i.e. CFD_D, CFU_D, CFD_U, CFU_U configurations), and pressure drops as well as temperature values, were noted for all the cases respectively using the probe tool. For taking measurements of temperature, two points were taken for probing the respective values in all the cases. One point (Point A) was 32 mm away from the tube center radially and located at the intersection of winglet center and tube center, the same point as that taken during experimentation using a thermocouple and the second point (Point B) was a random point taken downstream of the tube. The same has been depicted in the fig. 4.3. This point happened to lie after the winglets in all of the four cases. In case of the common flow down at downstream position, the point was right near the region where the formation of vortices was most pronounced. The reason behind making such a selection of point location was to study the effect of vortex formation on temperature values over the plate. In other words, the motive was to study the effect of winglets on heat transfer from the plate.

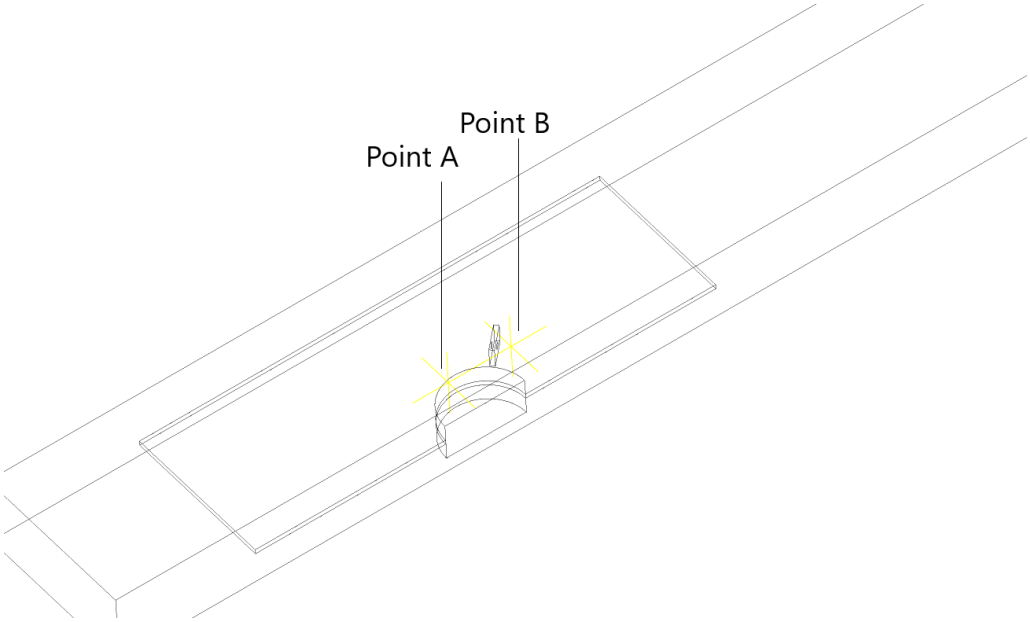

Figure 4.3 Depiction of probe points A and B

Figure 4.4 shows temperature contours for 4 m/s velocity for CFD_D configuration. Figure 4.5 shows pressure contour and figure 4.6 shows flow streamlines mapped over velocity contour for the same case. The temperature of the surface of the tube at steady state for this case is 302.89K.

One of the primary motives of this study is to analyze the pressure drop between two terminating edges of the fin plate. Manometer readings were taken at the center of the terminating edges of the plate in order to find the pressure drop. As a result, similar points were probed during post-processing for validation of numerical results.

The concept behind pressure drop is attributed to a few factors as may be explained. The free air stream enters the domain and approaches the fin plate which is at a higher temperature than ambient temperature due to heat transfer from the tube. As soon as air reaches the fin plate, it encounters a stagnation point where velocity energy nearly becomes zero. According to Bernoulli's principle, loss of velocity energy is tantamount to an increase in pressure energy. Thus, there is a high-pressure zone at the start of the fin plate as may be visible in figure 4.5. As air approaches the course of the plate, there is a gain in velocity energy and a loss of pressure energy. It again encounters an obstruction inflow from the tube which results in the decrement of velocity energy and gain in pressure energy. Moving further, air encounters the winglet in its path of flow. Winglet again causes a decrement in velocity energy and increment in pressure energy. A high-pressure region may be visible where air encounters the winglet following which, there is an inception of an interesting phenomenon.

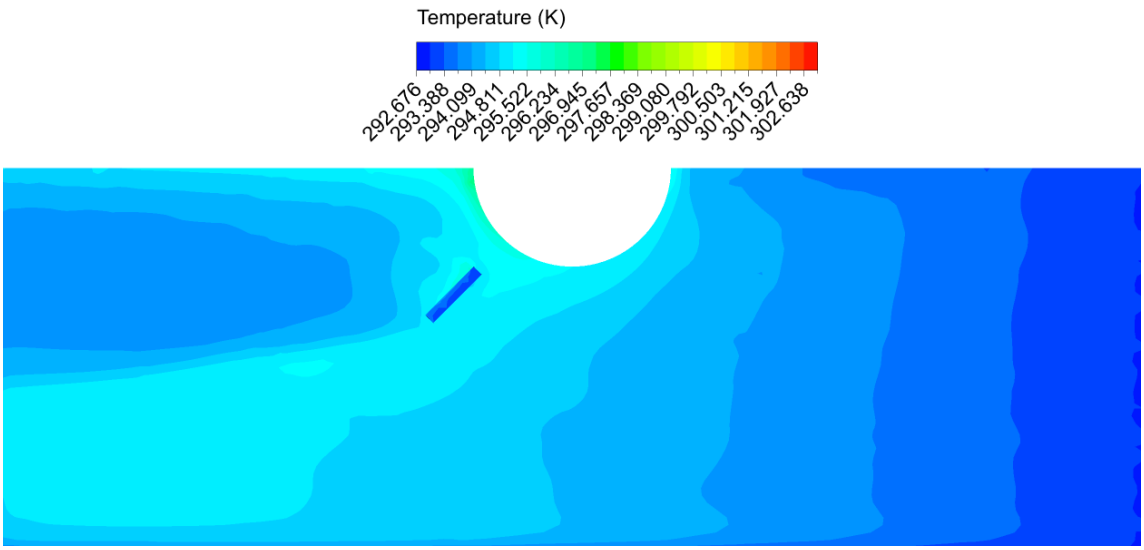

Figure 4.4 Temperature contour for CFD_D configuration at 4 m/s velocity

(flow Right to Left)

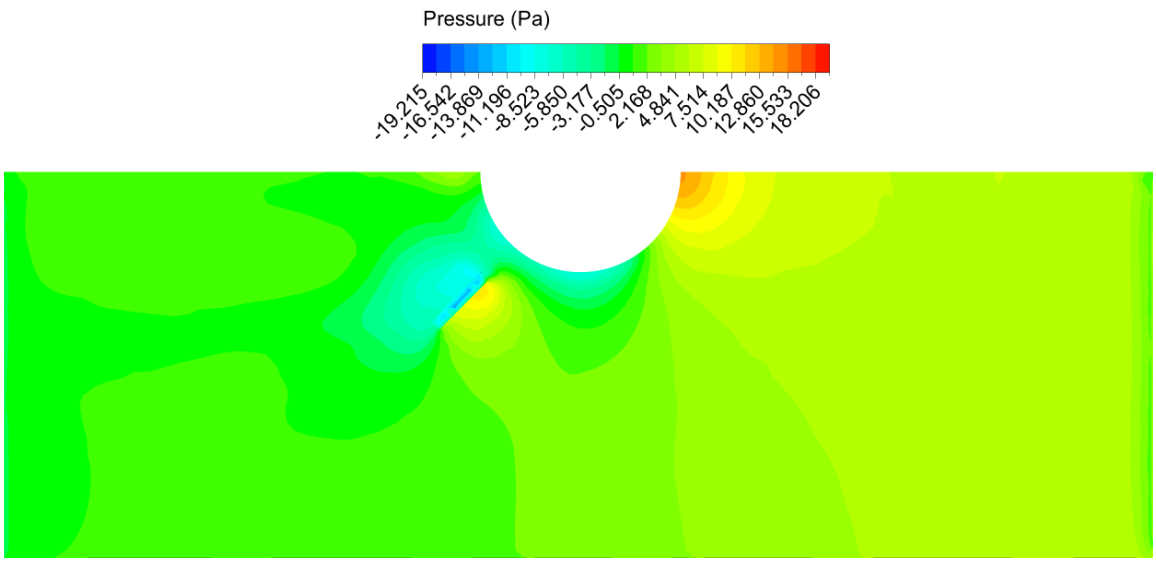

Figure 4.5 Pressure contour for CFD_D configuration at 4 m/s velocity

(flow Right to Left)

Being specific to CFD_D configuration wherein, the winglet is placed at 135 degrees to the horizontal, airstreams meet the vertex closest to the tube. Airstreams now have two directions to follow. Either they move towards their right-hand side or left-hand side. In the latter possibility, there is more resistance to flow as a result of which there is a high-pressure region. On the other hand, in moving towards the right-hand side, air streams

encounter lower resistance from the peripheries of the winglet due to which there is more velocity energy and less pressure energy. The concept of aerodynamics now comes into the picture. It may be seen that the edge of the winglet near the tube is shorter as compared to its adjacent edge. When air streams follow this edge, they encounter a break-in supporting flow path. This results in the inception of boundary layer separation. Pressure contours show a region of the negative high-pressure zone which means there should be some means for overcoming this negative pressure zone. Some streams of air tend to flow in the reverse direction in order to compensate for the negative pressure zone formed. Velocity streamlines shown in figure 4.6 indicate the mentioned fact. The formation of vortices results in the wake region as shown in figure 4.6. Farther from the wake region, airstream velocity is high. Due to disruption in flow caused by the winglet and subsequent formation of a wake region, there is a drop in pressure. Pressure drop varies with velocity of flow. Higher the flow velocity, the higher the pressure drop.

Moreover, it can also be observed that there are some area near to the tube where velocity of air is more than free stream velocity (i.e.4m/s in this case). This is the wake region near the tube, where more air will be pushed as a result of formation of vortices (resulting in turbulence) due to the winglet. This can be well understood from figure 4.6.

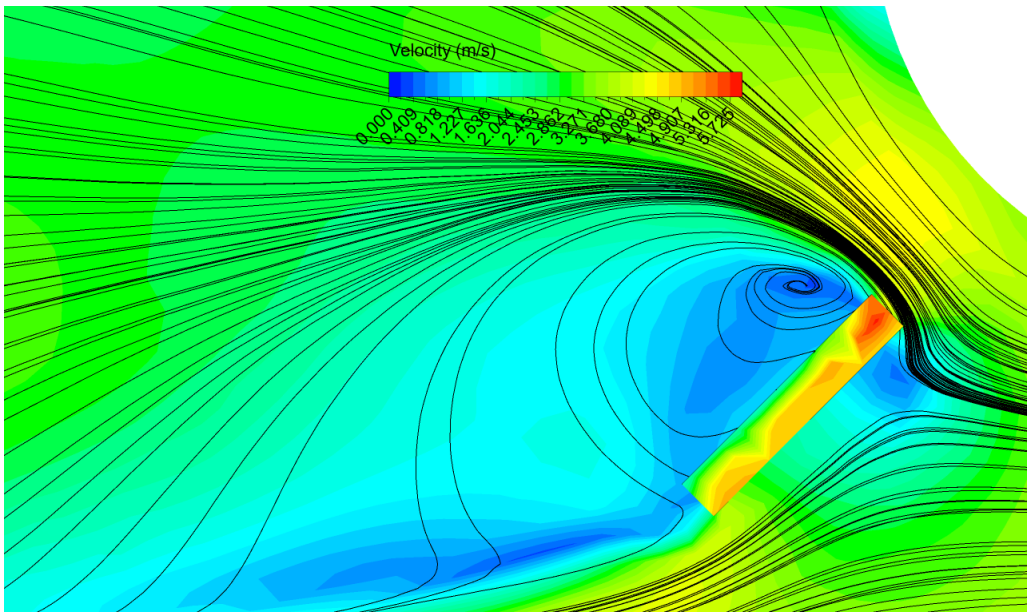

Figure 4.6 Velocity contour and streamlines for CFD_D configuration at 4 m/s velocity (flow Right to Left)

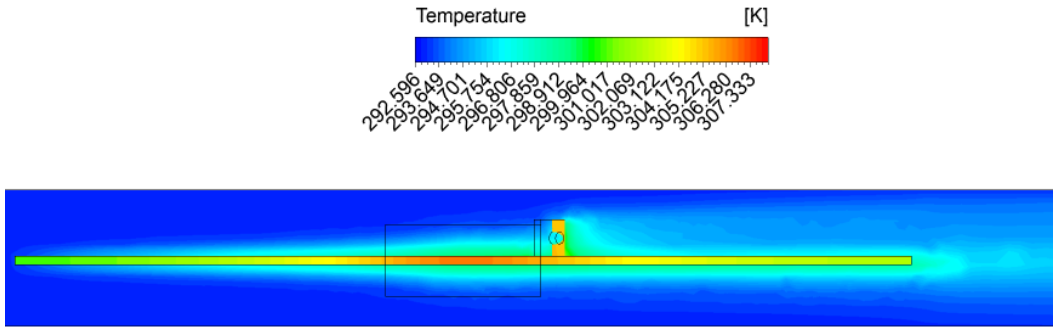

Figure 4.7 Temperature contour mapped on a vertical plane for CFD_D configuration at 1m/s velocity (flow Left to Right)

It is evident from the above figures that the rate of heat transfer improves as the velocity of flow increases. This is expected because of an increase in the convective heat transfer coefficient due to an increase in airflow velocity. It can be observed that the surface of the fin plate is cooler towards the upstream side at the start of the plate, as air enters nearly at ambient temperature. As air progresses towards the tube, from where heat is being generated, it certainly gets hotter due to contact with both, heated plates and tubes. The winglet has a non-uniform temperature contour due to heat transfer to airflow. As we move vertically upwards of the winglet, temperatures may be seen to decrease as compared to the vertically downward part of the same. This may be supported by figure 4.7 and explained as such: temperature of air stream flowing near the plate is higher than that of air stream flowing at some distance above the plate. As a matter of fact, the cooler air stream has more potential to gain heat from the winglet as compared to the hotter air stream. As a result, one observes the uneven temperature contour on the surface of the winglet. An interesting point to note is that temperature right after the winglet in each of the cases is higher than the adjacent regions. This is due to the formation of a wake region due to boundary layer separation as soon as airstream encounters the winglet. Velocity contours shown in figure 4.6 would make the explanation clearer. Figure 4.4 clearly highlights the high-temperature zone formed right after the winglet and subsequent formation of a relatively lower temperature zone after the wake region.

Figures 4.8 to 4.16 show temperature contours, pressure contours and velocity streamlines for all the four configurations at 4 m/s velocity except for CFD_D configuration as it has been already presented in the above figures. The characteristic variations in flow patterns due to the positioning of winglets in different cases and the resulting effects on pressure, temperature and velocity regimes may be observed.

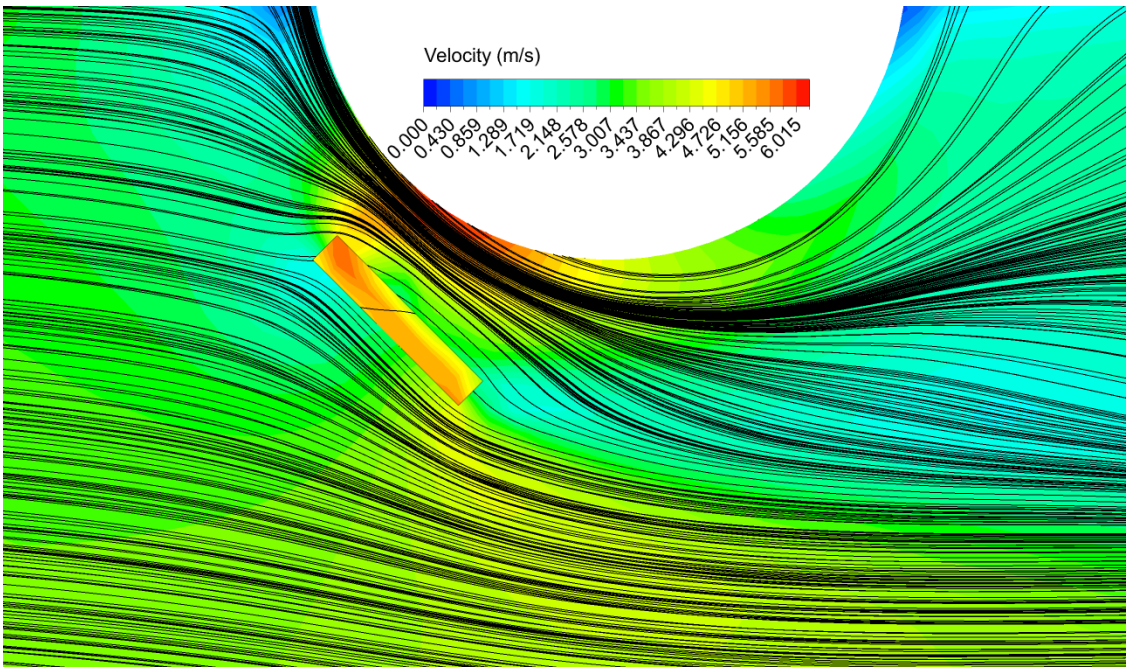

Figure 4.8 Velocity contour with streamlines for CFD_U configuration at 4m/s velocity (flow Left to Right)

Figure 4.8 shows the streamlines of airflow at 4 m/s velocity near the winglet and tube region in CFD_U configuration. An interesting observation has been made in this particular case. As might be evident from the figure, there is no formation of vortices anywhere near the winglet, as opposed to the other three cases. This could be attributed to more than one factor. Firstly, the orientation of the winglet is such that it is in alignment with the tube. As a result, when air streams turn towards the tube, they get a uniform path of flow to proceed further. For vortices to be formed, there should be an appreciable amount of obstructions in the flow path and also, there should be a boundary layer separation

resulting in the formation of wake region. In this case, due to the characteristic flow path offered by the alignment of the winglet and tube, there is an adequate amount of airflow directed towards the potential wake region. We know that the region of the wake is formed when a zone of pressure difference gets formed. Flow conditions, in this case, negate the zone of pressure difference from being formed as an outcome of which, there are no vortices. Moreover, the temperature of the surface of the tube at steady state for this case is 302.824K.

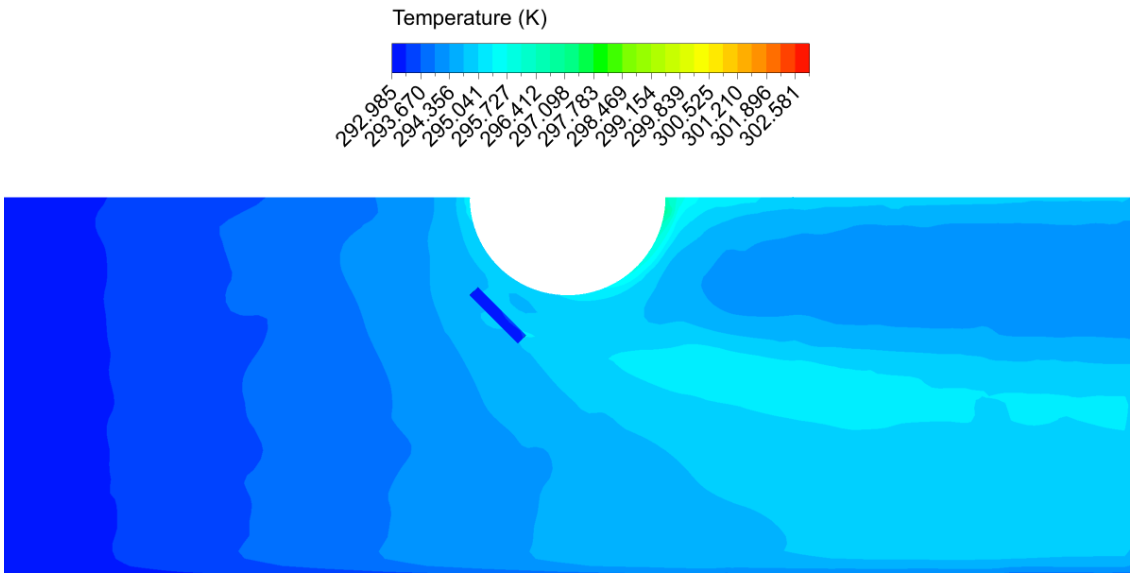

Figure 4.9 Temperature contour for CFD_U configuration at 4m/s velocity (flow Left to Right)

It can also be observed that there are some area near to the tube where velocity of air is more than free stream velocity (i.e.4m/s in this case). This is the wake region near the tube where more air will be pushed as a result of formation of vortices due to the winglet. Additionally, there is also some area where velocity of air is more than free stream velocity. It is also because of the formation of vortices, as a result of which more air will be pushed in that region. Figure 4.11explains the above mentioned fact.

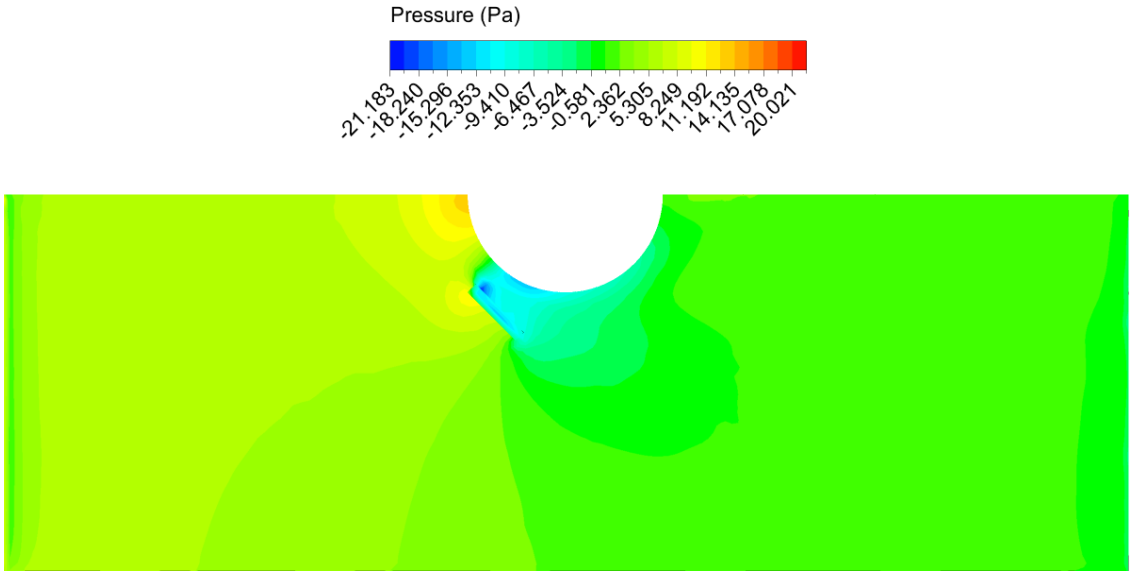

Figure 4.10 Pressure contour for CFD_U configuration at 4m/s velocity (flow Left to Right)

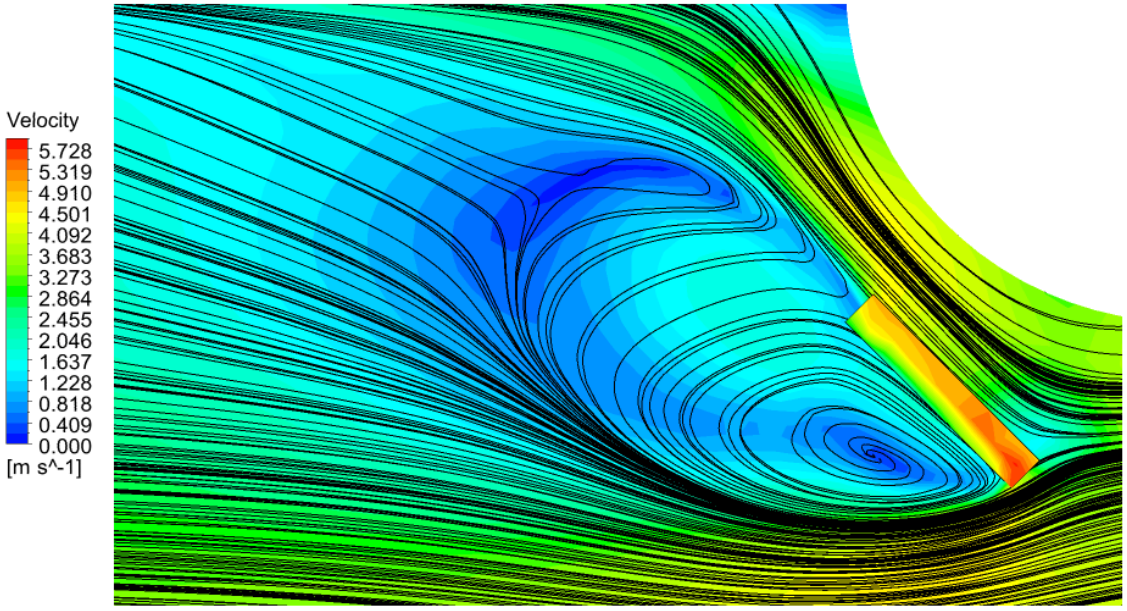

Figure 4.11 Velocity contour with streamlines for CFU_D configuration at 4m/s velocity (flow Right to Left)

The basic reason why using a winglet is beneficial in a fin tube heat exchanger is because it certainly offers a more effective surface area for better convection. One of the other motives of employing winglets on fin tube heat exchangers is to delay the formation of a wake region. In a similar heat exchanger without winglets, air streams encounter the bulge of the tube which leads to the formation of wake region immediately after that. When a winglet is present on a plate, either upstream or downstream of the tube, some obstruction gets offered to the airflow which leads to delay in the formation of the wake region. It is desirable to delay the wake region as much as possible because heat transfer in the wake region is the lowest. This could be attributed to the high negative pressure zone being formed with a minimum velocity of air streams. As mentioned above, lower the velocity of air flowing through region under consideration, more would be the temperature in that zone.

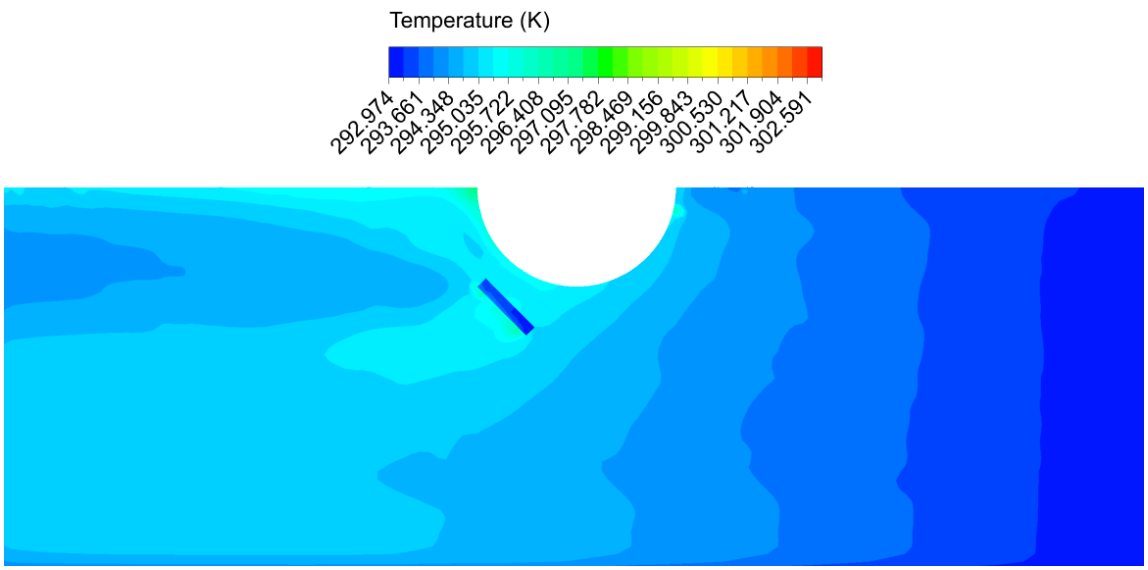

Figure 4.12 Temperature contour for CFU_D configuration at 4m/s velocity (flow Right to Left)

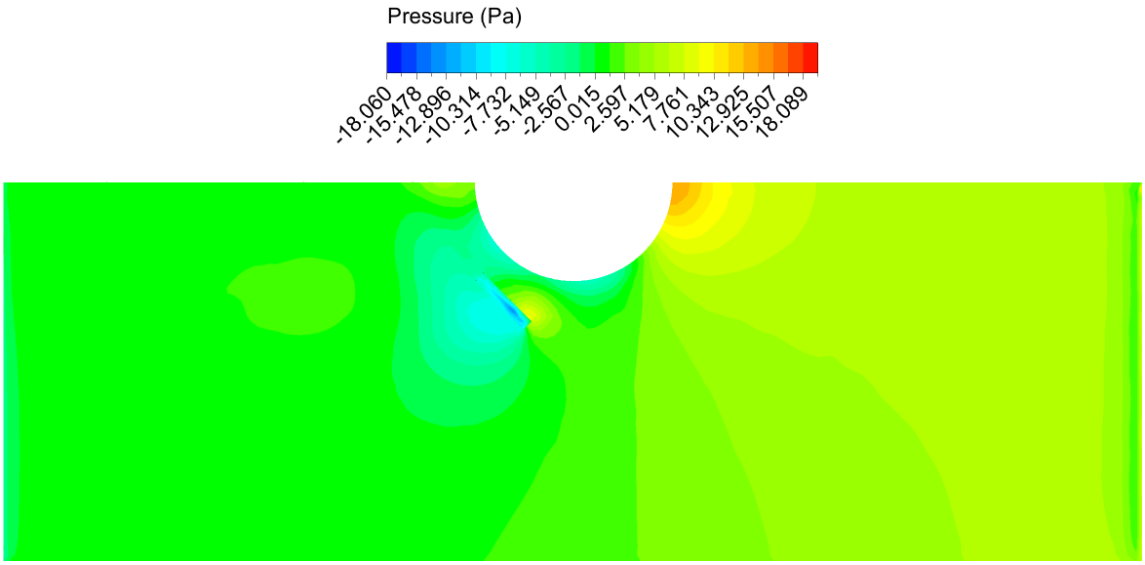

Figure 4.13 Pressure contour for CFU_D configuration at 4m/s velocity (flow Right to Left)

Being more specific to the results it translates to, the temperature at point A (figure 4.3) for 4 m/s flow velocity for CFD_U configuration is 294.758 K, as compared to 295.011 K, 294.997 K and 294.915 K for CFD_D, CFU_U and CFU_D configuration respectively. At Point B (figure 4.3), the temperature in CFD_U configuration is 294.216 K as compared to 294.778 K, 294.753 K and 294.3 K for CFD_D, CFU_U and CFU_D configuration respectively. CFD_U configuration offers the lowest temperatures at the two probe points of interest. Figure 4.9 shows the desired temperature contour for validation.

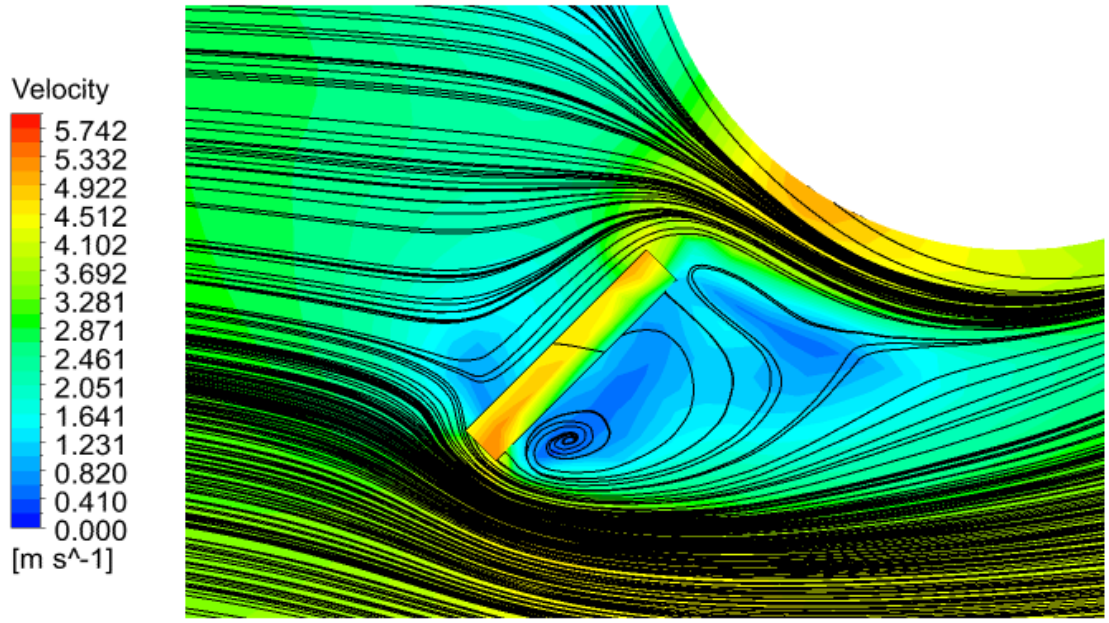

Figure 4.14 Velocity contour with streamlines for CFU_U configuration at 4m/s velocity (flow Left to Right)

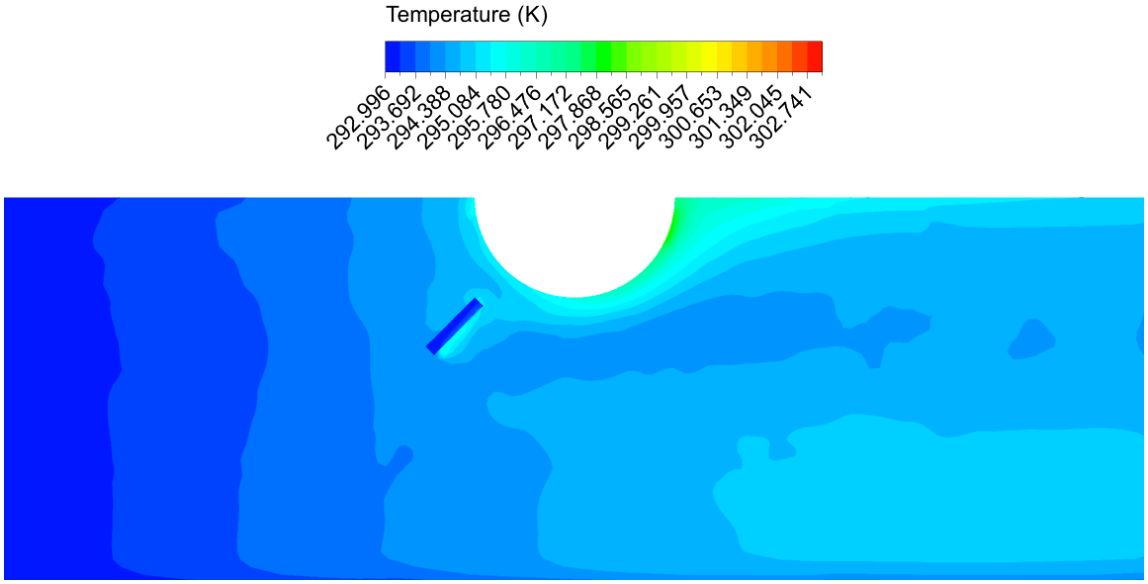

Figure 4.15 Temperature contour for CFU_U configuration at 4m/s velocity

(flow Left to Right)

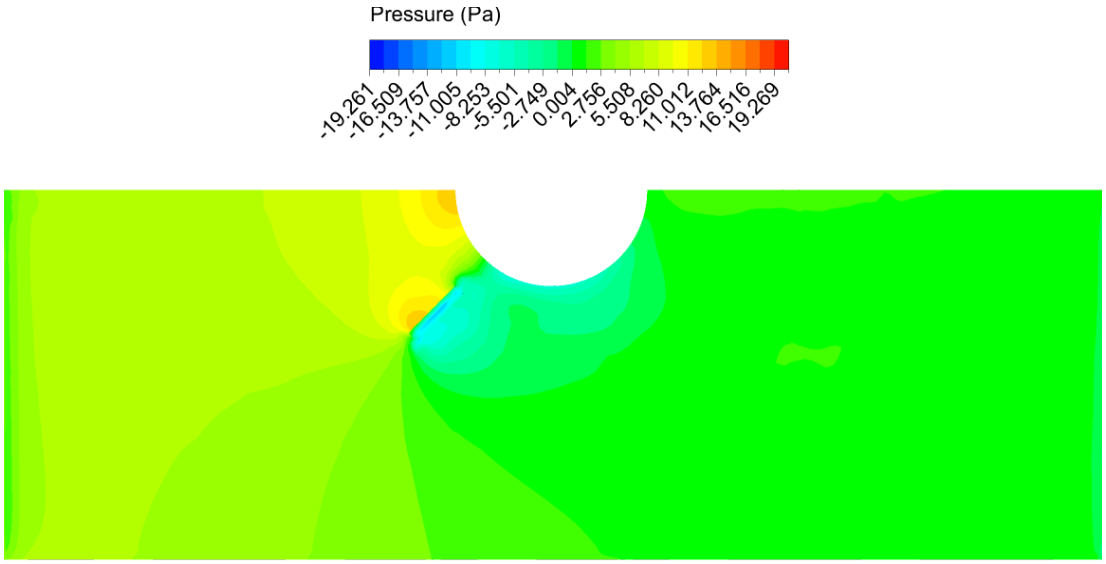

Figure 4.16 Pressure contour for CFU_U configuration at 4m/s velocity (flow Left to Right)

4.4. SELECTION OF OPTIMUM CONFIGURATION

The present section discusses the effects produced on heat transfer characteristics and parameters such as convective heat transfer coefficient, Nusselt number, and Colburn's factor because of variations in orientation and location of the winglet. The effects on pressure drop and friction factor will also be talked about.

4.4.1. Heat Transfer Characteristics

Figure 4.17 shows a plot between the convective heat transfer coefficient and Reynolds number. CFD_U configuration has the highest value of the heat transfer coefficient. This is because of the peculiar flow path offered by the winglet in conjunction with the tube. CFU_U configuration follows the trend of the high heat transfer coefficient. CFU_U configuration is the only one in which airflow first encounters the face of the winglet

before being pushed to the wake region caused by the tube. This is the reason behind its high heat transfer coefficient. The difference between heat transfer coefficients offered by CFD_D configuration and CFU_D configuration is very small as a result of which, we need to look for other parameters for deciding the better one of these two. Nusselt number is directly proportional to the convective heat transfer coefficient and inversely proportional to the thermal conductivity, which is the same for all the cases. Thus, the variation of Nusselt number with Reynolds number (figure 4.18) follows the same trend as the convective heat transfer coefficient. It may be seen from the below two figures that the addition of a winglet in any configuration has a significant benefit over the baseline case with no winglet.

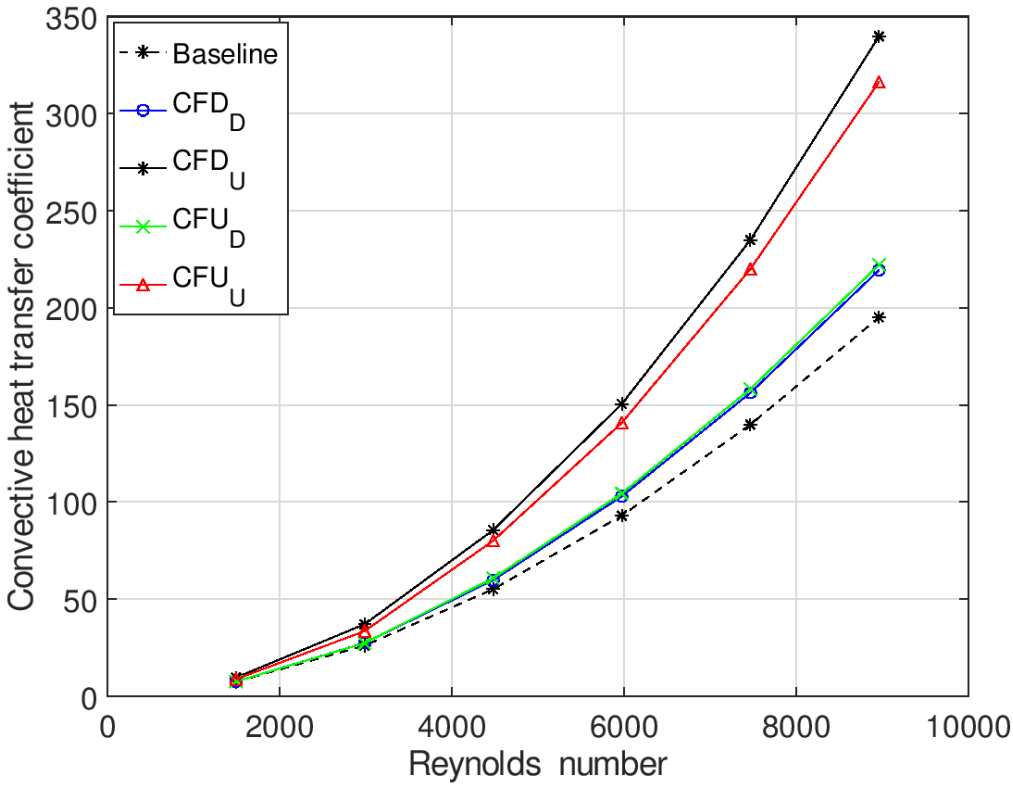

Figure 4.17 Variation of convective heat transfer coefficient with Reynolds number

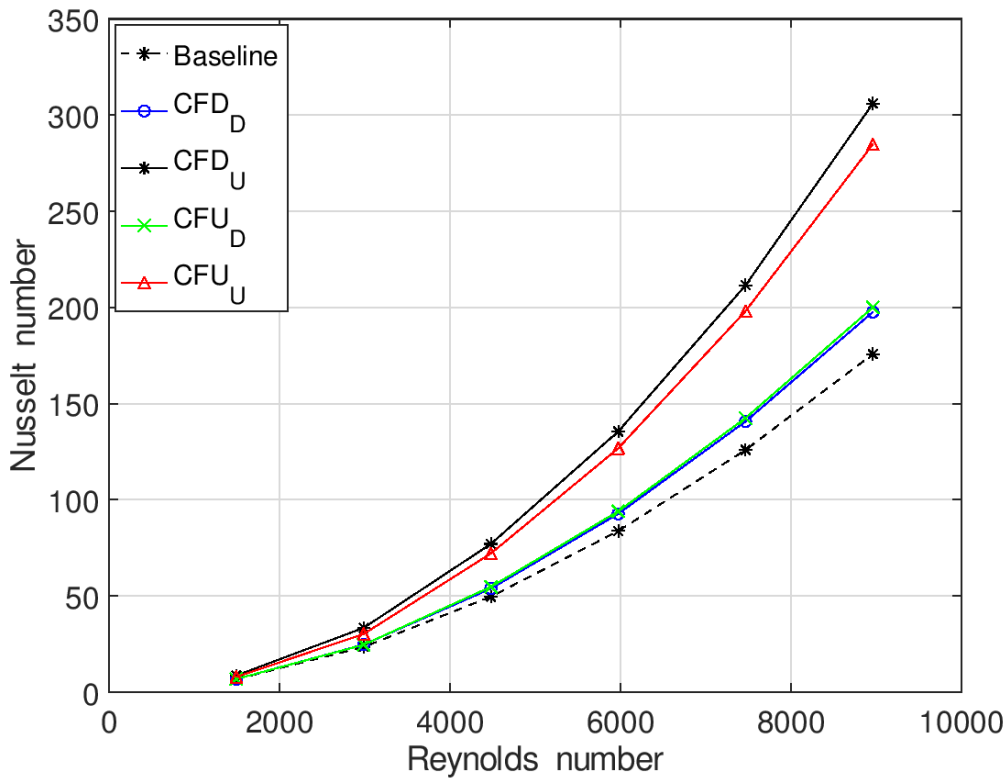

Figure 4.18 Variation of Nusselt number with Reynolds number

Colburn's factor considers Nusselt number as well as Prandtl number and is thus, a better measure of heat transfer characteristic than Nusselt number. Figure 4.19 shows the plot of Colburn's factor against Reynolds number. Although the trend of heat transfer efficiency among the four cases is similar to that shown by the plot of Nusselt number, there is rather a linear improvement in heat transfer characteristics with an increase in velocity of flow, as shown in the figure.

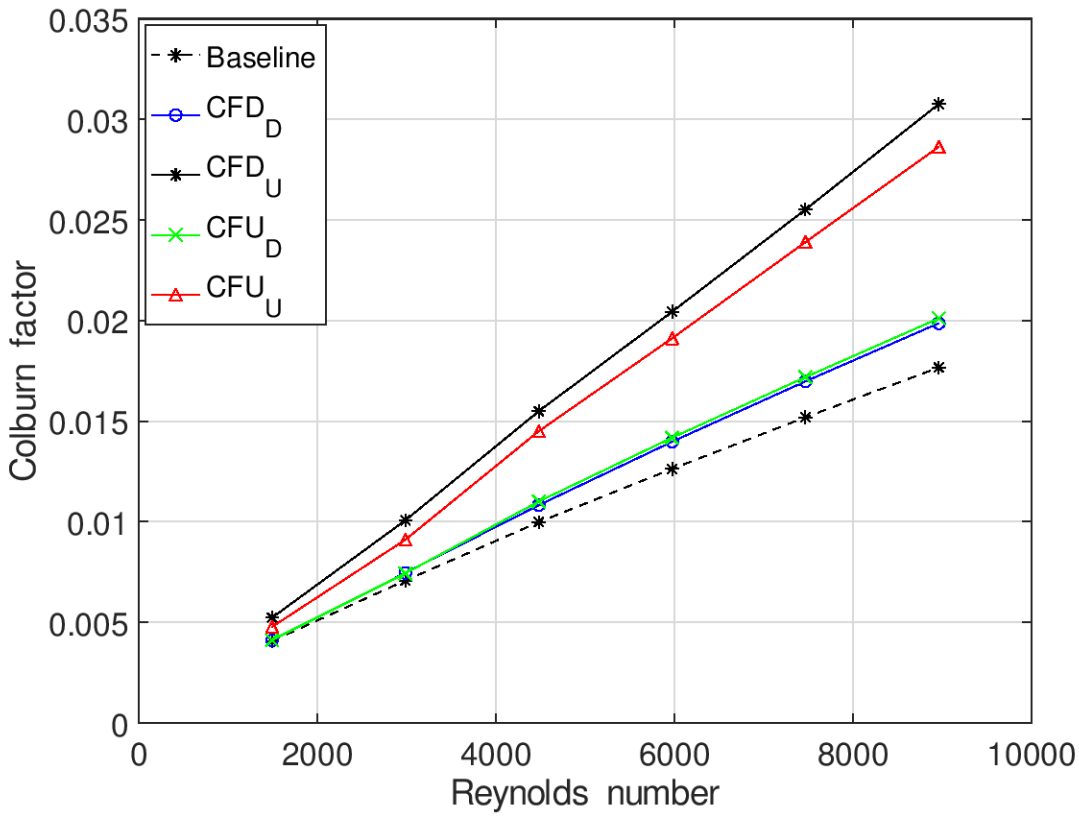

Figure 4.19 Variation of Colburn's factor with Reynolds number

4.4.2. Flow Resistance Characteristics

Figure 4.20 shows the variation of pressure drop with the Reynolds number. It is always desired that pressure drop in a heat exchanger be as minimal as possible. The only drawback of employing a winglet in the fin and tube heat exchanger is the increment in pressure drop. Thus, the configuration with the least pressure drop values out of the four would be desirable.

The average increase in the pressure drop value over baseline case for CFD_D, CFD_U, CFU_D and CFU_U configurations are 2.95%, 7.48%, 7.81% and 10.38% respectively for the considered range of Reynolds no. CFD_D configuration offers the least pressure drop while CFU_U configuration offers the highest pressure drop. Figure 4.5 could be interpreted for a suitable analysis. In CFD_D configuration, when air streams encounter the tube, they deviate from their free flow path and move further towards the winglet. Resistance to flow offered

by the winglet causes delayed vortices (as compared to baseline case). The point lies in the fact that although the winglet is causing resistance to flow, the presence of a hole allows a significant decrement in resistance. Another factor is that the winglet is aligned with its face away from the tube, which further causes a decrement in resistance. On the contrary, CFU_D configuration has its winglet aligned towards the tube because of which the pressure drop is higher than the CFD_D configuration. CFU_U configuration offers the highest pressure drop because the free airstream faces resistance upstream from both, the tube and winglet nearly at the same time.

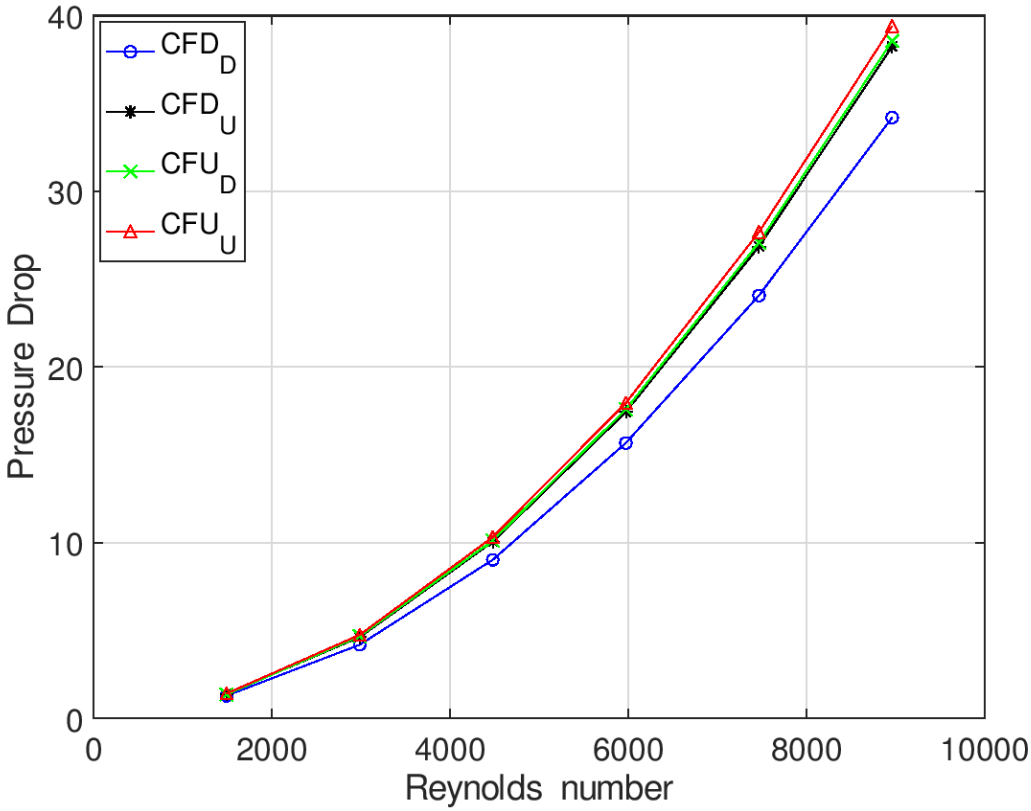

Figure 4.20 Variation of Pressure drop with Reynolds number

Figure 4.21 shows the variation of friction factor with Reynolds number. The friction factor is directly proportional to pressure drop and inversely proportional to the square of flow velocity. The friction factor decreases linearly and rapidly from 1m/s till

2m/s velocity and then follows a rather slower trend since it is a function of the squared exponent of velocity. As the velocity of flow increases, the viscous resistance decreases and thus, the friction factor decreases. The trend is quite similar to that shown by the plot of pressure drop in figure 4.20.

Moreover, it can also be observed from figure 4.21 that all the curves are almost parallel to each other. This may be attributed to the variation in pressure drop. As it can be observed from the plot of pressure drop with Reynolds number that increase in pressure drop with increase in Reynolds number follows almost the same trend for different configurations, the variation in friction factor also follows the same trend.

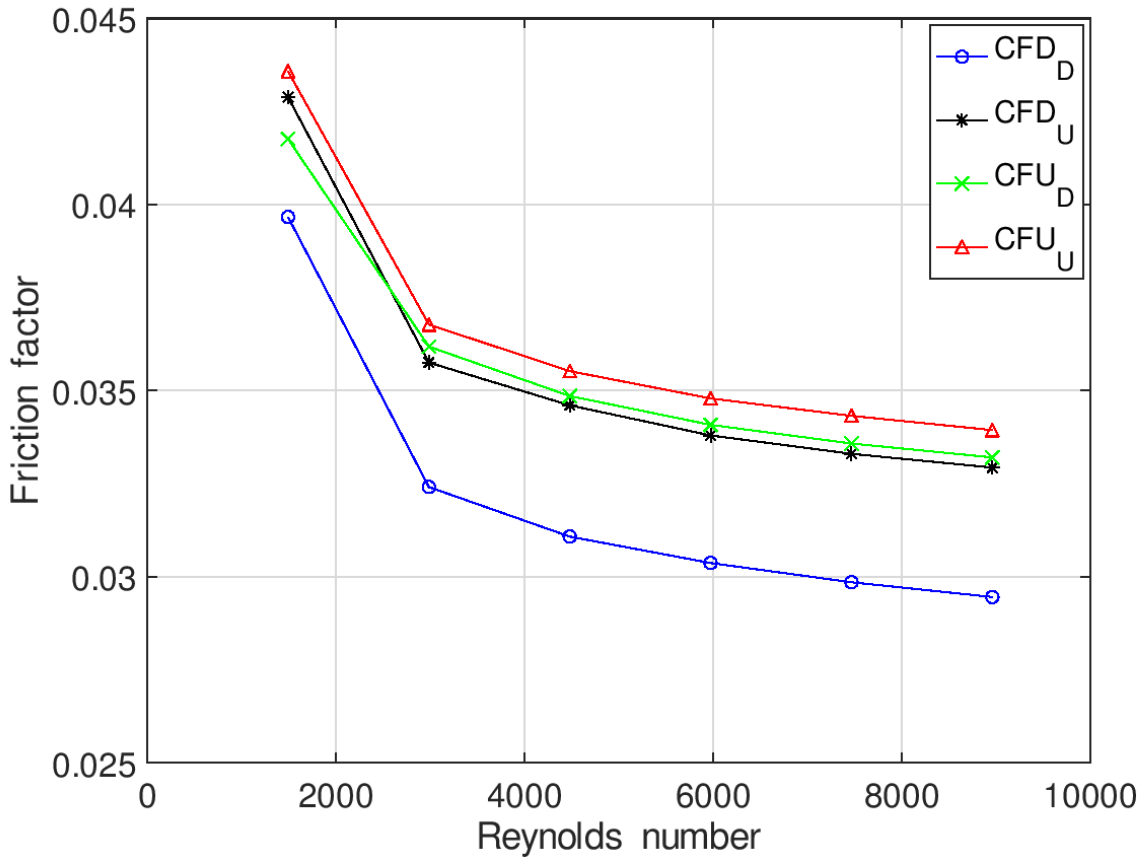

Figure 4.21 Variation of Friction factor with Reynolds number

4.4.3. Overall Thermohydraulic Performance

Overall thermohydraulic performance is the cumulative effect of thermal characteristics and flow resistance characteristics, and can be best assessed by the Performance Evaluation Criterion, PEC (2) = $(j/j_0)/(f/f_0)^{1/3}$ (where j and f are the Colburn's factor and friction factor respectively for the heat exchanger using winglet, while j_o and f_o are the same without using winglet i.e. the baseline case), also known as JF factor which is used to evaluate improvement over the baseline case. PEC takes into consideration, both the Colburn's factor and friction factor of the modified heat exchanger relative to the baseline heat exchanger without winglets. Higher the PEC, better will be the overall thermohydraulic performance and vice versa.

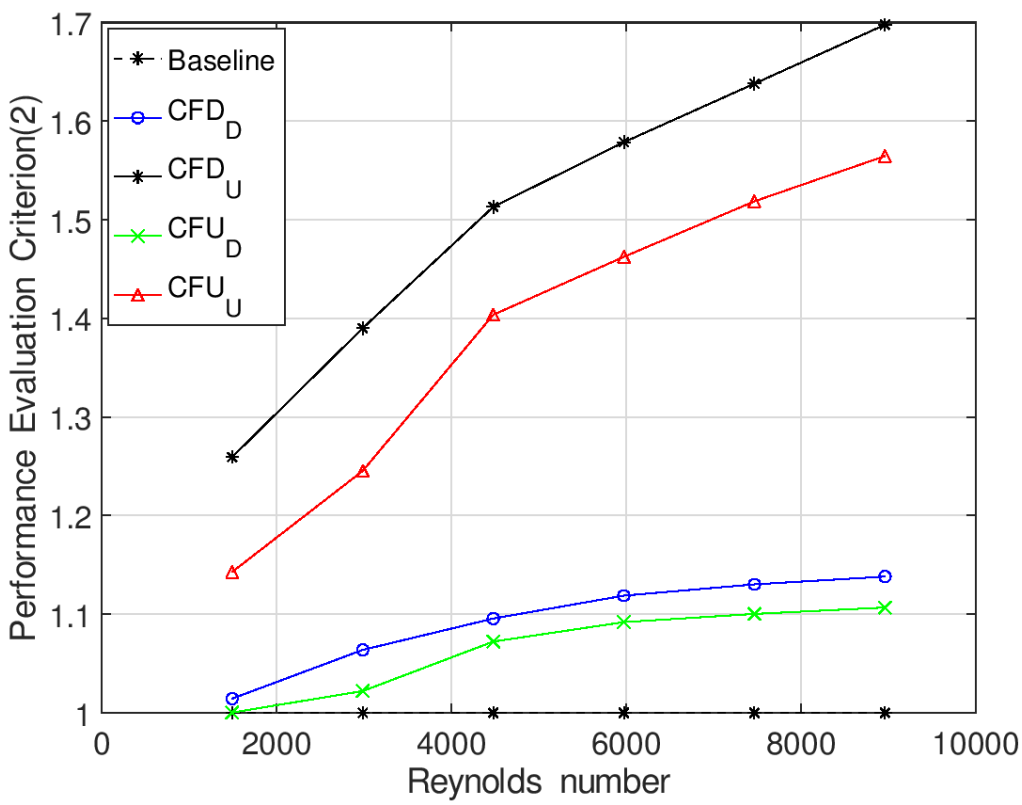

Figure 4.22 Variation of Performance Evaluation Criteria (PEC) with Reynolds number

Figure 4.22 shows the plot of performance evaluation criteria against Reynolds number. It can be observed that CFD_U configuration has the highest value of PEC followed by CFU_U configuration, CFD_D configuration, and CFU_D configuration respectively. CFD_U upstream case offers the best performance. CFD_U configuration exhibits the best thermohydraulic performance with an average improvement of 51.28% over the baseline case, whereas CFU_D configuration reported an average improvement of 6.56% over the baseline case for the same which is the lowest from among the considered configurations.

It could be seen that the upstream location of both the configurations offers better heat transfer enhancement as compared to a downstream location. For CFD configuration, located in upstream location the average improvement in overall thermohydraulic performance is 38.02% over the same located in downstream location. Similarly, for CFU configuration, located in upstream location the average improvement in overall thermo-hydraulic performance is 30.05% over the same located in downstream location.

It can also be interpreted that common flow down configuration offers better heat transfer enhancement than common flow up configuration. For winglet located in upstream location, CFD configuration gives an average improvement of 8.23% in overall thermohydraulic performance over CFU configuration. Similarly, for winglet located in downstream location, CFD configuration gives an average improvement of 2.54% in overall thermohydraulic performance over CFU configuration. This is in agreement with the literature studied (Md Salleh et al., 2018).

4.5. SUMMARY

- The main disadvantage associated with using the winglet is the induction of some pressure drop. To reduce this, winglets with punched holes as vortex generators have been used which improves the overall thermohydraulic performance by up to 65% for CFD_D configuration. Figure 4.2 can be referred for the same.

- CFD_D configuration provides the least value of pressure drop whereas CFU_U configuration has the maximum pressure drop. The average increase in the pressure drop for CFU_U configuration is of the order of 13.74% over CFD_D configuration for the considered range of Reynolds no. Figure 4.20 can be referred for the same.

- CFD_U configuration provides maximum augmentation in heat transfer characteristics with an average improvement of 55% over the baseline case for the considered range of Reynolds no. Figure 4.19 can be referred for the same.

- Winglet located in the upstream position exhibits better thermal performance as compared to a downstream position irrespective of its configuration. For CFD configuration, located in upstream location the average improvement in thermal performance is 42.83% over the same located in downstream location. Similarly, for CFU configuration, located in upstream location the average improvement in thermal performance is 31.07% over the same located in downstream location. Figure 4.19 can be referred for the same.

- Overall thermohydraulic performance is the cumulative effect of thermal characteristics and flow resistance characteristics which have been assessed by Performance Evaluation Criterion (PEC) also known as the JF factor. CFD_U configuration exhibits the best thermohydraulic performance with an average improvement of 51.28% over the baseline case, whereas CFU_D configuration reported an average improvement of 6.56% over the baseline case for the same which is the lowest from among the considered configurations. Figure 4.22 can be referred for the same.

- Winglet located in CFD configuration reported superior thermohydraulic performance than CFU configuration irrespective of whether it is located upstream or downstream. For winglet located in upstream location, CFD configuration gives an average improvement of 8.23% in overall thermohydraulic performance over CFU configuration. Similarly, for winglet located in downstream location, CFD configuration gives an average improvement of 2.54% in overall thermohydraulic performance over CFU configuration. Figure 4.22 can be referred for the same.

- Winglet located in the upstream position exhibits better thermohydraulic performance as compared to a downstream position irrespective of its configuration. For CFD configuration, located in upstream location the average improvement in overall thermohydraulic performance is 38.02% over the same located in downstream location. Similarly, for CFU configuration, located in upstream location the average improvement in overall thermohydraulic performance is 30.05% over the same located in downstream location. Figure 4.22 can be referred for the same.

CHAPTER - 5

(PERFORMANCE OF RECTANGULAR WINGLET (GLOBAL STUDY))

5.1. INTRODUCTION

In the next phase of the investigations, I focused my attention on studying the globalized effect of employing a rectangular winglet having a punched hole at its center as the vortex generator, i.e. the whole of the fin-plate has been considered for the analysis. Firstly, the effect of orientation of the vortex generator has been presented and afterward the effect of the location of the same has been discussed in detail. Lastly, at the end of the chapter, a section has been added which compares the performance of the considered vortex generator in various configurations and suggest the optimum configuration of vortex generator, for maximum heat transfer augmentation and minimum flow resistance using various performance parameters (i.e. Colburn's factor (j), friction factor (f) and performance evaluation criterion (PEC) = $(j/j_0)/(f/f_0)^{1/3}$)

5.2. EFFECT OF ORIENTATION

A comparison between two orientations of common flow up and common flow down is being drawn here on the basis of two important performance parameters viz., Colburn's factor over the fin-plate surface and pressure drop across two terminating faces of the fin-plate.

5.2.1. Flow Resistance Characteristics

Fig. 5.1 shows a variation of pressure drop with Reynolds number for the two mentioned cases. CFU orientation shows a higher pressure drop than CFD and the difference between the same tends to increase as we move up the range of Reynolds number values. The average increment of pressure drop in CFU orientation over CFD is 10.28% and reasons for the same could be investigated from pressure contours plotted over the fin-plate surface, as shown in fig. 5.2 & fig. 5.3. Pressure contours show how airflow interacts with the stagnation zone offered by tube and winglet in its path. In the case of CFU orientation, the alignment of the winglet is such that free airflow experiences stagnation zone from the face of longer edge. Due to a relatively larger stagnation zone as compared to CFD orientation, the high-pressure zone formed in CFU is larger in size, as can be

inferred from the region in red color near winglet. In a way, some of the airstreams first interact with the winglet and then are directed towards the tube in case of CFU and this results in another allied phenomenon. As shown in fig. 5.2, resulting stagnation zone formed in front of the tube becomes more pronounced due to interaction with the high-pressure zone created in front of the winglet. Resulting wake region due to flow moving past winglet involving negative pressures, formed behind the same is larger in case of CFU and there is some visible interaction between the wake flow phenomena of winglet and tube. On the contrary, the wake region formed behind winglet in CFD is smaller in size, as can be seen in fig. 5.3, in addition to meeker stagnation zones involved. This forms basis for higher pressure drop values in CFU orientation than CFD counterpart.

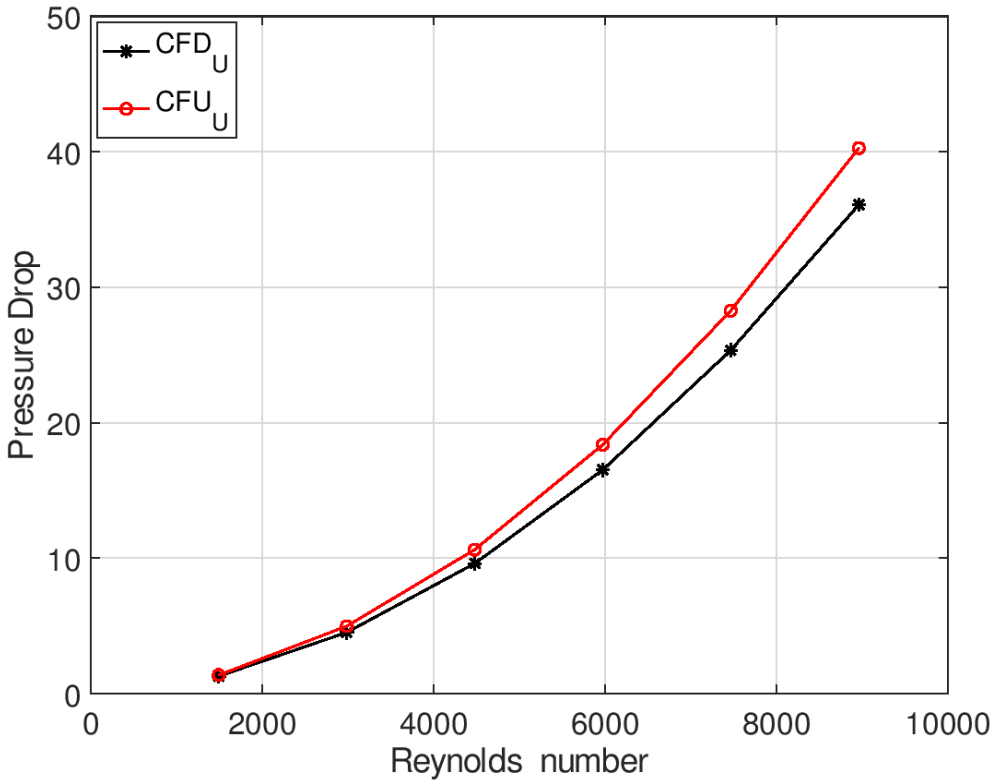

Figure 5.1 Variation of pressure drop with Reynolds number for CFU_U and CFD_U configurations

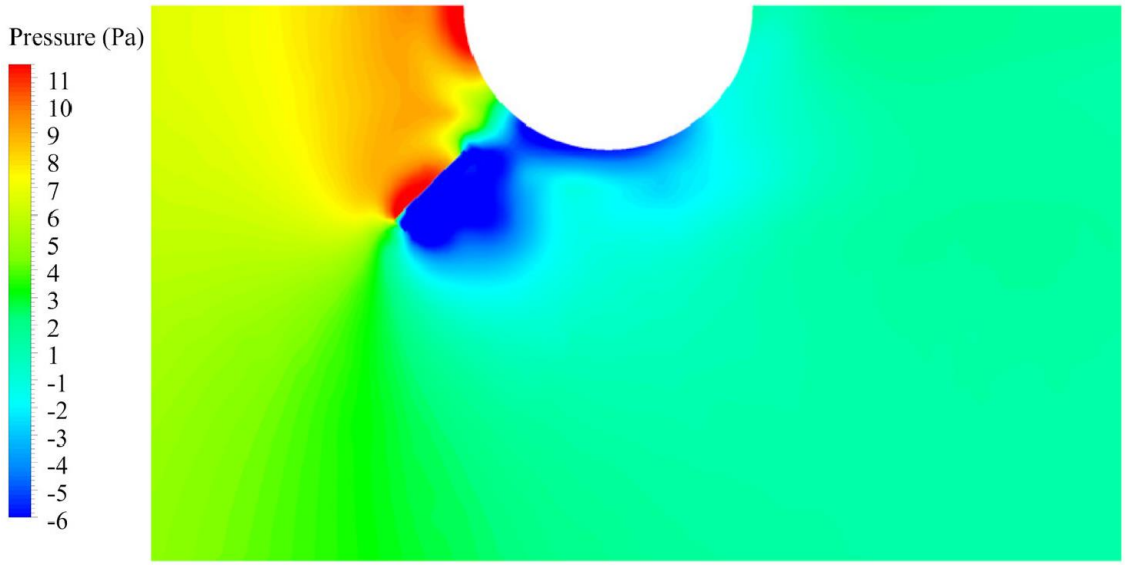

Figure 5.2 Pressure contours of CFU_U configuration and at inlet 4 m/s velocity

(flow Left to Right)

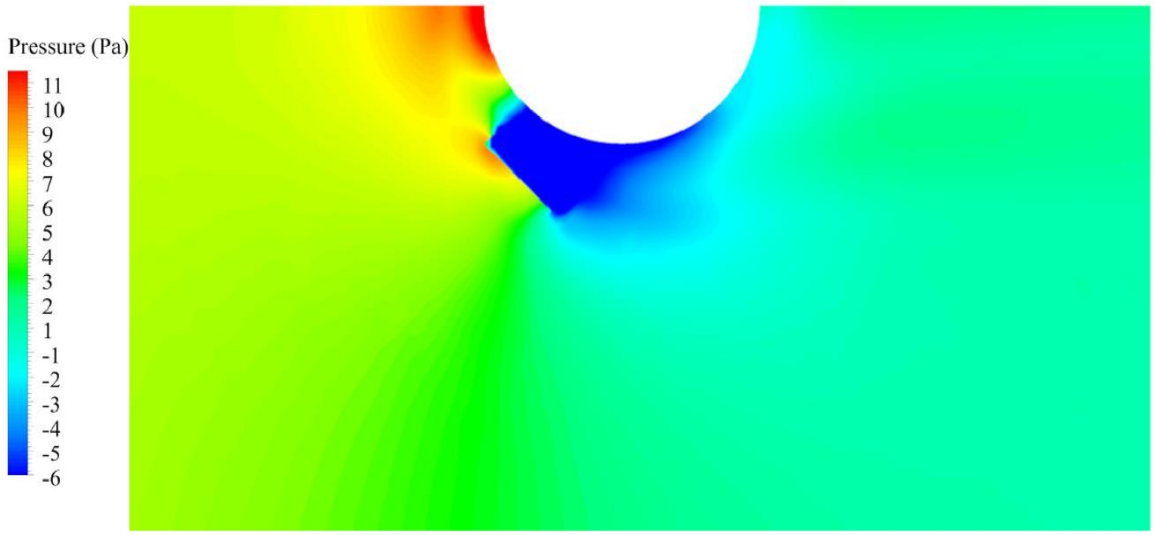

Figure 5.3 Pressure contours of CFD_U configuration at inlet 4 m/s velocity

(flow Left to Right)

5.2.2. Heat Transfer Characteristics

Fig. 5.4 shows a variation of Colburn's factor with Reynolds number for the two mentioned cases. It is quite evident from the plot of *j* versus *Re* that CFD orientation performs better as compared to CFU when it comes to thermal performance. There is an average improvement of 47.78% in Colburn's factor on the overall range of investigated Reynolds numbers on using CFD configuration with an increasing trend of improvement from the lowest to the highest value of *Re*. In order to analyze the reasons behind the same, insights may be drawn from fig. 5.5 and fig. 5.6 showing temperature contours drawn on plate surface for each of the two orientations at a flow velocity of 4 m/s. Due to a direct relationship between the two, velocity contours have been shown in fig. 5.7 and fig. 5.8 corresponding to fig. 5.5 and fig. 5.6 respectively for presenting a better elucidation of temperature contours. Airflow is seen to slow down at regions of hindrance caused by winglet and tubes. Due to stagnation zones caused by the two, some of the air streams slow down to nearly zero velocity whereas some air streams deviate from the zone. Wake region is associated with velocity gradients because of flow recirculation. The above-mentioned factors govern the characteristic temperature contour as shown in figures.

Speaking of the portion of the fin-plate near heat generating source, that is the tube, low-temperature zones are encountered either when flow deviation from stagnation zone occurs or when flow moves past the wake zone, whose effect can especially be seen in case of CFU orientation (fig. 5.5). The difference between resultant wake zones formed as a result of winglet and tube towards the outlet side of the domain can be easily pointed out in CFU and CFD orientations. The resultant wake zone is larger in size for CFD orientation because of which recirculation zone formed solely due to tube is small, thus enhancing heat transfer in the vicinity of heat-generating source and reverse of this statement is true for CFU case. Given that thermal performance being studied here is based on area-averaged global temperature values, which in fact provides a better metric for thermal efficiency comparison, CFD orientation offers an edge over its CFU counterpart.

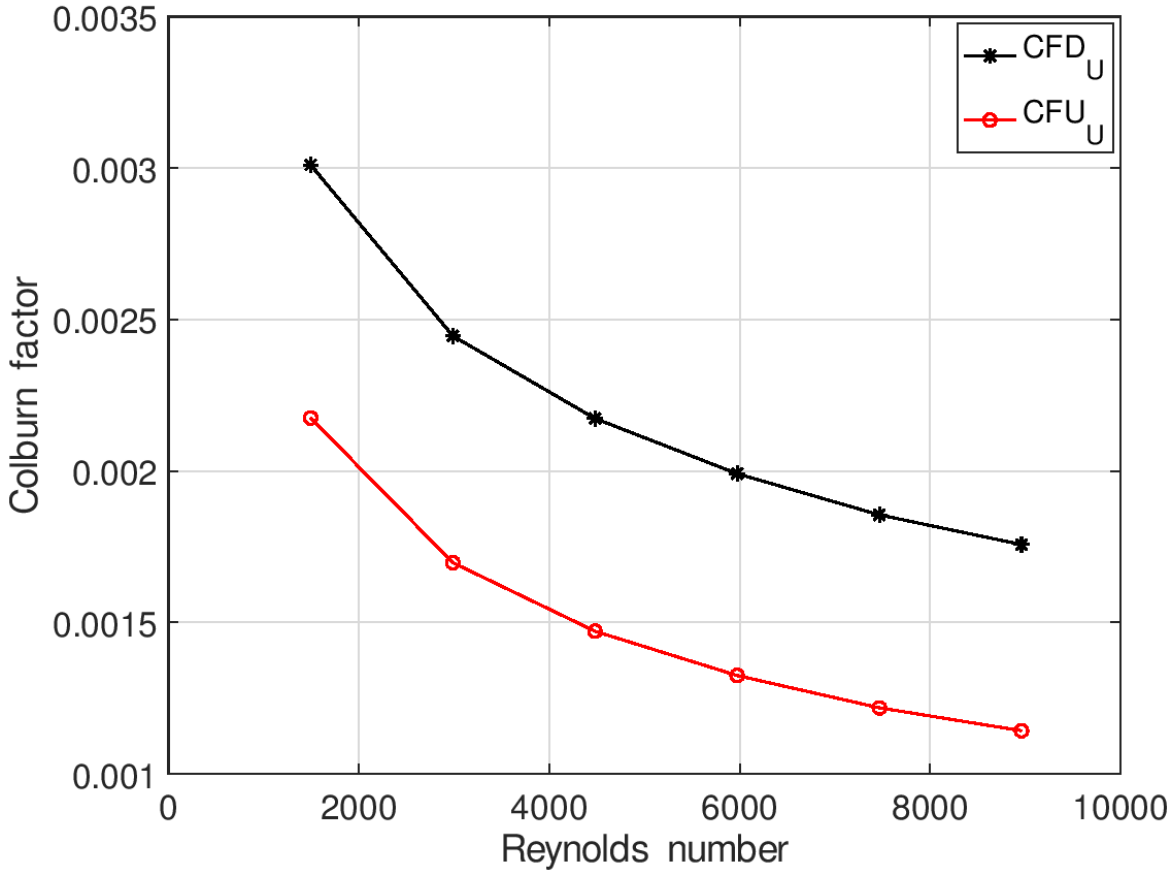

Figure 5.4 Variation of Colburn's factor with Reynolds number for CFU_U and CFD_U configurations

It can be observed from the velocity contours of CFU_U and CFD_U configurations that there is some area near to the tube where velocity of air is more than free stream velocity (i.e.4m/s in this case). This is the wake region near the tube where more air will be pushed as a result of formation of vortices due to the winglet. Additionally, there is also some area where velocity of air is more than free stream velocity. It is also because of the formation of vortices, as a result of which more air will be pushed in that region. Figure 5.7 & 5.8 explains the above mentioned fact.

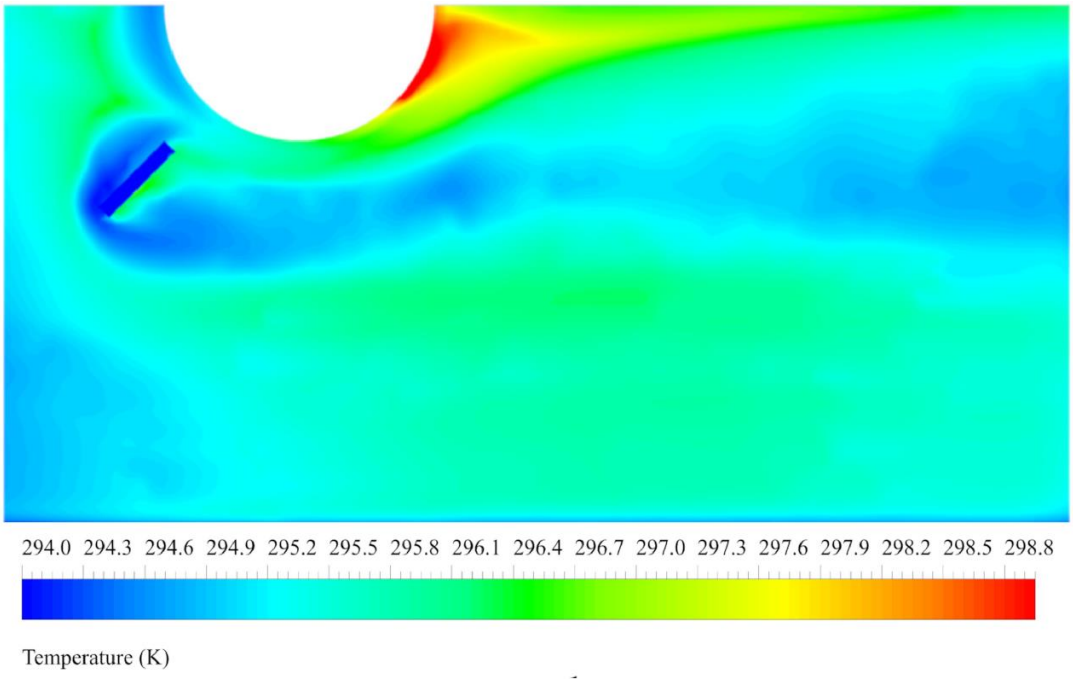

Figure 5.5 Temperature contours of CFU_U configuration at 4 m/s inlet velocity (flow Left to Right)

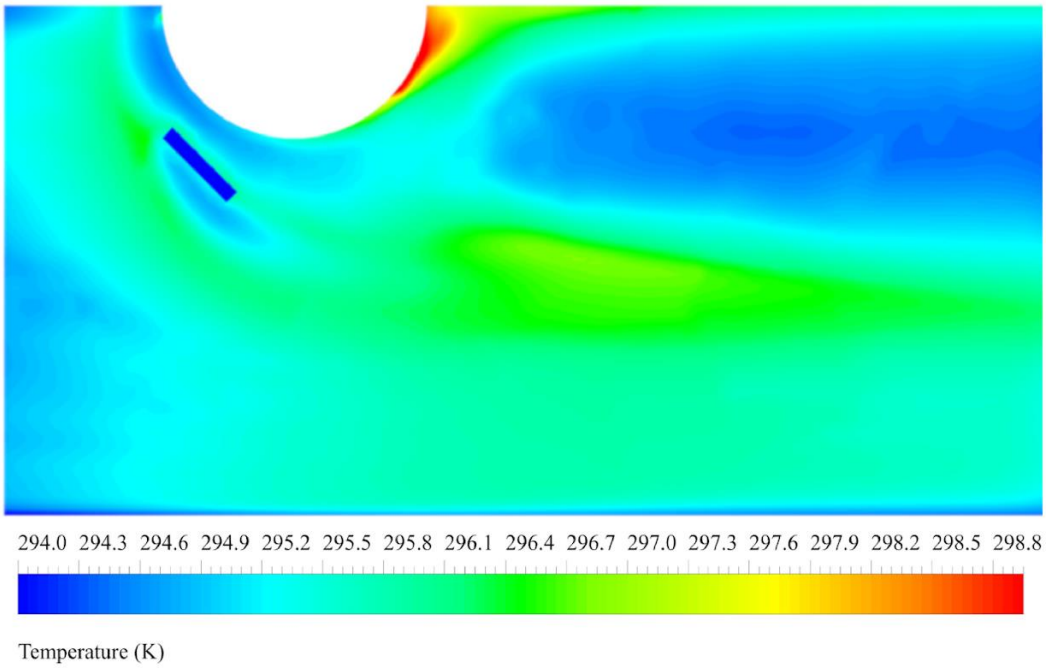

Figure 5.6 Temperature contours of CFD_U configuration at 4 m/s inlet velocity (flow Left to Right)

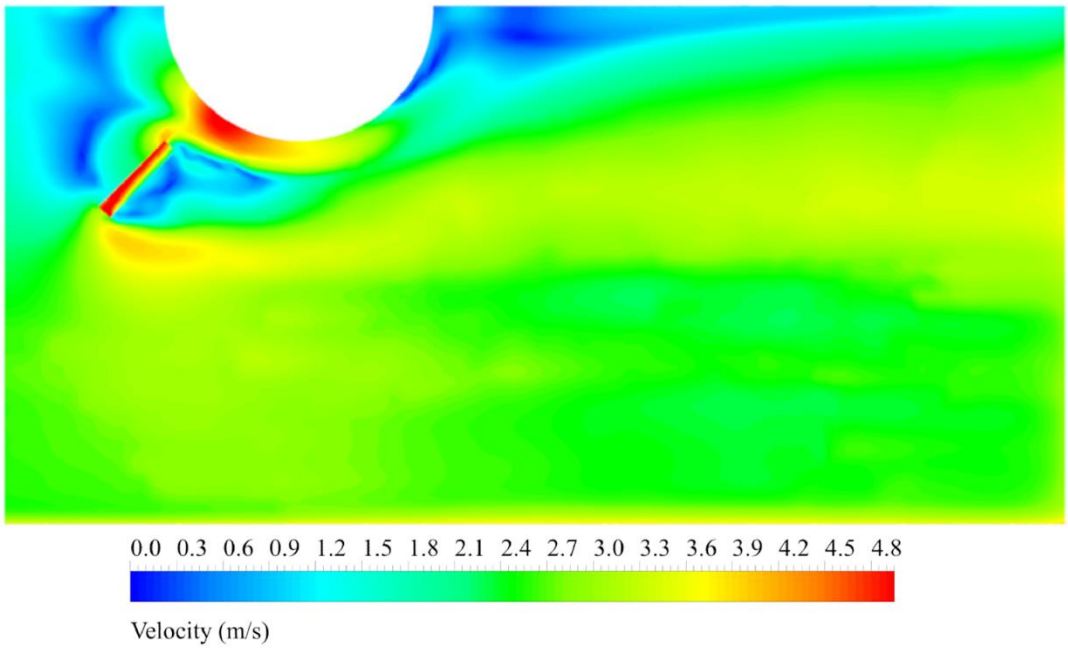

Figure 5.7 Velocity contours of CFU_U configuration at 4 m/s inlet velocity

(flow Left to Right)

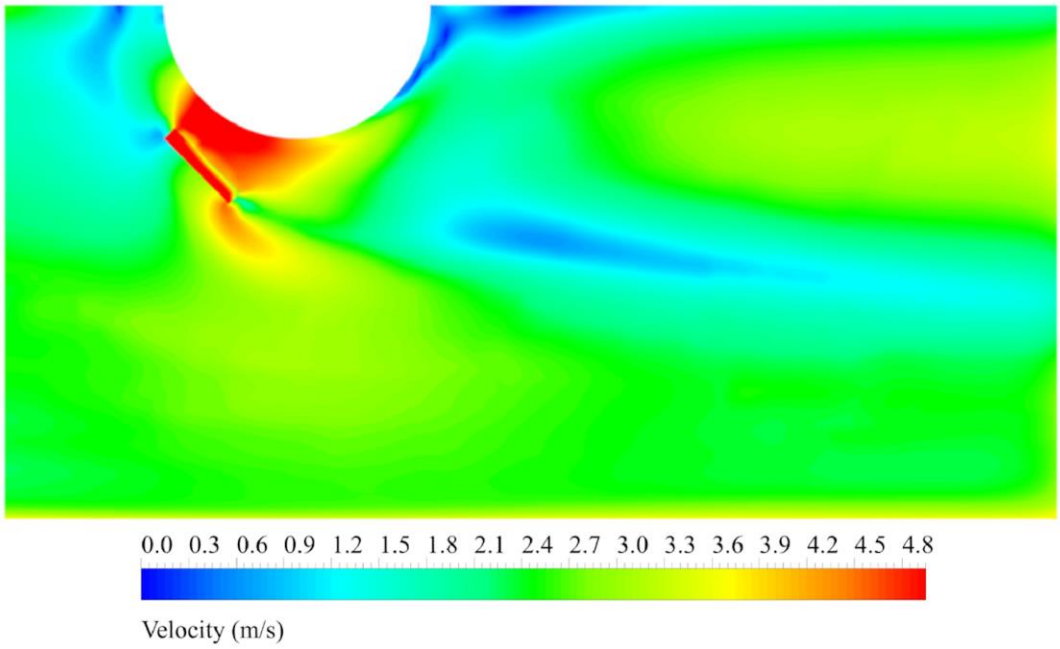

Figure 5.8 Velocity contours of CFD_U configuration at 4 m/s inlet velocity

(flow Left to Right)

5.3. EFFECT OF LOCATION

A study on the effect of placing the non-punched winglet upstream or downstream of the tube on two critical performance parameters viz., the pressure drop across fin-plate and Colburn's factor is being presented in this section. Fig. 5.9 and fig. 5.12 shows variations of pressure drop and Colburn's factor with Reynolds number.

5.3.1. Flow Resistance Characteristics

It may be inferred from fig. 5.9 that there is a marginal difference between pressure drops in the two cases under consideration here, especially at the beginning of the *Re* range. CFD_D configuration shows a higher pressure drop when compared with CFD_U with a range of pressure difference between 1.4 Pa and 5 Pa, the average difference in pressure drop over all the investigated *Re* values being 4%.

Fig. 5.10 and fig. 5.11 shows pressure contours for upstream and downstream cases respectively at an inlet velocity of 4 m/s. We know that one of the most important factors governing pressure drop in fluid flow is that of hindrance caused in the path of free-flowing fluid and associated recirculation. We have already seen above how airflow interacts with hindrances caused by tube and winglet at the upstream location of CFD orientation.

Speaking of the downstream location of the same orientation, it may be observed from fig. 5.9 that the high-pressure zone formed in front of the tube, solely because of the tube is similar to that formed in the upstream case. In fact, in upstream location, the high-pressure zone is more pronounced because of the interaction of high-pressure zones caused due to winglet and tube but we see from fig. 5.9 that pressure drop caused in downstream location is more than that of upstream location. This means there should be some other over-ruling factor within the flow field that acts as the deciding factor when considering pressure drop. The same is contributed by recirculation zones caused by the two winglets as may be understood from the difference in sizes of regions in blue color in fig. 5.10 and fig. 5.11. Negative low-pressure zones due to winglet and tube are seen to be fully interacting due to the characteristic arrangement of the CFD_U case and they coalesce to form a high negative pressure zone, which is smaller in size than the downstream case. On

the contrary, individual low-pressure zones of tube and winglet show less interaction without any scope for coalescence and are seen to be larger in size. The size factor dominates here and overall pressure drop is more in downstream configuration than upstream. It can thus be stated that the upstream location of the CFD configuration provides an edge above the downstream location due to lower pressure drop.

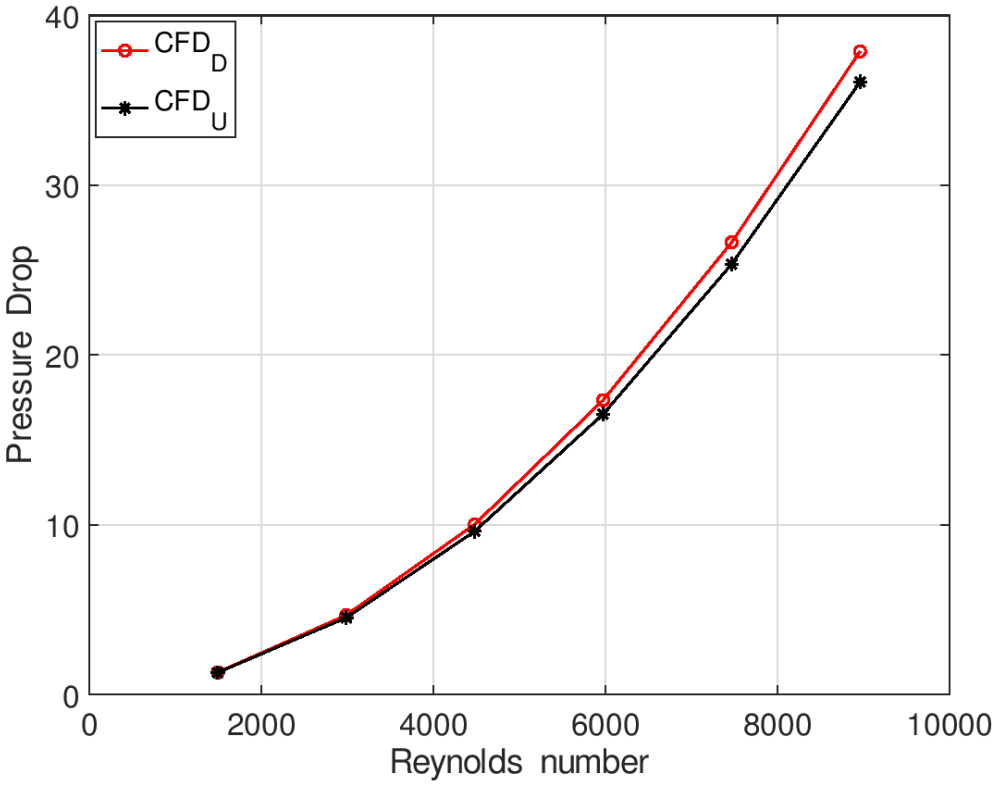

Figure 5.9 Variation of Pressure drop with Reynolds number for CFD_U and CFD_D configurations

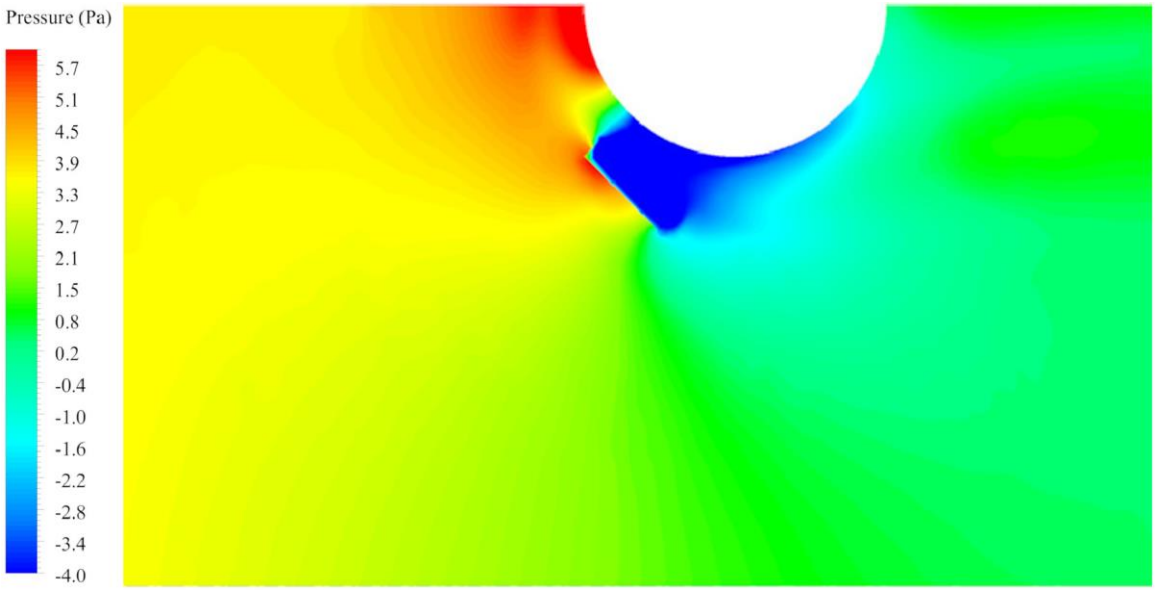

Figure 5.10 Pressure contours of CFD_U configuration at inlet 4 m/s velocity

(flow Left to Right)

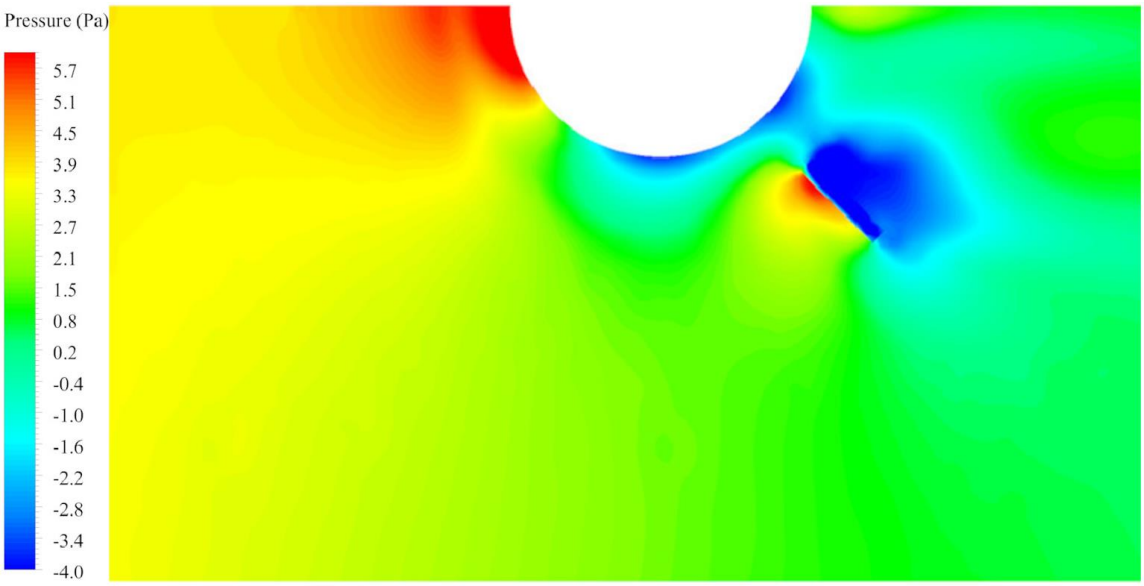

Figure 5.11 Pressure contours of CFD_D configuration at inlet 4 m/s velocity

(flow Left to Right)

5.3.2. Heat Transfer Characteristics

Fig. 5.12 shows that there is an appreciable difference in values of Colburn's factor when the two mentioned cases are compared head to head. The upstream configuration presents superior thermal performance with an average improvement of 17.27% over downstream configuration. Fig. 5.13 & fig. 5.14 shows temperature contours for both the configurations under consideration. In order to avoid redundancy in reasoning with the above sub-section, velocity contours have been omitted here. Due to the characteristic coalescence of winglet and tube induced low-pressure zones in upstream locations, there is the formation of a highly negative net effective pressure region, as explained above. Due to the incompressibility of flow assumed in our study, airflow always tends to move from high pressure to the low-pressure zone. This results in higher velocity air streams being associated in the region between tube and winglet thus enhancing heat transfer, as may be evident from temperature contours shown in the figure. Following another interaction with the recirculation zone of the tube, high-velocity air streams flow past the effective wake region of tube and winglet thus taking away heat. This would be evident from the blue colored wake region in fig. 5.13. Above mentioned fact also explains the reason for formation of low temperature zone in the right hand side of the tube.

On the other hand, while the arrangement of the winglet at a downstream location is able to produce a larger wake region due to collective interaction with the recirculation zone of the tube, the velocity of air streams associated in the region is seen to be less than upstream configuration. Therefore, in spite of a larger wake area in the downstream case, thermal performance is better in the upstream case because of enhanced heat transfer near the generation source and wake region. This also proves to be one of the reasons why global area-averaged study gives us a better metric for thermal performance than localized point-dominated study.

It can be noticed from figure 5.14 that there is low temperature zone in the right hand side of the winglet. The reason for same may be attributed to the formation of vortices just after the winglet.

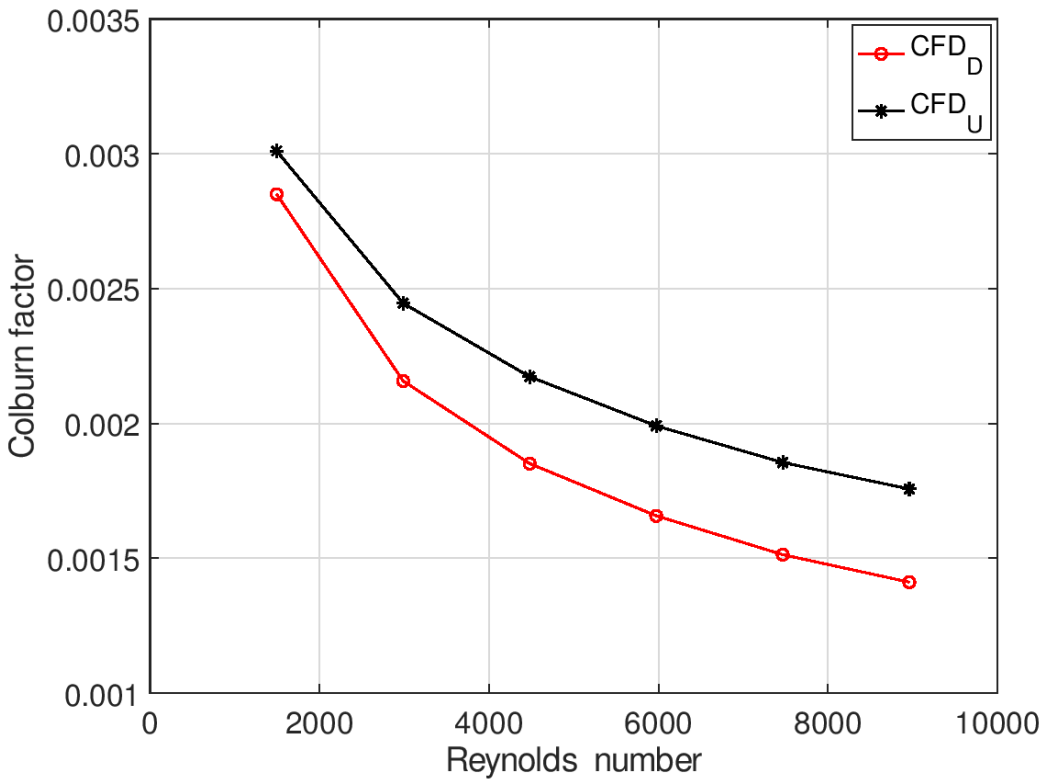

Figure 5.12 Variation of Colburn's factor with Reynolds number for CFD_U and CFD_D configurations

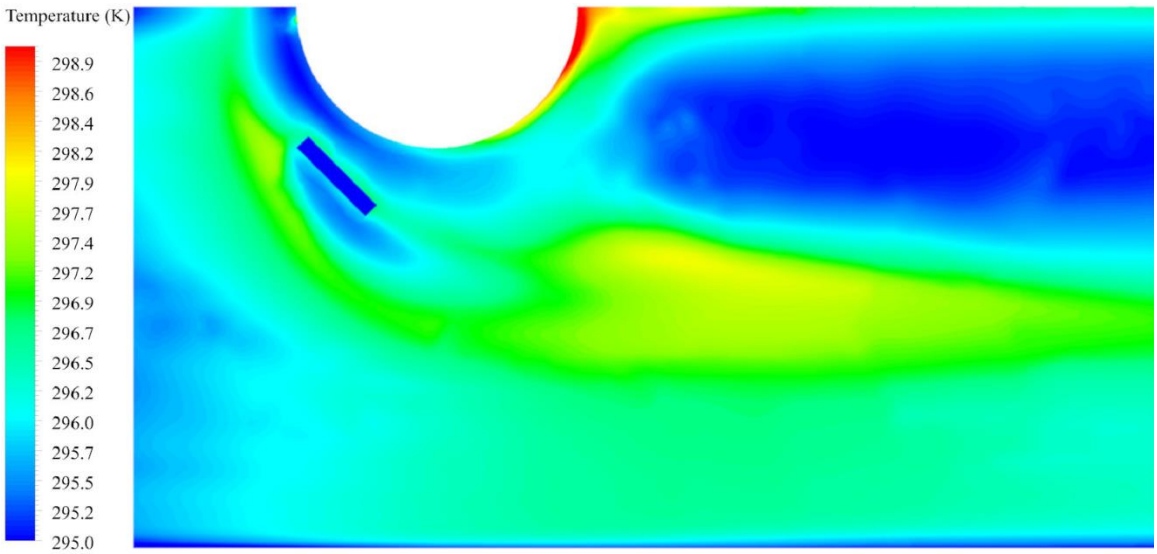

Figure 5.13 Temperature contours of CFD_U configuration at 4 m/s inlet velocity

(flow Left to Right)

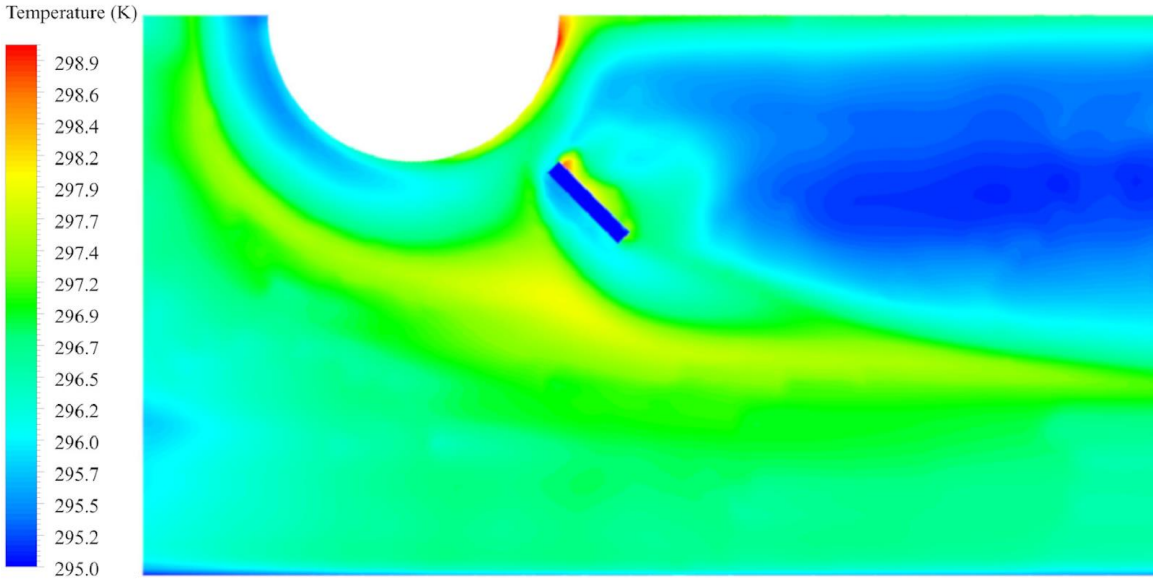

Figure 5.14 Temperature contours of CFD_D configuration at 4 m/s inlet velocity (flow Left to Right)

5.4. SELECTION OF OPTIMUM CONFIGURATION

After having talked about the effect of orientation and location of the winglet, we now discuss the selection of optimum configuration using performance parameters such as Colburn's factor, friction factor, and performance evaluation criterion.

5.4.1. Heat Transfer Characteristics

Figure 5.15 to figure 5.18 represents the temperature contours for all the considered configurations of winglet viz., CFU_U, CFU_D, CFD_U, and CFD_D configurations respectively and can be suitably interpreted to select the optimum configuration of winglet for maximum heat transfer augmentation. In order to relate the temperature contours with the heat transfer, variation of convective heat transfer with Reynolds no. have also been depicted in figure 5.19. Nusselt number is directly proportional to the convective heat transfer coefficient and inversely proportional to the thermal conductivity, which is the same for all the cases. Thus, the variation of Nusselt number with Reynolds number (figure 5.20) follows the same trend as of convective heat transfer coefficient.

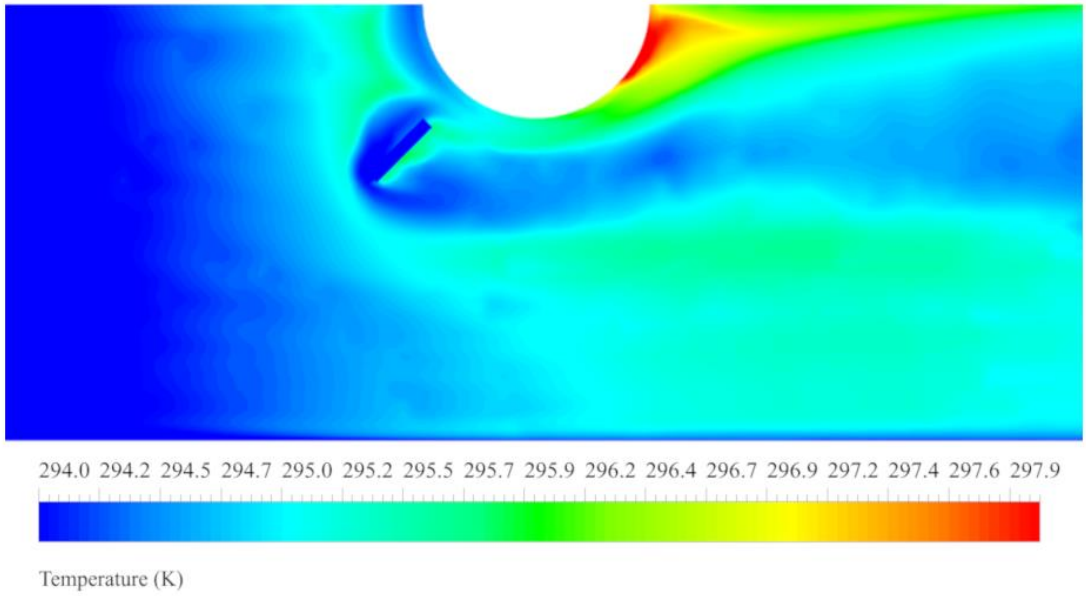

Figure 5.15 Temperature contour of CFU_U configuration at 5 m/s inlet velocity.

(flow Left to Right)

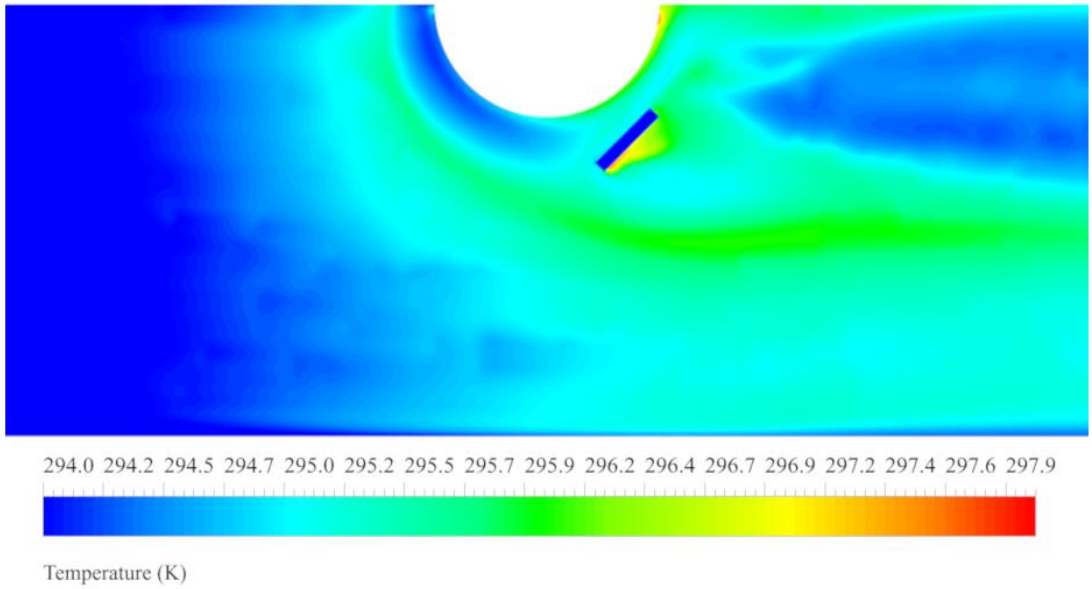

Figure 5.16 Temperature contour of CFU_D configuration at 5 m/s inlet velocity.

(flow Left to Right)

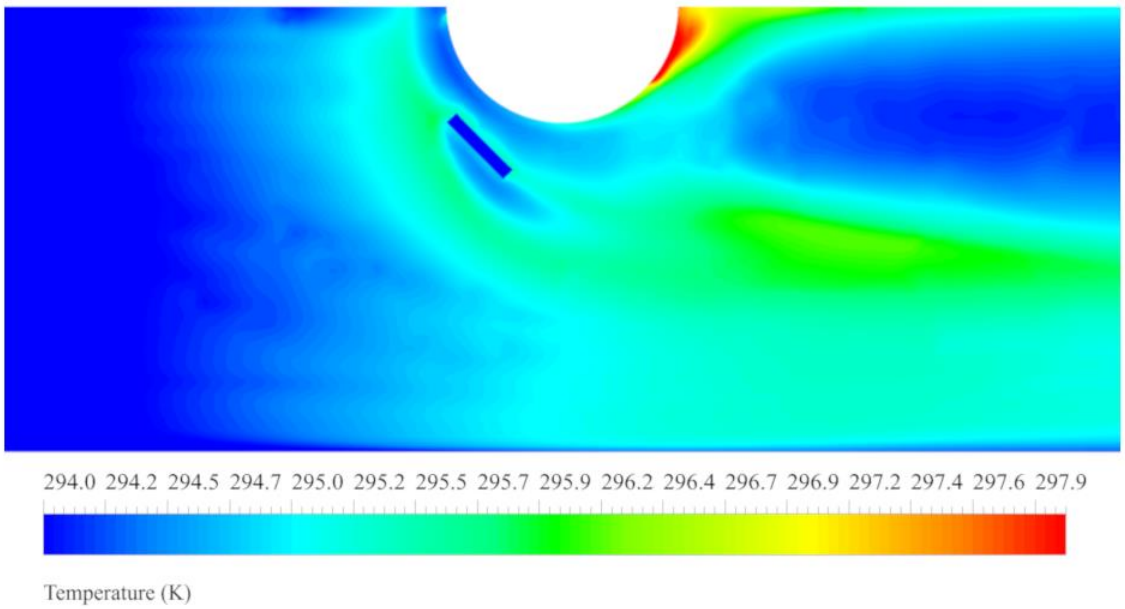

Figure 5.17 Temperature contour of CFD_U configuration at 5 m/s inlet velocity.

(flow Left to Right)

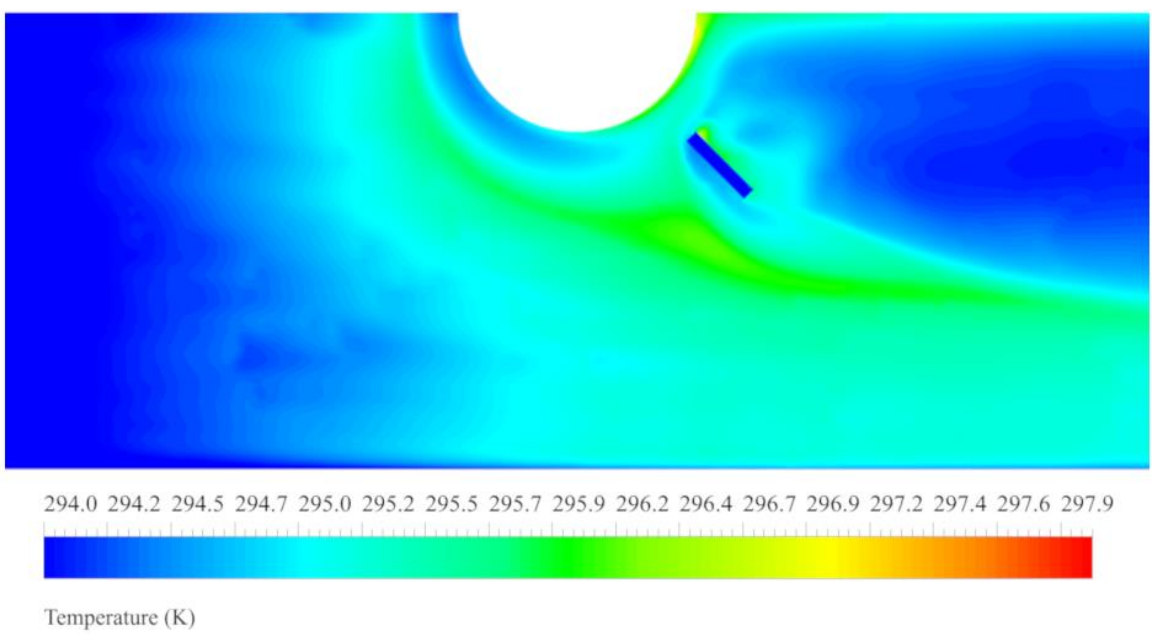

Figure 5.18 Temperature contours of CFD_D configuration at 5 m/s inlet velocity

(flow Left to Right)

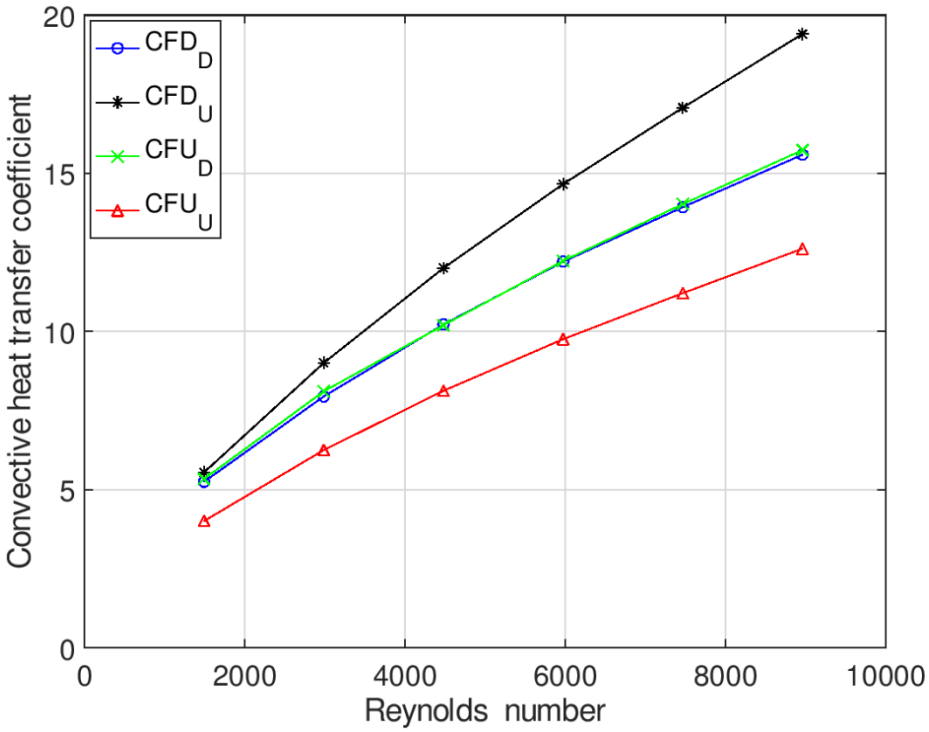

Figure 5.19 Variation of Convective heat transfer coefficient with Reynolds number

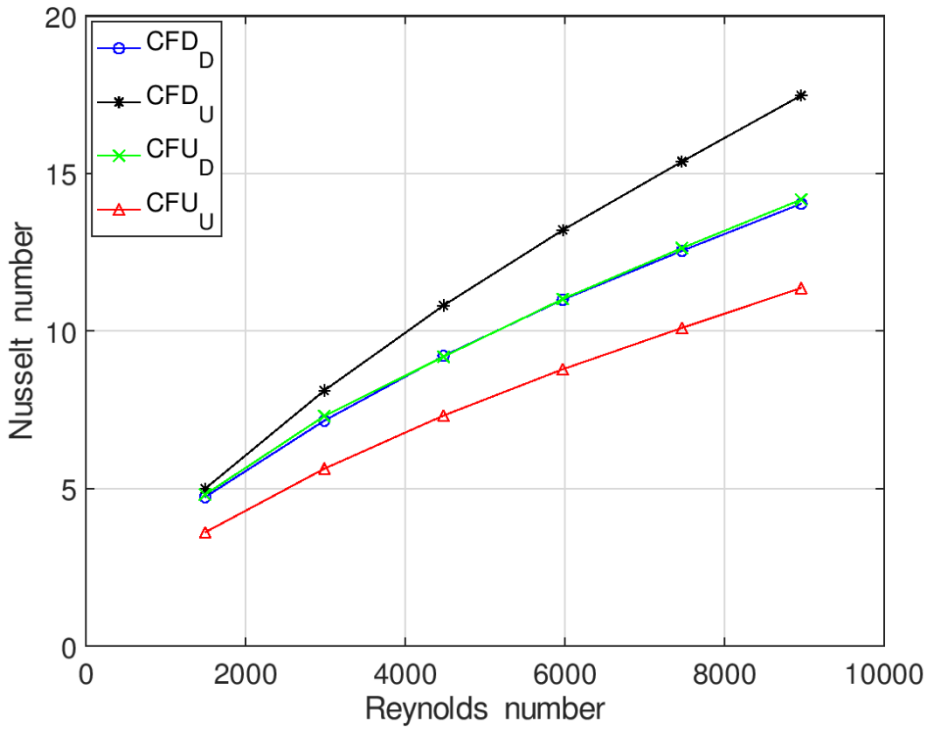

Figure 5.20 Variation of Nusselt number with Reynolds number

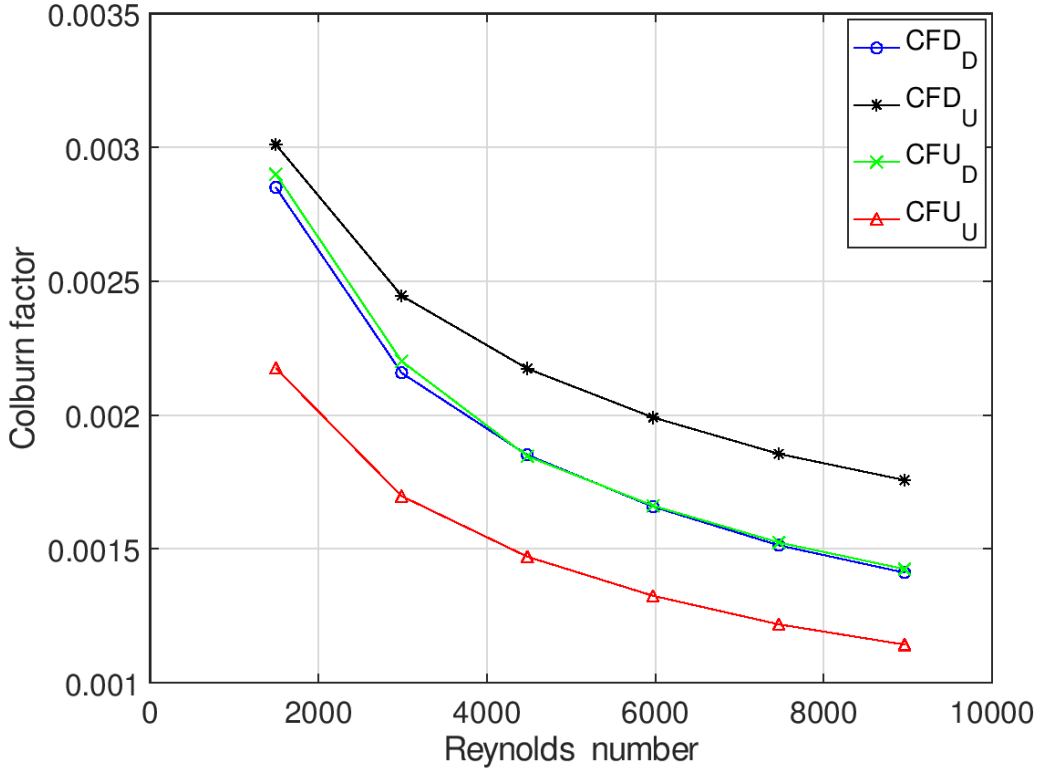

Figure 5.21 Variation of Colburn's factor with Reynolds number

Colburn's factor considers Nusselt number as well as Prandtl number and is thus, a better measure of heat transfer characteristic than Nusselt number. Fig. 5.21 which shows the variation of Colburn's factor with Reynolds number, clearly indicates that for CFD_U configuration heat transfer augmentation is highest while for CFU_U configuration, it is the lowest. An explanation for this has already been given in the previous section. For CFD_D and CFU_D configuration difference is not considerable. CFU_D configuration has a slightly higher value of Colburn's factor than CFD_D configuration. This is due to the fact that in CFU_D configuration, the wake region adjacent to the tube is minimized to a large extent. More air will be pushed to the wake region due to the winglet having its face aligned towards the tube.

5.4.2. Flow Resistance Characteristics

Figure 5.22 shows the variation of pressure drop with Reynolds number for all the configurations of the winglet. It is always desired that pressure drop in a heat exchanger be as minimal as possible. The only drawback of employing a winglet in the fin and tube heat exchanger is the increment in pressure drop. Thus, the configuration with the least pressure drop values out of the four would be desirable.

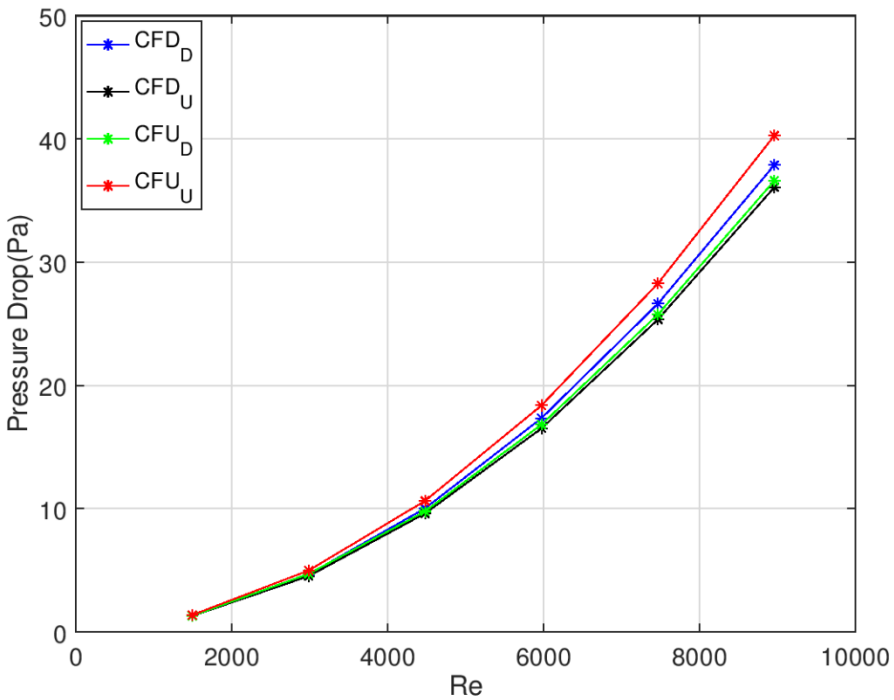

Figure 5.22 Variation of Pressure drop with Reynolds number

Figure 5.23 to figure 5.26 represents the pressure contours for all the considered configurations of winglet viz., CFU_U, CFU_D, CFD_U, and CFD_D configurations respectively and can be suitably interpreted to select the optimum configuration of winglet for minimum pressure drop penalty.

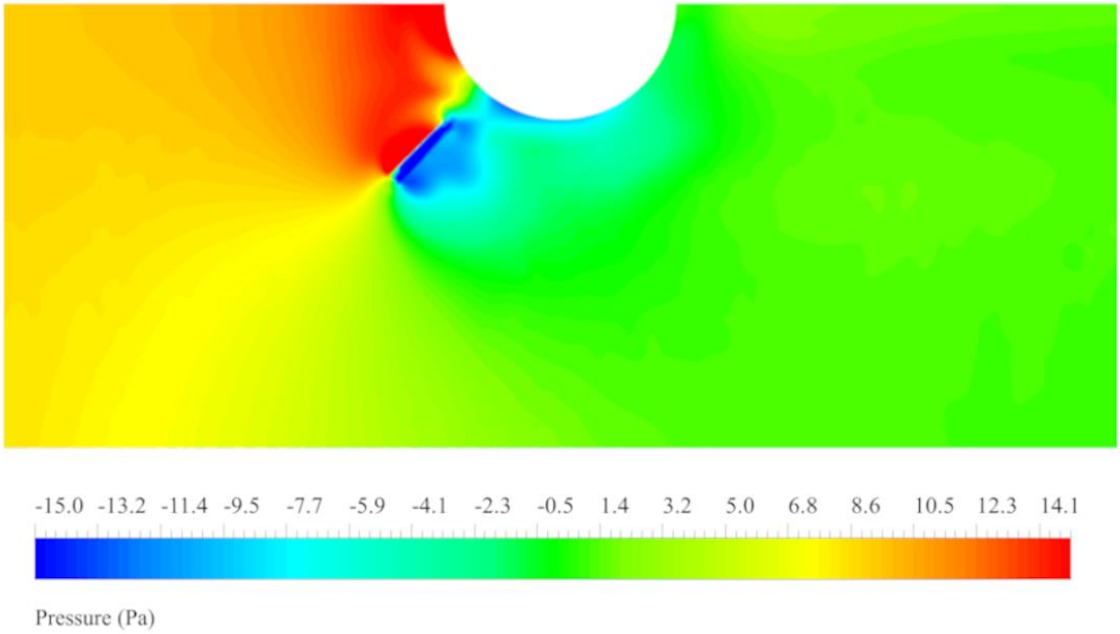

Figure 5.23 Pressure contour of CFU_U configuration at 5 m/s inlet velocity (flow Left to Right)

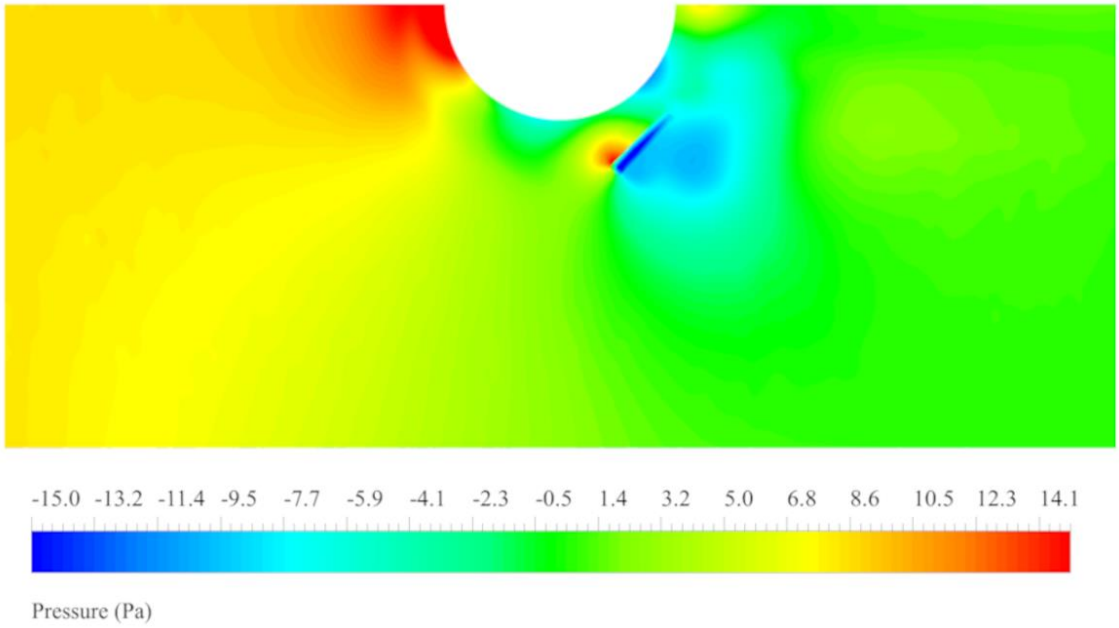

Figure 5.24 Pressure contour of CFU_D configuration at 5 m/s inlet velocity (flow Left to Right)

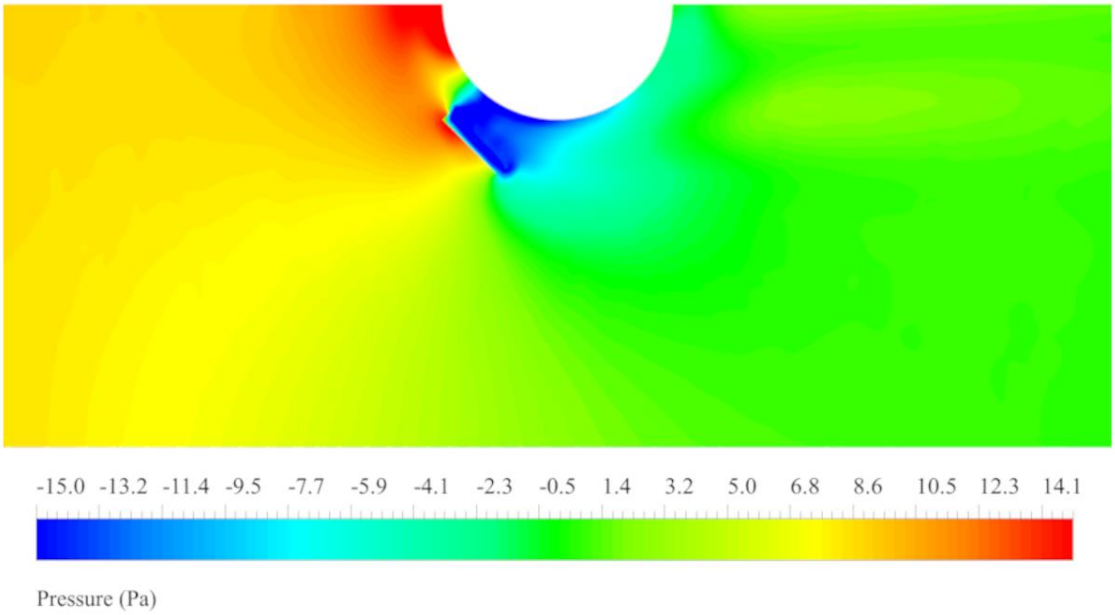

Figure 5.25 Pressure contour of CFD_U configuration at 5 m/s inlet velocity (flow Left to Right)

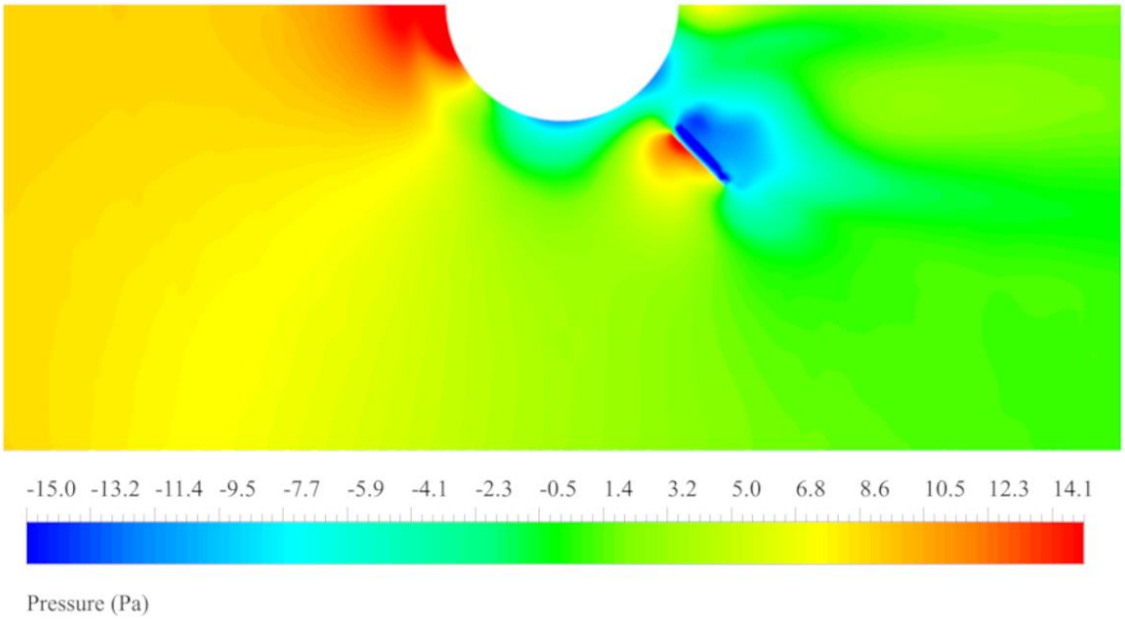

Figure 5.26 Pressure contour of CFD_D configuration at 5 m/s inlet velocity (flow Left to Right)

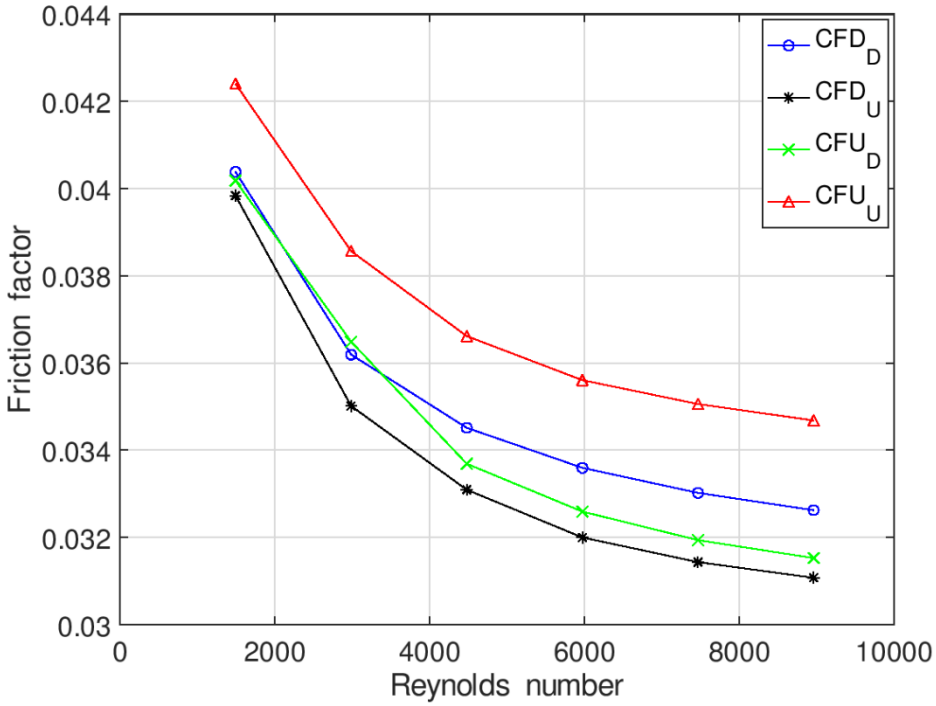

Figure 5.27 Variation of Friction factor with Reynolds number

Figure 5.27 shows the variation of friction factor with Reynolds number. The friction factor is directly proportional to pressure drop and inversely proportional to the square of flow velocity. The friction factor decreases linearly and rapidly from 1m/s till 3m/s velocity and then follows a rather slower trend since it is a function of the squared exponent of velocity. As the velocity of flow increases, the viscous resistance decreases and thus, the friction factor decreases. The trend is quite similar to that shown by the plot of pressure drop in figure 5.22.

From the plots of friction factor, it can be interpreted that the friction factor is higher for CFD_D configuration while it is lower for CFU_D configuration. This could be because, in CFD_D configuration, the winglet is aligned with its face away from the tube while in CFU_D configuration, the winglet has its face aligned towards the tube. Moreover, as explained earlier, CFU_U configuration has the highest value of friction factor while CFD_U configuration has the least value from among the configurations considered.

5.4.3. Overall Thermohydraulic Performance

In order to select the best configuration from among the considered one, I have used PEC, also known as area goodness factor which takes into account the cumulative effect of Colburn's factor as well as friction factor. It can be concluded from fig. 5.28 that PEC has the highest value for CFD_U configuration because of favorable results in both, Colburn's factor and the Friction factor. On the contrary, CFU_U configuration has the least value of PEC because of unfavorable results in both, Colburn's factor and Friction factor. As far as the other two configurations are concerned, CFU_D configuration performs better than CFD_D configuration mainly because of low friction factor as opposed to the other configuration. So, conclusively we can say that CFD_U configuration outperforms from the rest of the configurations and can be considered as the optimum one.

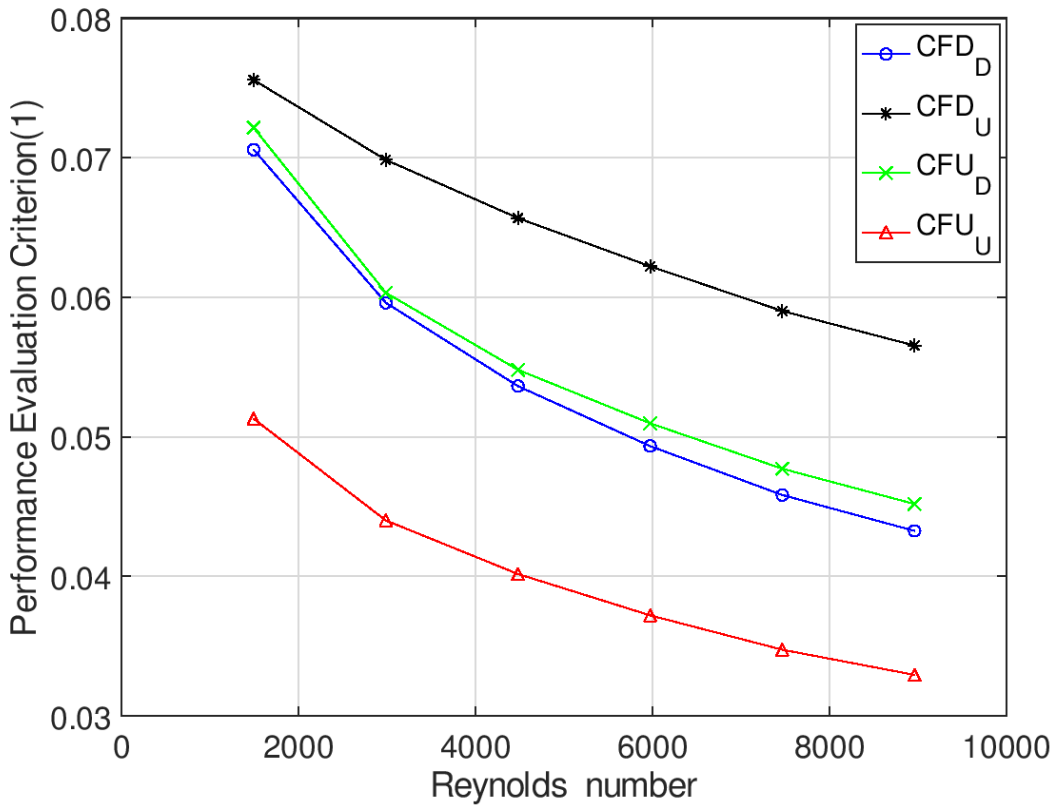

Figure 5.28 Variation of Performance Evaluation Criteria (PEC) with Reynolds number

5.5. SUMMARY

- As far as the global performance is concerned, the winglet attached in CFD_U configuration provides the least value of pressure drop whereas CFU_U configuration has the maximum pressure drop. It is because in CFU_U configuration, the free airstream faces resistance upstream from both, the tube and winglet nearly at the same time while in CFD_U configuration, the orientation of winglet is such that it is in alignment with the tube. The average increase in the pressure drop for CFU_U configuration is of the order of 10.28% over CFD_U configuration for the considered range of Reynolds no. Figure 5.22 can be referred for the same.
- Winglet located in CFD_U configuration provides maximum augmentation in heat transfer characteristics with an average improvement of 61.78% in Colburn's factor over baseline case whereas CFU_U configuration reported the least augmentation with an average improvement of 9.31% for the same over baseline case for the considered range of Reynolds no. Figure 5.21 can be referred for the same.
- From among the considered configuration, CFD_U configuration exhibits the superior thermal performance with an average improvement of 47.78% in Colburn's factor over CFU_U configuration which reported the least improvement. Figure 5.21 can be referred for the same.
- Winglet located in CFD_U configuration reported maximum augmentation in overall thermohydraulic performance with an average improvement of 62.47% over baseline case whereas CFU_U configuration reported the least augmentation with an average improvement of 6.25% over baseline case. Figure 5.28 can be referred for the same.
- The cumulative effect of thermal characteristics and flow resistance characteristics was observed with the help of area goodness factor, termed as a performance evaluation criterion. Winglet having CFD_U configuration reported a significant augmentation up to 71% in overall thermohydraulic performance over CFU_U configuration because of favorable results in both, heat transfer and pressure drop characteristics.

CHAPTER - 6

(PERFORMANCE OF PUNCHED-OUT WINGLET)

6.1. INTRODUCTION

In the last phase of the investigations, I focused my attention on studying the effect of a punched-out / stamped-out rectangular winglet having a circular hole at its center from the fin plate surface. Firstly, this chapter presents a relative comparison between the performance of punched-out winglet (i.e. winglet with hole at its center and punched out from the fin plate surface) over non-punched winglet (i.e. winglet with hole at its center and mounted over the fin plate surface) in three different configurations viz., CFD configuration at downstream as well as upstream location and CFU at an upstream location only because plate punching interferes with the tube placement for the fourth case that is, CFU at a downstream location. Lastly, a relative comparison between the performance of all of the investigated cases has been presented with the help of various performance parameters in order to select an optimum configuration of the punched-out winglet for maximum improvements in the performance over its non-punched counterpart.

6.2. EFFECT OF USING PUNCHED OUT WINGLET

Effect of punching the winglets out of fin-plate surface will now be discussed and a comparison with non-punched counterpart cases will be drawn. For doing so, I will first present an intra-case study (for example CFD_D punched versus CFD_D non-punched, etc.) and then move on to an overall inter-case comparison between all of the investigated cases. Fig. 6.1 and fig. 6.3 shows variations of pressure drop and Colburn's factor with Reynolds number, both for punched and non-punched cases.

6.2.1. Flow Resistance Characteristics

Starting with intra-case comparison, we can see that while plate punching has a positive impact on pressure drop (fig. 6.1) in CFU_U and CFD_D configurations by causing a reduction in the overall pressure drop by 0.6% and 3.05% respectively, CFD_U configuration rather shows an increase in the same by 2.3%.

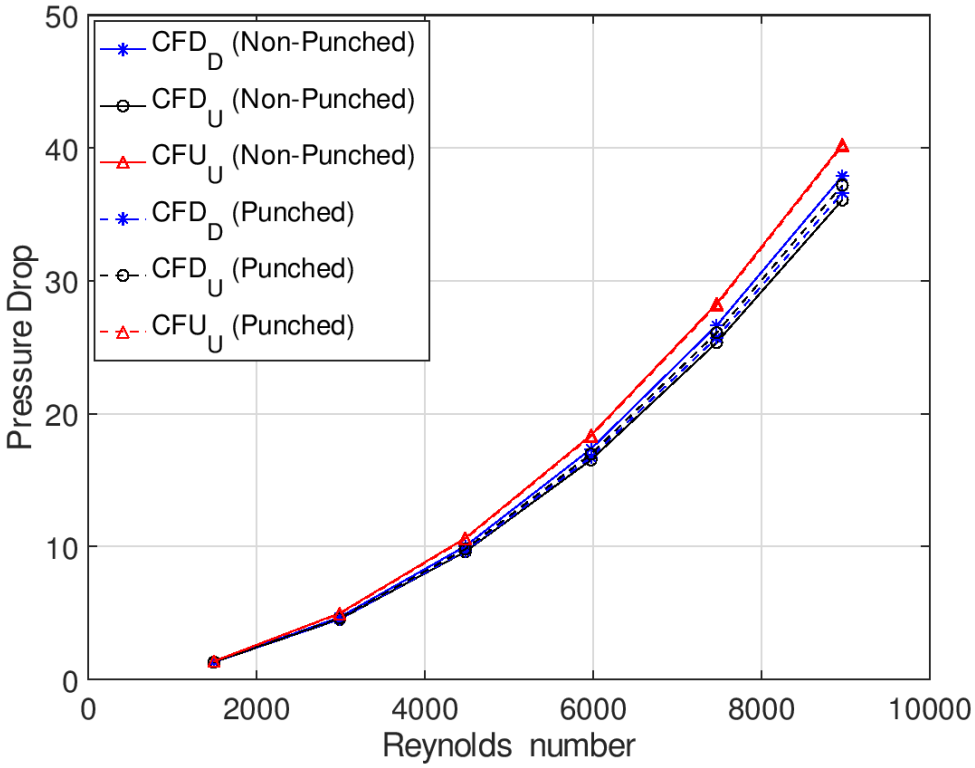

Figure 6.1 Variation of Pressure drop with Reynolds number for all the investigated configurations

Figure 6.2 portrays contours of pressure for all cases under consideration from both top and bottom view at an inlet flow velocity of 5 m/s. On comparing all the non-punched cases with their corresponding punched cases, we may say that the effect of the stagnation zone on pressure drop due to hindrance caused by winglet in the path of flow is less significant in punched-out cases than in non-punched cases. This is primarily because of the fact that the presence of a hole on the plate before the winglet acts as a vent which provides an alternate path for air to flow towards the outlet. This could be made out from lesser intensities of red-colored regions in the stagnation zone of all the punched cases, when seen from a top view (fig. 6.2(a), fig. 6.2(b), fig. 6.2(e), fig. 6.2(f), fig. 6.2(i), fig. 6.2(j). The second factor that plays a major role in evaluating pressure drop across the fin-plate is the formation of the recirculation zone behind the winglet and tube as talked about in detail in the above sections. When seen from the top view, we may notice that all the punched cases have a smaller winglet-dominated recirculation zone.

On noticing closely fig. 6.2(e) and fig. 6.2(f), we find that there is a significant difference between the talked about recirculation zones in CFD_D configuration and this partly accounts for the highest pressure drop being obtained from creating a punched hole on its surface. It is to be realized that this is the only configuration where venting creates a direct path for airflow to interact with the wake zone of the tube at its rear whereas the same is not the case with the other two configurations. Because of the creation of a low-pressure zone of an appreciable size at the back of the tube, fluid would always have a tendency to fill in the void if given an opportunity.

Another important factor is to consider the flow phenomena taking place near the lower face of the plate because of venting. The contours showing a bottom view of the fin-plate portray how there is the addition of a minor low-pressure region at one of the edges of the hole. Although this factor acts as a detrimental one to the reduction of pressure drop, we need to consider the cumulative effect of all the three factors mentioned here. An interesting phenomenon taking place here is in the case of CFD_U configuration. The orientation of the winglet and hole, in this case, is such that venting promotes fluid to directly hit the tube on its side. The low-pressure zone on the lower face due to hole happens to get formed at very close proximity to the low-pressure zone of the tube on its side which further promotes coalescence. This becomes a dominating factor in the punched CFD_U configuration that accounts for an increment in pressure drop over the non-punched case.

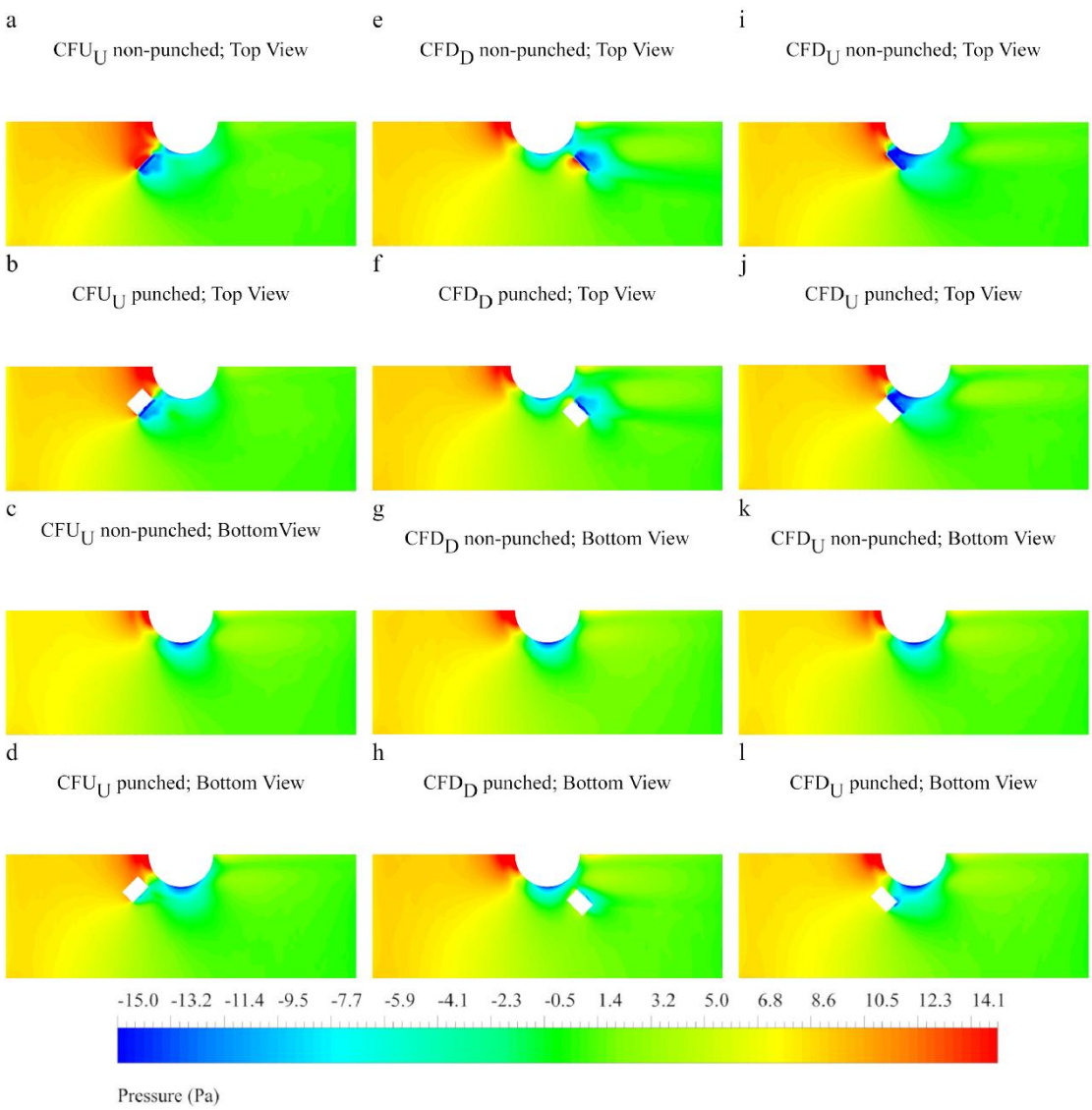

Figure 6.2 Pressure contours for all the investigated configurations from the top and bottom view of fin-plate at an inlet velocity of 5 m/s.

6.2.2. Heat Transfer Characteristics

Figure 6.3 shows a variation of Colburn's factor with *Re* for all the cases under consideration from which, inferences regarding the thermal performance of the heat exchanger could be made. Employing the concept of punched-out winglets from plate surface shows the maximum effect in CFU$_U$ configuration, as can be pointed out from the drastic difference in performance enhancement of 48.3%, from figure 6.3. CFD$_U$

configuration shows an enhancement of 0.53% whereas CFD_D shows a decrement of 0.53%.

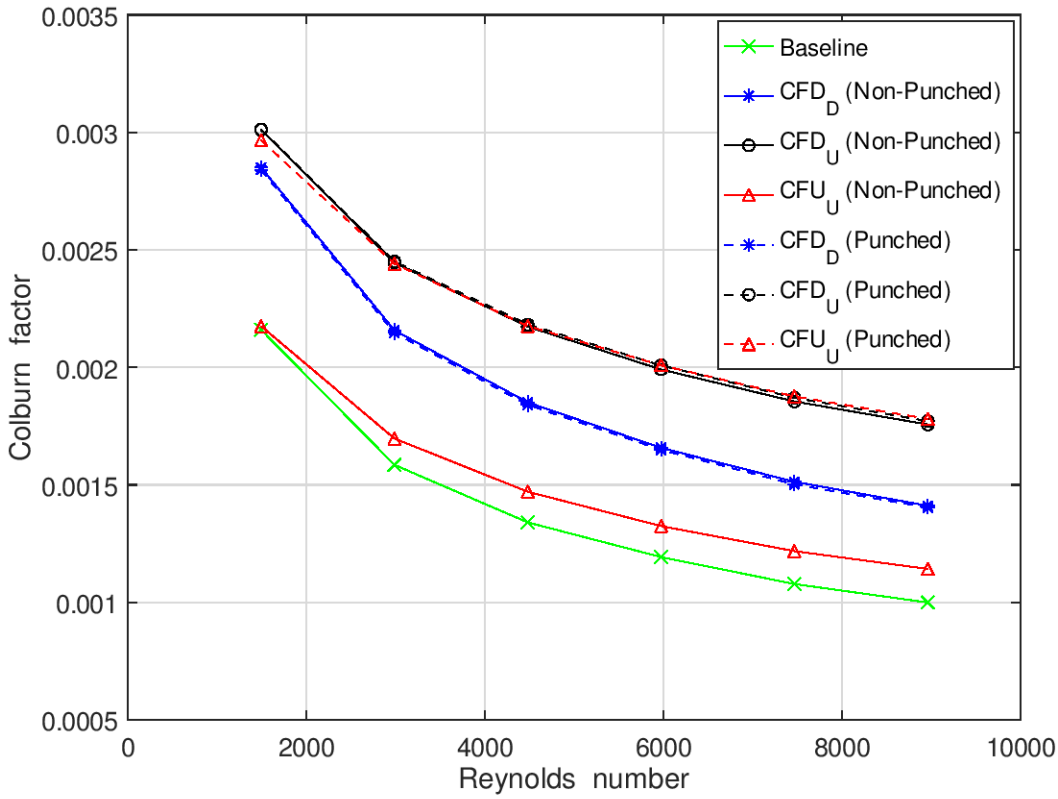

Figure 6.3 Variation of Colburn's factor with Reynolds number for all the investigated configurations

In order to understand the reasons behind these results, temperature contours shown in fig. 6.4 may be referred to. The contours of CFU_U show that winglet dominated recirculation zone formed in the case of the punched-out winglet is significantly smaller than the non-punched case. Higher velocity air streams flow from the region between winglet and tube in the punched-out case and this could be attributed to flow turning due to the presence of additional faces on the plate before winglet. This could also be verified from the presence of a low-temperature zone right at the edge of the winglet between the winglet and tube, which indicates a high-velocity zone. Due to high-velocity air streams, heat transfer characteristics improve in the vicinity of the tube in addition to its wake region. Figure 6.4(b) shows the region of the drastic difference in temperature at the rear

of the tube. Figure 6.4(c) and figure 6.4(d) shows a more or less, similar temperature distribution on the top face of the plate in CFD_D cases. The only difference between the two cases (punched and non-punched) lies in the winglet dominated wake zone. Due to the winglet facing away from the tube and being located downstream, high-velocity air streams turn more towards the back of the tube in the punched-out case. This creates a very small region of higher temperatures being formed right behind the winglet, as can be seen in figure 6.4(d). The same attributes to a minor reduction in thermal performance in the punched-out case of CFD_D configuration. Along the aforementioned lines of reasoning, the tube-dominated recirculation zone shows lower temperature values in the punched-out case of CFD_U configuration (figure 6.4(e) and figure 6.4(f)) and this accounts for a minor enhancement in thermal performance in the punched-out case over the non-punched case.

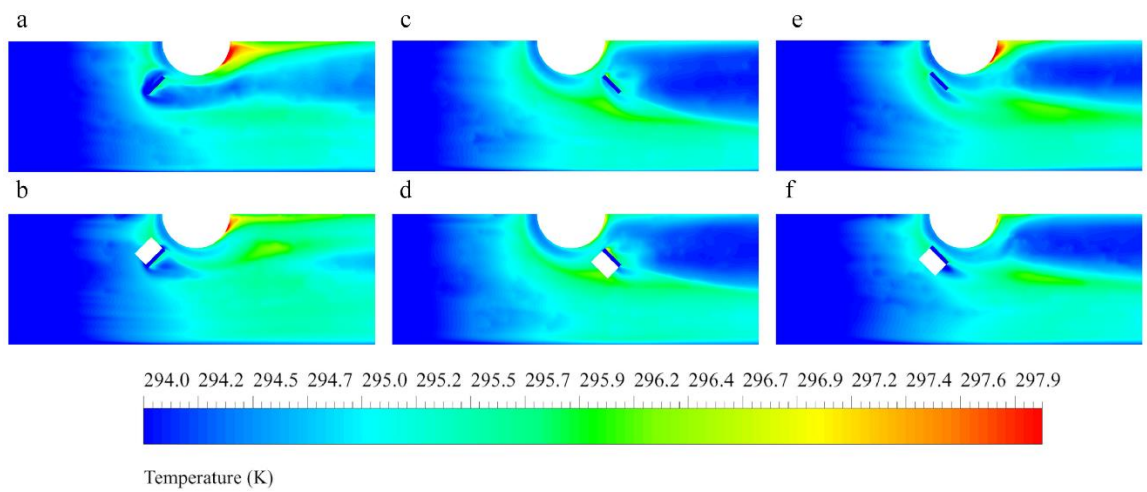

Figure 6.4 Temperature contours for (a), (b) CFU_U, (c), (d) CFD_D, and (e), (f) CFD_U configurations at inlet velocity of 5 m/s.

(flow Left to Right)

Vortex formations are depicted in figure 6.5 which shows the velocity streamlines at 5m/s inlet velocity for all the configurations. It may be observed that CFD_U configuration provides a conducive path of flow for streamlines due to the characteristic alignment of the

winglet and tube. The effect of the same would be evident from the low average friction factor values and high heat transfer coefficients in performance curves.

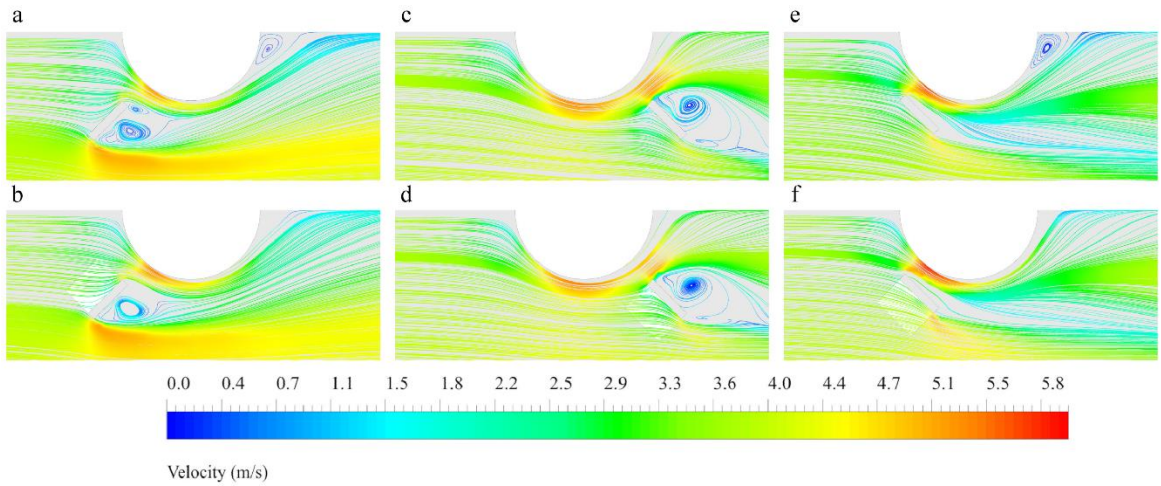

Figure 6.5 Velocity streamlines for (a), (b) CFU_U; (c), (d) CFD_D; and (e), (f) CFD_U configurations at inlet velocity of 5 m/s.

(flow Left to Right)

6.2.3. Overall Thermohydraulic Performance

After having talked about the intra-case comparison of each configuration, an inter-case discussion is in order for making concluding comments on overall performance evaluation. Figure 6.6 shows a plot of friction factor (*f*) against the Reynolds number (*Re*). Friction factor shows a directly proportional relationship with pressure drop and inversely proportional relationship with the square of velocity, hence the shape of indicated curves. Due to the nature of the proportional relationship, the trend of friction factor is the same as that of pressure drop, shown in figure 6.1. There is a sharp drop in friction factor between the two initial Reynolds number values after which the decline keeps becoming more subtle. The punched-out case of CFD_D configuration exhibits the best performance when talking in terms of overall pressure drop due to the maximum drop in friction factor.

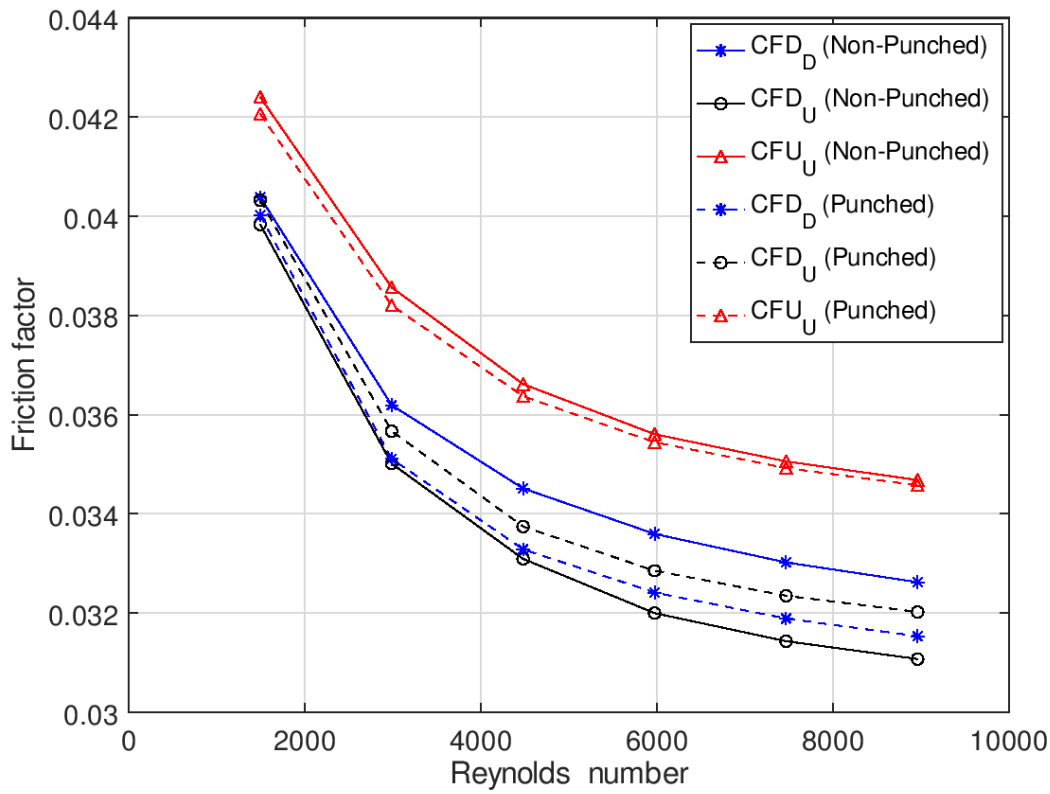

Figure 6.6 Variation of Friction factor with Reynolds number for all the investigated configurations

Figure 6.7 shows a variation of the convective heat transfer coefficient (*h*) with *Re*. Trend exhibited by these curves is similar to that shown by Colburn's factor (fig. 6.3) because of the direct proportionality of both with Nusselt number. The difference between intra-case heat transfer coefficients increases as we move up the range of *Re* values. Punching shows the maximum positive impact on CFU_U configuration when talking in terms of convective heat transfer.

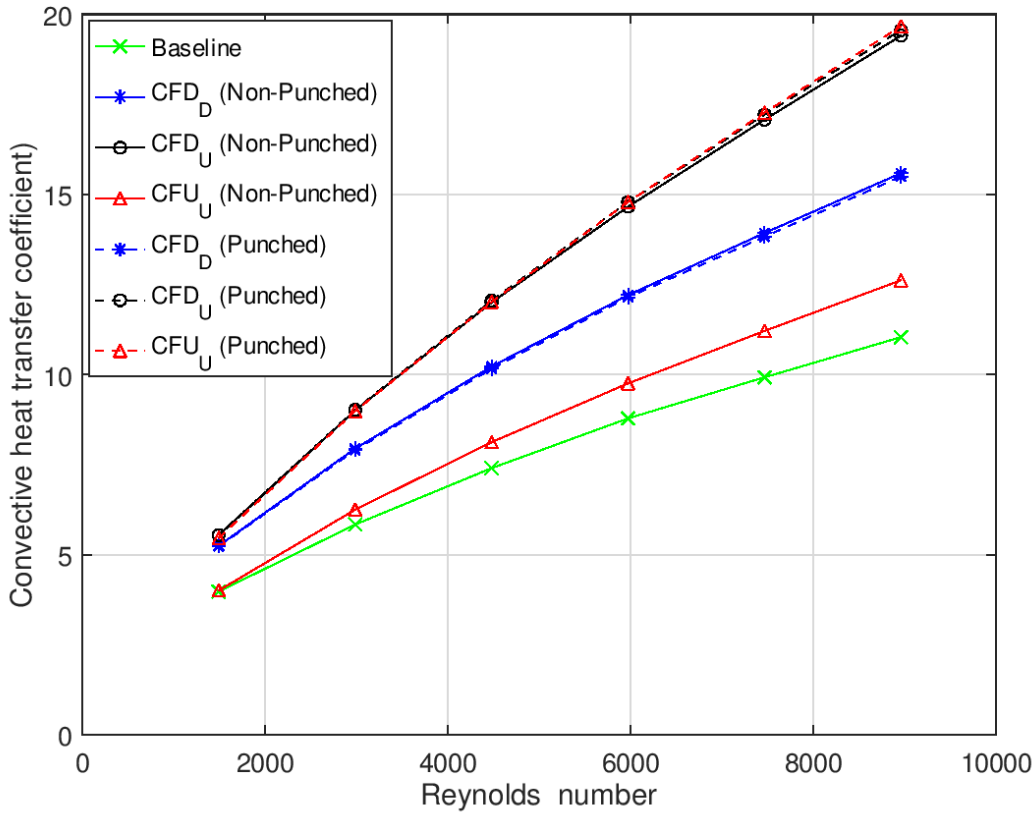

Figure 6.7 Variation of Convective heat transfer coefficient with Reynolds number for all the investigated configurations

JF factor as the performance evaluation criterion being considered as the scale for performance evaluation in my study provides the best indication of performance comparison between punched and non-punched cases. The plot of the variation of PEC with *Re* shown in figure 6.8 considers the cumulative effect of Colburn's factor and friction factor. Although there is a minor enhancement in heat transfer characteristics in punched cases of CFD_U configuration, the factor of increment in pressure drop dominates and thus a reduction in PEC is seen in this configuration due to punching out of winglet from the plate.

On the other hand, while punching shows a negative impact on heat transfer characteristics in CFD_D configuration, the factor of decrement in pressure drop dominates. There is thus an appreciable increase in PEC for this configuration. The CFU_U configuration is rather an obvious one due to the positive impacts of punching on both, pressure drop and heat transfer characteristics. The cumulative effect of the same can be seen from the drastic increase in PEC of the punched case of CFU_U configuration, showing an enhancement of the same by 34%. It may thus be concluded that as predicted by the employed modeling technique, the concept of punching out the winglet is not recommended in the case of CFD_U configuration. On the contrary, punching the winglet out of the plate surface plays the most significant positive role in CFU_U configuration followed by CFD_D configuration.

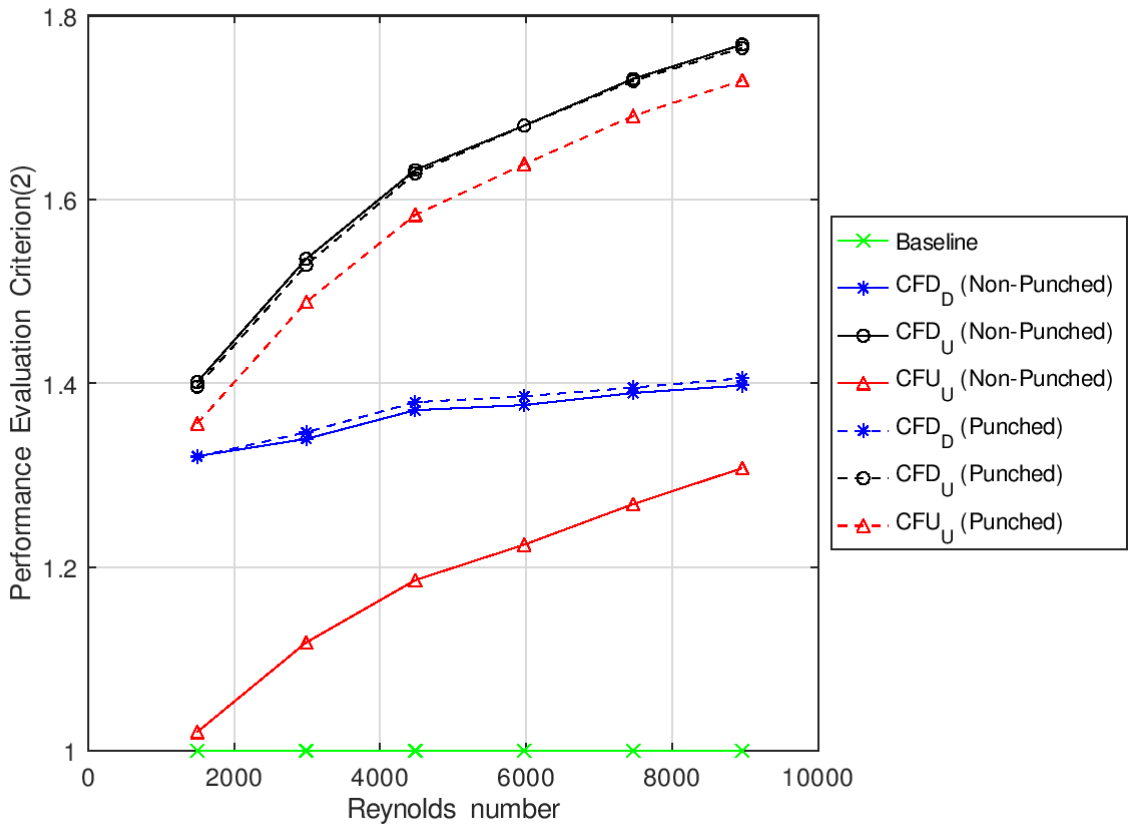

Figure 6.8 Variation of Performance Evaluation Criterion (PEC (2)) with Reynolds no. for all the investigated configurations

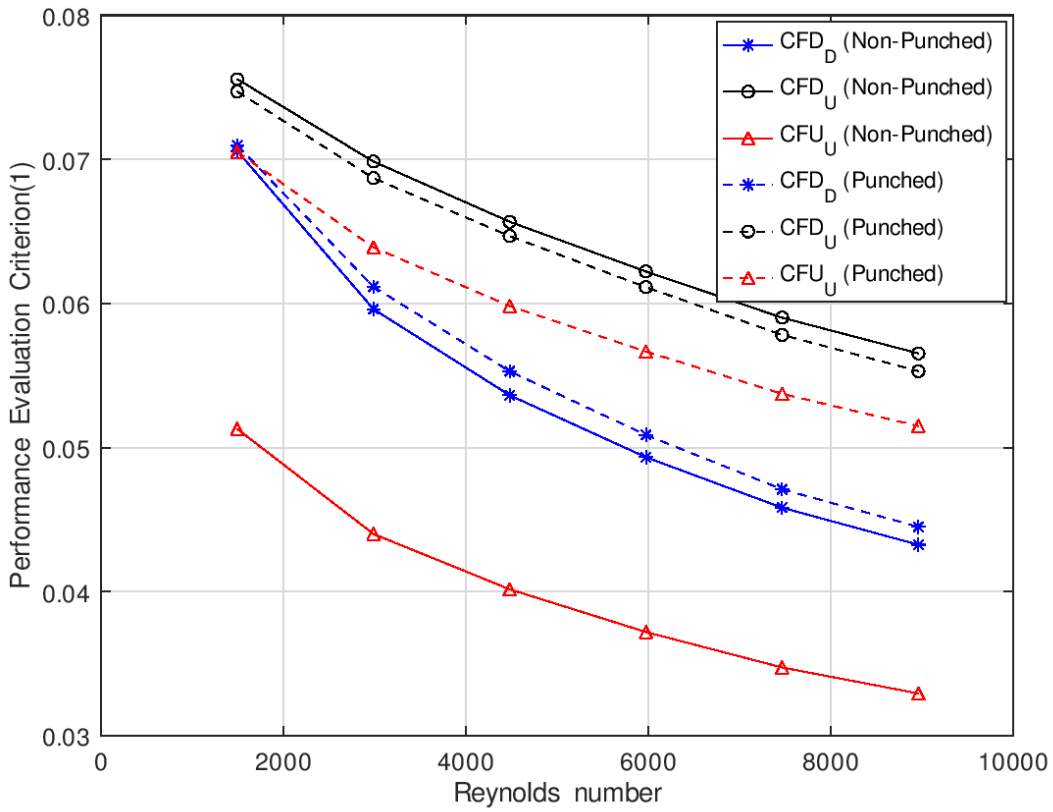

Figure 6.9 Variation of Performance Evaluation Criterion (PEC (1)) with Reynolds no. for all the investigated configurations

In order to evaluate the improvement of punched cases over non-punched cases, we can also use area goodness factor (*j/f*) which takes into account the cumulative effect of Colburn's factor as well as friction factor and also known as a performance evaluation criterion. Figure 6.9 depicts the plot of the variation of performance evaluation criterion with Reynolds no. and exhibits the same trend as shown by the plot of the JF factor for different configurations of the punched and non-punched winglet.

6.3. SUMMARY

- The main drawback associated with using the winglet is the induction of some pressure drop. To reduce this, considered winglet was punched-out from the fin plate surface. CFU_U configuration and CFD_D configuration proved to be advantageous in terms of pressure drop obtained with CFU_U configuration shows a maximum reduction of up to 4% in the pressure drop value over the non-punched case. Figure 6.1 can be referred for the same.
- Winglet located in CFU_U configuration provides maximum augmentation in heat transfer characteristics with an average improvement of 48.29% in Colburn's factor over the non-punched case for the considered range of Reynolds no. Figure 6.3 can be referred for the same.
- Winglet located in CFD_U configuration provides a very small augmentation in heat transfer characteristics with an average improvement of 0.53% in Colburn's factor over non-punched cases whereas CFD_D configuration reported an average decrement of 0.53% in Colburn's factor over its non-punched case. Figure 6.3 can be referred for the same.
- Overall thermohydraulic performance is the cumulative effect of thermal characteristics and flow resistance characteristics and was observed with the help of area goodness factor, termed as a performance evaluation criterion. Winglet mounted in CFU_U configuration reported a major enhancement of the order of 34% for the same over the non-punched case. Figure 6.9 can be referred for the same.
- CFD_U configuration was the only one among the three considered configurations to exhibit a drop in overall thermohydraulic performance when compared with non-punched cases for the same.
- For punched out rectangular winglet, common flow down configuration at upstream location exhibits the best thermal performance, followed by common flow up configuration at an upstream location and, common flow down configuration at a downstream location. Figure 6.3 can be referred for the same.

CHAPTER – 7

(CONCLUSIONS AND FUTURE SCOPE)

7.1. CONCLUSION

This chapter enumerates the major findings reported from the investigations on employing a rectangular winglet having a circular hole at the center, as a vortex generator in a fin-and-tube heat exchanger. The considered winglet has been used as a pair and the same has been attached as well as punched out in the Common Flow Down and Common Flow Up configuration at upstream as well as downstream location. The conclusions have been presented as chapter wise.

7.2. PERFORMANCE OF THE RECTANGULAR WINGLET (LOCALISED STUDY) (CHAPTER 4)

- The main disadvantage associated with using the winglet is the induction of some pressure drop. To reduce this, winglets with punched holes as vortex generators have been used which reduces the pressure drop by up to 7% for CFD_D configuration.
- CFD_D configuration provides the least value of pressure drop whereas CFU_U configuration has the maximum pressure drop. The average increase in the pressure drop for CFU_U configuration is of the order of 13.74% over CFD_D configuration for the considered range of Reynolds no.
- CFD_U configuration provides maximum augmentation in heat transfer characteristics with an average improvement of 55% over the baseline case for the considered range of Reynolds no.
- Overall thermohydraulic performance is the cumulative effect of thermal characteristics and flow resistance characteristics which have been assessed by Performance Evaluation Criterion (PEC) also known as the JF factor. CFD_U configuration exhibits the best thermohydraulic performance with an average improvement of 51.28% over the baseline case whereas CFU_D configuration reported an average improvement of 6.56% over the baseline case for the same which is the lowest from among the considered configurations.

- Winglet located in CFD configuration reported superior thermohydraulic performance than CFU configuration irrespective of whether it is located upstream or downstream.
- Winglet located in the upstream position exhibits better thermohydraulic performance as compared to a downstream position irrespective of its configuration.

7.3. PERFORMANCE OF THE RECTANGULAR WINGLET (GLOBAL STUDY) (CHAPTER 5)

- For the global performance study, the winglet attached in CFD_U configuration provides the least value of pressure drop whereas CFU_U configuration has the maximum pressure drop. The average increase in the pressure drop for CFU_U configuration is of the order of 10.28% over CFD_U configuration for the considered range of Reynolds no.
- Winglet located in CFD_U configuration provides maximum augmentation in heat transfer characteristics with an average improvement of 61.78% in Colburn's factor over baseline case whereas CFU_U configuration reported the least augmentation with an average improvement of 9.31% for the same over baseline case for the considered range of Reynolds no.
- From among the considered configuration, CFD_U configuration exhibits the superior thermal performance with an average improvement of 47.78% in Colburn's factor over CFU_U configuration which reported the least improvement.
- Winglet located in CFD_U configuration reported maximum augmentation in overall thermohydraulic performance with an average improvement of 62.47% over baseline case whereas CFU_U configuration reported the least augmentation with an average improvement of 6.25% over baseline case.
- The cumulative effect of thermal characteristics and flow resistance characteristics was observed with the help of area goodness factor, termed as

a performance evaluation criterion. Winglet having CFD_U configuration reported a significant augmentation up to 71% in overall thermohydraulic performance over CFU_U configuration because of favorable results in both, heat transfer and pressure drop characteristics.

- The implemented numerical model indicated towards CFD_U configuration as exhibiting the best thermal performance, followed by CFU_D, CFD_D, and CFU_U configuration.

7.4. PERFORMANCE OF THE PUNCHED-OUT WINGLET (CHAPTER 6)

- The main drawback associated with using the winglet is the induction of some pressure drop. To reduce this, considered winglet was punched-out from the fin plate surface. CFU_U configuration and CFD_D configuration proved to be advantageous in terms of pressure drop obtained with CFU_U configuration shows a maximum reduction of up to 4% in the pressure drop value over the non-punched case.
- Winglet located in CFU_U configuration provides maximum augmentation in heat transfer characteristics with an average improvement of 48.29% in Colburn's factor over the non-punched case for the considered range of Reynolds no.
- Winglet located in CFD_U configuration provides a very small augmentation in heat transfer characteristics with an average improvement of 0.53% in Colburn's factor over non-punched cases whereas CFD_D configuration reported an average decrement of 0.53% in Colburn's factor over its non-punched case.
- Overall thermohydraulic performance is the cumulative effect of thermal characteristics and flow resistance characteristics and was observed with the help of area goodness factor, termed as a performance evaluation criterion. Winglet mounted in CFU_U configuration reported a major enhancement of the order of 34% for the same over the non-punched case.

- CFD_U configuration was the only one among the three considered configurations to exhibit a drop in overall thermohydraulic performance when compared with non-punched cases for the same.
- For punched out rectangular winglet, common flow down configuration at upstream location exhibits the best thermal performance, followed by common flow up configuration at an upstream location and, common flow down configuration at a downstream location.

7.5. SCOPE FOR FUTURE WORK

Although the present study gives very interesting results, there is still enough scope left for future work which can be summarized as follows.

- The present investigations can be further extended to estimate the optimum value for the angle of attack as well as the aspect ratio of the rectangular winglet for the maximum heat transfer augmentation.
- The present investigations consider circular tube but this study can also be extended for oval tube as well as for a flat tube for the relative comparison and to judge the optimum shape of the tube for improvement in the overall thermohydraulic performance of the heat exchanger.
- The present study considers flat fin plate surface but the same analysis can be performed for wavy fin plate surface and a relative comparison can be made between the two different fin surfaces.
- In the present study, only one tube has been considered for the investigations, but this analysis could be extended for multiple tubes in an inline and staggered arrangement.
- Flat rectangular winglet can be replaced by the curved rectangular winglet for estimating the heat transfer augmentation and a relative comparison can be made between the two different types of the winglet.

- Delta winglet with a circular hole at the center may also be considered for estimating the heat transfer and flow resistance characteristics and a relative comparison between the performance of delta and rectangular winglet can be made.
- The current work considers only one row of winglet pair, but it can also be extended for multiple rows of winglet pair in an inline and staggered arrangement to evaluate the overall performance.

REFERENCES &
LIST OF PUBLICATIONS

REFERENCES

[1] Allison, C. B., & Dally, B. B. (2007). Effect of a delta-winglet vortex pair on the performance of a tube-fin heat exchanger. *International Journal of Heat and Mass Transfer*, *50*(25–26), 5065–5072. https://doi.org/10.1016/j.ijheatmasstransfer.2007.08.003

[2] Aris, M. S., Owen, I., & Sutcliffe, C. J. (2011). The development of active vortex generators from shape memory alloys for the convective cooling of heated surfaces. *International Journal of Heat and Mass Transfer*, *54*(15–16), 3566–3574. https://doi.org/10.1016/j.ijheatmasstransfer.2011.03.030

[3] Arora, A., Subbarao, P. M. V., & Agarwal, R. S. (2015). Numerical optimization of location of "common flow up" delta winglets for inline aligned finned tube heat exchanger. *Applied Thermal Engineering*, *82*, 329–340. https://doi.org/10.1016/j.applthermaleng.2015.02.071

[4] BENARD, & H. (1908). Formation of centers of circulation behind a moving obstacle. *Compte Rendus Academie Des Sciences*, *147*, 839–842.

[5] Biswas, G., Mitra, N. K., & Fiebig, M. (1994). Heat transfer enhancement in fin-tube heat exchangers by winglet type vortex generators. *International Journal of Heat and Mass Transfer*, *37*(2), 283–291. https://doi.org/10.1016/0017-9310(94)90099-X

[6] Chen, Y., Fiebig, M., & Mitra, N. K. (1998). Heat transfer enhancement of a finned oval tube with punched longitudinal vortex generators in-line. *International Journal of Heat and Mass Transfer*, *41*(24), 4151–4166. https://doi.org/10.1016/S0017-9310(98)00130-6

[7] Chimres, N., Wang, C. C., & Wongwises, S. (2018a). Effect of elliptical winglet on the air-side performance of fin-and-tube heat exchanger. *International Journal of Heat and Mass Transfer*, *123*, 583–599. https://doi.org/10.1016/j.ijheatmasstransfer.2018.02.079

[8] Chimres, N., Wang, C. C., & Wongwises, S. (2018b). Optimal design of the semi-dimple vortex generator in the fin and tube heat exchanger. *International Journal of Heat and Mass Transfer*, *120*, 1173–1186. https://doi.org/10.1016/j.ijheatmasstransfer.2017.11.121

[9] Chomdee, S., & Kiatsiriroat, T. (2006). Enhancement of air cooling in staggered array of electronic modules by integrating delta winglet vortex generators. *International Communications in Heat and Mass Transfer*, *33*(5), 618–626. https://doi.org/10.1016/j.icheatmasstransfer.2006.01.002

[10] Chu, P., He, Y. L., Lei, Y. G., Tian, L. T., & Li, R. (2009). Three-dimensional numerical study on fin-and-oval-tube heat exchanger with longitudinal vortex generators. *Applied Thermal Engineering*, *29*(5–6), 859–876. https://doi.org/10.1016/j.applthermaleng.2008.04.021

[11] Datta, A., Sanyal, D., & Das, A. K. (2016). Numerical investigation of heat transfer in microchannel using inclined longitudinal vortex generator. *Applied Thermal Engineering*, *108*. https://doi.org/10.1016/j.applthermaleng.2016.07.165

[12] Du, X., Feng, L., Yang, Y., & Yang, L. (2013). Experimental study on heat transfer enhancement of wavy finned flat tube with longitudinal vortex generators. *Applied Thermal Engineering*, *50*(1), 55–62. https://doi.org/10.1016/j.applthermaleng.2012.05.024

[13] Dyke, M. Van. (1988). An Album of Fluid Motion, Fourth Printing.

[14] Esmaeilzadeh, A., Amanifard, N., & Deylami, H. M. (2017). Comparison of simple and curved trapezoidal longitudinal vortex generators for optimum flow characteristics and heat transfer augmentation in a heat exchanger. *Applied Thermal Engineering*, *125*. https://doi.org/10.1016/j.applthermaleng.2017.07.115

[15] Fiebig, M. (1998). Vortices, generators and heat transfer. *Chemical Engineering Research and Design*, *76*(2), 108–123. https://doi.org/10.1205/026387698524686

[16] Fiebig, M., Güntermann, T., & Mitra, N. K. (1995). Numerical analysis of heat transfer and flow loss in a parallel plate heat exchanger element with longitudinal vortex generators as fins. *Journal of Heat Transfer*, *117*(4), 1064–1067. https://doi.org/10.1115/1.2836284

[17] Fiebig, M., Valencia, A., & Mitra, N. K. (1993). Wing-type vortex generators for fin-and-tube heat exchangers. *Experimental Thermal and Fluid Science*,

7(4), 287–295. https://doi.org/10.1016/0894-1777(93)90052-K

[18] Fiebig, Martin. (1995). Embedded vortices in internal flow: heat transfer and pressure loss enhancement. *International Journal of Heat and Fluid Flow*, *16*(5), 376–388. https://doi.org/10.1016/0142-727X(95)00043-P

[19] Fiebig, Martin, Mitra, N. K., & Dong, Y. (2019). SIMULTANEOUS HEAT TRANSFER ENHANCEMENT AND FLOW LOSS REDUCTION OF FIN-TUBES. In *International Heat Transfer Conference 9* (pp. 51–55). Begell House. https://doi.org/10.1615/ihtc9.1290

[20] Gong, B., Wang, L. B., & Lin, Z. M. (2015). Heat transfer characteristics of a circular tube bank fin heat exchanger with fins punched curve rectangular vortex generators in the wake regions of the tubes. *Applied Thermal Engineering*, *75*, 224–238. https://doi.org/10.1016/j.applthermaleng.2014.09.043

[21] Han, H., Wang, S., Sun, L., Li, Y., & Wang, S. (2019). Numerical study of thermal and flow characteristics for a fin-and-tube heat exchanger with arc winglet type vortex generators. *International Journal of Refrigeration*. https://doi.org/10.1016/j.ijrefrig.2018.10.021

[22] He, J., Liu, L., & Jacobi, A. M. (2010). Air-Side Heat-Transfer Enhancement by a New Winglet-Type Vortex Generator Array in a Plain-Fin Round-Tube Heat Exchanger. *Journal of Heat Transfer*, *132*(7), 071801. https://doi.org/10.1115/1.4000988

[23] He, Y. L., Han, H., Tao, W. Q., & Zhang, Y. W. (2012). Numerical study of heat-transfer enhancement by punched winglet-type vortex generator arrays in fin-and-tube heat exchangers. *International Journal of Heat and Mass Transfer*, *55*(21–22), 5449–5458. https://doi.org/10.1016/j.ijheatmasstransfer.2012.04.059

[24] He, Ya Ling, Chu, P., Tao, W. Q., Zhang, Y. W., & Xie, T. (2013). Analysis of heat transfer and pressure drop for fin-and-tube heat exchangers with rectangular winglet-type vortex generators. *Applied Thermal Engineering*, *61*(2), 770–783. https://doi.org/10.1016/j.applthermaleng.2012.02.040

[25] Holman, J. P. (2001). Experimental methods for engineers /. *McGraw-Hill*

Series in Mechanical Engineering.

[26] Hu, W., Wang, L., Guan, Y., & Hu, W. (2017). The effect of shape of winglet vortex generator on the thermal–hydrodynamic performance of a circular tube bank fin heat exchanger. *Heat and Mass Transfer/Waerme- Und Stoffuebertragung*, *53*(9), 2961–2973. https://doi.org/10.1007/s00231-017-2042-3

[27] Jacobi, A. M., & Shah, R. K. (1995). Heat transfer surface enhancement through the use of longitudinal vortices: A review of recent progress. *Experimental Thermal and Fluid Science*, *11*(3), 295–309. https://doi.org/10.1016/0894-1777(95)00066-U

[28] Jalil, J., Abdulla, H., & Yusuf, A. (2006). Effect of Winglet Shape on Heat Transfer from Heated Cylinder in Cross Flow تأثير شكل مولد الدوامات على انتقال الحرارة من أسطوانة مسخنة. *Journal of King Abdulaziz University-Engineering Sciences*, *17*(2), 117–128. https://doi.org/10.4197/eng.17-2.6

[29] Jedsadaratanachai, W., & Boonloi, A. (2015). Thermal performance assessment in a fin-and-oval-tube heat exchanger with delta winglet vortex generators. *Journal of Mechanical Science and Technology*, *29*(4), 1765–1779. https://doi.org/10.1007/s12206-015-0350-4

[30] Joardar, A., & Jacobi, A. M. (2008). Heat transfer enhancement by winglet-type vortex generator arrays in compact plain-fin-and-tube heat exchangers. *International Journal of Refrigeration*, *31*(1), 87–97. https://doi.org/10.1016/j.ijrefrig.2007.04.011

[31] Kakaç, S. (Sadık), Shah, R. K., & Aung, W. (1987). *Handbook of single-phase convective heat transfer*. Wiley. Retrieved from https://inis.iaea.org/search/search.aspx?orig_q=RN:18090434

[32] Ke, Z., Chen, C. L., Li, K., Wang, S., & Chen, C. H. (2019). Vortex dynamics and heat transfer of longitudinal vortex generators in a rectangular channel. *International Journal of Heat and Mass Transfer*, *132*. https://doi.org/10.1016/j.ijheatmasstransfer.2018.12.064

[33] Khoshvaght-Aliabadi, M., Sartipzadeh, O., & Alizadeh, A. (2015). An experimental study on vortex-generator insert with different arrangements of

delta-winglets. *Energy*, *82*, 629–639. https://doi.org/10.1016/j.energy.2015.01.072

[34] Kwak, K. M., Torii, K., & Nishino, K. (2002). Heat transfer and flow characteristics of fin-tube bundles with and without winglet-type vortex generators. *Experiments in Fluids*, *33*(5), 696–702. https://doi.org/10.1007/s00348-002-0528-2

[35] Lemouedda, A., Breuer, M., Franz, E., Botsch, T., & Delgado, A. (2010). Optimization of the angle of attack of delta-winglet vortex generators in a plate-fin-and-tube heat exchanger. *International Journal of Heat and Mass Transfer*, *53*(23–24), 5386–5399. https://doi.org/10.1016/j.ijheatmasstransfer.2010.07.017

[36] Li, L., Du, X., Zhang, Y., Yang, L., & Yang, Y. (2015). Numerical simulation on flow and heat transfer of fin-and-tube heat exchanger with longitudinal vortex generators. *International Journal of Thermal Sciences*, *92*, 85–96. https://doi.org/10.1016/j.ijthermalsci.2015.01.030

[37] Li, M. J., Zhang, H., Zhang, J., Mu, Y. T., Tian, E., Dan, D., … Tao, W. Q. (2018). Experimental and numerical study and comparison of performance for wavy fin and a plain fin with radiantly arranged winglets around each tube in fin-and-tube heat exchangers. *Applied Thermal Engineering*, *133*, 298–307. https://doi.org/10.1016/j.applthermaleng.2018.01.012

[38] Li, W., Khan, T. A., Tang, W., & Minkowycz, W. J. (2018). Numerical Study and Optimization of Corrugation Height and Angle of Attack of Vortex Generator in the Wavy Fin-and-Tube Heat Exchanger. *Journal of Heat Transfer*, *140*(11), 111801. https://doi.org/10.1115/1.4040609

[39] Lotfi, B., Sundén, B., & Wang, Q. (2016). An investigation of the thermo-hydraulic performance of the smooth wavy fin-and-elliptical tube heat exchangers utilizing new type vortex generators. *Applied Energy*, *162*, 1282–1302. https://doi.org/10.1016/j.apenergy.2015.07.065

[40] Lu, G., & Zhai, X. (2019). Effects of curved vortex generators on the air-side performance of fin-and-tube heat exchangers. *International Journal of Thermal Sciences*, *136*. https://doi.org/10.1016/j.ijthermalsci.2018.11.009

[41] Lu, G., & Zhou, G. (2016a). Numerical simulation on performances of plane and curved winglet - Pair vortex generators in a rectangular channel and field synergy analysis. *International Journal of Thermal Sciences*, *109*. https://doi.org/10.1016/j.ijthermalsci.2016.06.024

[42] Lu, G., & Zhou, G. (2016b). Numerical simulation on performances of plane and curved winglet type vortex generator pairs with punched holes. *International Journal of Heat and Mass Transfer*, *102*, 679–690. https://doi.org/10.1016/j.ijheatmasstransfer.2016.06.063

[43] Lyczkowski, R. W. (1984). Heat exchangers—theory and practice, J. Taborek, G. F. Hewitt, and N. Afgan, Editors Hemisphere Publishing Corp., Washington, D.C., 1983 992 pages,$69.95. *AIChE Journal*, *30*(2), 350–350. https://doi.org/10.1002/aic.690300229

[44] Md Salleh, M. F., Gholami, A., & Wahid, M. A. (2018). Numerical Evaluation of Thermal Hydraulic Performance in Fin-and-Tube Heat Exchangers With Various Vortex Generator Geometries Arranged in Common-Flow-Down or Common-Flow-Up. *Journal of Heat Transfer*, *141*(2), 021801. https://doi.org/10.1115/1.4041832

[45] Menter, F. R. (1994). Two-equation eddy-viscosity turbulence models for engineering applications. *AIAA Journal*, *32*(8), 1598–1605. https://doi.org/10.2514/3.12149

[46] Min, C., Qi, C., Kong, X., & Dong, J. (2010). Experimental study of rectangular channel with modified rectangular longitudinal vortex generators. *International Journal of Heat and Mass Transfer*, *53*(15–16), 3023–3029. https://doi.org/10.1016/j.ijheatmasstransfer.2010.03.026

[47] Naik, H., Harikrishnan, S., & Tiwari, S. (2018). Numerical investigations on heat transfer characteristics of curved rectangular winglet placed in a channel. *International Journal of Thermal Sciences*, *129*. https://doi.org/10.1016/j.ijthermalsci.2018.03.028

[48] Naik, H., & Tiwari, S. (2018). Effect of winglet location on performance of fin-tube heat exchangers with inline tube arrangement. *International Journal of Heat and Mass Transfer*, *125*, 248–261.

https://doi.org/10.1016/j.ijheatmasstransfer.2018.04.071

[49] Oneissi, M., Habchi, C., Russeil, S., Bougeard, D., & Lemenand, T. (2016). Novel design of delta winglet pair vortex generator for heat transfer enhancement. *International Journal of Thermal Sciences*, *109*, 1–9. https://doi.org/10.1016/j.ijthermalsci.2016.05.025

[50] PAULEY, W. R., & EATON, J. K. (2008). Experimental study of the development of longitudinal vortex pairs embedded in a turbulent boundary layer. *AIAA Journal*, *26*(7), 816–823. https://doi.org/10.2514/3.9974

[51] Pearcy, H. (1961). Stock-Induced Separation in Boundary Layers and Flow Control, 2.

[52] Pesteei, S. M., Subbarao, P. M. V., & Agarwal, R. S. (2005). Experimental study of the effect of winglet location on heat transfer enhancement and pressure drop in fin-tube heat exchangers. *Applied Thermal Engineering*, *25*(11–12), 1684–1696. https://doi.org/10.1016/j.applthermaleng.2004.10.013

[53] Saboya, F. E. M., & Sparrow, E. M. (1974). Local and average transfer coefficients for one-row plate fin and tube heat exchanger configurations. *Journal of Heat Transfer*, *96*(3), 265–272. https://doi.org/10.1115/1.3450189

[54] Sahiti, N., Lemouedda, A., Stojkovic, D., Durst, F., & Franz, E. (2006). Performance comparison of pin fin in-duct flow arrays with various pin cross-sections. *Applied Thermal Engineering*, *26*(11–12), 1176–1192. https://doi.org/10.1016/j.applthermaleng.2005.10.042

[55] Salviano, L. O., Dezan, D. J., & Yanagihara, J. I. (2016). Thermal-hydraulic performance optimization of inline and staggered fin-tube compact heat exchangers applying longitudinal vortex generators. *Applied Thermal Engineering*, *95*, 311–329. https://doi.org/10.1016/j.applthermaleng.2015.11.069

[56] Samadifar, M., & Toghraie, D. (2018). Numerical simulation of heat transfer enhancement in a plate-fin heat exchanger using a new type of vortex generators. *Applied Thermal Engineering*, *133*. https://doi.org/10.1016/j.applthermaleng.2018.01.062

[57] Sarangi, S. K., & Mishra, D. P. (2017). Effect of winglet location on heat

transfer of a fin-and-tube heat exchanger. *Applied Thermal Engineering*, *116*. https://doi.org/10.1016/j.applthermaleng.2017.01.106

[58] Shi, B., Wang, L., Gen, F., & Zhang, Y. (2006). The optimal fin spacing for three-row flat tube bank fin mounted with vortex generators. *Heat and Mass Transfer/Waerme- Und Stoffuebertragung*, *43*(1), 91–101. https://doi.org/10.1007/s00231-006-0093-y

[59] Singh, S., Sørensen, K., & Condra, T. (2018). Investigation of Vortex Generator Enhanced Double-Fin and Tube Heat Exchanger. *Journal of Heat Transfer*, *141*(2), 021802. https://doi.org/10.1115/1.4042050

[60] Sinha, A., Chattopadhyay, H., Iyengar, A. K., & Biswas, G. (2016). Enhancement of heat transfer in a fin-tube heat exchanger using rectangular winglet type vortex generators. *International Journal of Heat and Mass Transfer*, *101*, 667–681. https://doi.org/10.1016/j.ijheatmasstransfer.2016.05.032

[61] Song, K. W., Tagawa, T., Chen, Z. H., & Zhang, Q. (2019). Heat transfer characteristics of concave and convex curved vortex generators in the channel of plate heat exchanger under laminar flow. *International Journal of Thermal Sciences*. https://doi.org/10.1016/j.ijthermalsci.2018.11.002

[62] Song, K. W., Wang, L. B., Fan, J. F., Zhang, Y. H., & Liu, S. (2008). Numerical study of heat transfer enhancement of finned flat tube bank fin with vortex generators mounted on both surfaces of the fin. *Heat and Mass Transfer/Waerme- Und Stoffuebertragung*, *44*(8), 959–967. https://doi.org/10.1007/s00231-007-0339-3

[63] Song, K. W., Xi, Z. P., Su, M., Wang, L. C., Wu, X., & Wang, L. B. (2017). Effect of geometric size of curved delta winglet vortex generators and tube pitch on heat transfer characteristics of fin-tube heat exchanger. *Experimental Thermal and Fluid Science*, *82*, 8–18. https://doi.org/10.1016/j.expthermflusci.2016.11.002

[64] Tang, L. H., Chu, W. X., Ahmed, N., & Zeng, M. (2016). A new configuration of winglet longitudinal vortex generator to enhance heat transfer in a rectangular channel. *Applied Thermal Engineering*, *104*, 74–84.

https://doi.org/10.1016/j.applthermaleng.2016.05.056

[65] Tang, Ling Hong, Tan, S. C., Gao, P. Z., & Zeng, M. (2016). Parameters Optimization of Fin-and-Tube Heat Exchanger with a Novel Vortex Generator Fin by Taguchi Method. *Heat Transfer Engineering*, *37*(3–4), 369–381. https://doi.org/10.1080/01457632.2015.1052715

[66] Tian, L., Liu, B., Min, C., Wang, J., & He, Y. (2015). Study on the effect of punched holes on flow structure and heat transfer of the plain fin with multi-row delta winglets. *Heat and Mass Transfer/Waerme- Und Stoffuebertragung*, *51*(11), 1523–1536. https://doi.org/10.1007/s00231-015-1521-7

[67] Tian, L. T., He, Y. L., Lei, Y. G., & Tao, W. Q. (2009). Numerical study of fluid flow and heat transfer in a flat-plate channel with longitudinal vortex generators by applying field synergy principle analysis. *International Communications in Heat and Mass Transfer*, *36*(2), 111–120. https://doi.org/10.1016/j.icheatmasstransfer.2008.10.018

[68] Tian, X. L., Jin, H., Song, K. W., Wang, L. C., Liu, S., & Wang, L. B. (2018). Effects of fin pitch and tube diameter on the air-side performance of tube bank fin heat exchanger with the fins punched plane and curved rectangular vortex generators. *Experimental Heat Transfer*, *31*(4), 297–316. https://doi.org/10.1080/08916152.2017.1410503

[69] Tiggelbeck, St., Mitra, N. K., & Fiebig, M. (2008). Comparison of Wing-Type Vortex Generators for Heat Transfer Enhancement in Channel Flows. *Journal of Heat Transfer*, *116*(4), 880. https://doi.org/10.1115/1.2911462

[70] Tiggelbeck, Stefan, Mitra, N., & Fiebig, M. (1992). Flow structure and heat transfer in a channel with multiple longitudinal vortex generators. *Experimental Thermal and Fluid Science*, *5*(4), 425–436. https://doi.org/10.1016/0894-1777(92)90029-5

[71] Tiwari, S., Maurya, D., Biswas, G., & Eswaran, V. (2003). Heat transfer enhancement in cross-flow heat exchangers using oval tubes and multiple delta winglets. *International Journal of Heat and Mass Transfer*, *46*(15), 2841–2856. https://doi.org/10.1016/S0017-9310(03)00047-4

[72] Torii, K., Kwak, K. M., & Nishino, K. (2002). Heat transfer enhancement

accompanying pressure-loss reduction with winglet-type vortex generators for fin-tube heat exchangers. *International Journal of Heat and Mass Transfer*, *45*(18), 3795–3801. https://doi.org/10.1016/S0017-9310(02)00080-7

[73] Torii, Kahoru, Nishino, K., & Nakayama, K. (2019). Mechanism of Heat Transfer Augmentation by Longitudinal Vortices in a Flat Plate Boundary Layer. In *International Heat Transfer Conference 10* (pp. 123–128). Begell House. https://doi.org/10.1615/ihtc10.2420

[74] Valencia, A., Fiebig, M., & Mitra, N. K. (1996). Heat Transfer Enhancement by Longitudinal Vortices in a Fin-Tube Heat Exchanger Element With Flat Tubes. *Journal of Heat Transfer*, *118*(1), 209. https://doi.org/10.1115/1.2824039

[75] Wang, C. C., Lo, J., Lin, Y. T., & Wei, C. S. (2002). Flow visualization of annular and delta winlet vortex generators in fin-and-tube heat exchanger application. *International Journal of Heat and Mass Transfer*, *45*(18), 3803–3815. https://doi.org/10.1016/S0017-9310(02)00085-6

[76] Wang, W., Bao, Y., & Wang, Y. (2015). Numerical investigation of a finned-tube heat exchanger with novel longitudinal vortex generators. *Applied Thermal Engineering*, *86*, 27–34. https://doi.org/10.1016/j.applthermaleng.2015.04.041

[77] Wendt, B. J., & Hingst, W. R. (1994). Flow structure in the wake of a wishbone vortex generator. *AIAA Journal*, *32*(11), 2234–2240. https://doi.org/10.2514/3.12282

[78] Wilcox, D. C. (1993). *Turbulence Modeling for CFD*. Retrieved from http://inis.jinr.ru/sl/vol2/Physics/Механика сплошной среды/Wilcox,_Turbulence_Modeling_for_CFD,1994/contents.pdf

[79] Wu, J. M., & Tao, W. Q. (2011). Impact of delta winglet vortex generators on the performance of a novel fin-tube surfaces with two rows of tubes in different diameters. *Energy Conversion and Management*, *52*(8–9), 2895–2901. https://doi.org/10.1016/j.enconman.2011.03.002

[80] Wu, J. M., & Tao, W. Q. (2012). Effect of longitudinal vortex generator on heat transfer in rectangular channels, *37*, 67–72.

https://doi.org/10.1016/j.applthermaleng.2012.01.002

[81] Wu, X., Liu, D. D., Zhao, M., Lu, Y. L., & Song, X. (2016). The optimization of fin-tube heat exchanger with longitudinal vortex generators using response surface approximation and genetic algorithm. *Heat and Mass Transfer/Waerme- Und Stoffuebertragung*, *52*(9), 1871–1879. https://doi.org/10.1007/s00231-015-1709-x

[82] Yoo, S. Y., Park, D. S., Chung, M. H., & Lee, S. Y. (2002). Heat transfer enhancement for fin-tube heat exchanger using vortex generators. *KSME International Journal*, *16*(1), 109–115. https://doi.org/10.1007/BF03185161

[83] Yun, J., & Lee, K. (2000). In ¯ uence of design parameters on the heat transfer and ¯ ow friction characteristics of the heat exchanger with slit ® ns, *43*, 2529–2539.

[84] Zeeshan, M., Nath, S., Bhanja, D., & Das, A. (2018). Numerical investigation for the optimal placements of rectangular vortex generators for improved thermal performance of fin-and-tube heat exchangers. *Applied Thermal Engineering*, *136*, 589–601. https://doi.org/10.1016/j.applthermaleng.2018.03.006

[85] Zhou, G., & Feng, Z. (2014). Experimental investigations of heat transfer enhancement by plane and curved winglet type vortex generators with punched holes. *International Journal of Thermal Sciences*. https://doi.org/10.1016/j.ijthermalsci.2013.11.010

LIST OF PUBLICATIONS

During the residency period of Ph.D. work

S.No.	Title	Authors	Journal / Conference	Indexing
Published / Accepted				
1.	Numerical investigation towards implementation of punched winglet as vortex generator for performance improvement of a fin-and-tube heat exchanger	Arvind Gupta, Aditya Roy, Sachin Gupta, Munish Gupta	International Journal of Heat and Mass Transfer, Elsevier Publications, Volume 149, 2020, 119171, (Published)	SCI *(Impact factor 4.346)*
2.	Computer-aided engineering analysis for the performance improvement of a fin-and-tube heat exchanger using vortex generator	Sachin Gupta, Aditya Roy, Arvind Gupta	Concurrent Engineering: Research and Applications, Sage Publications, 2019 (Published)	SCI *(Impact factor 1.127)*
3.	Numerical investigations to find the optimal placement of winglet for improvement of air side performance of cross-flow heat exchanger	Sachin Gupta, Arvind Gupta, Munish Gupta,	Heat Transfer-Asian Research, John Wiley & Sons, 2020 (Accepted)	ESCI, SCOPUS

4.	Numerical Simulations of Performance of Plate Fin Tube Heat Exchanger Using Rectangular Winglet Type Vortex Generator with Punched Holes	Sachin Gupta, Aditya Roy, Arvind Gupta, Munish Gupta	SAE Technical Paper 2019-01-0145, 2019, Published by SAE International, doi: 0.4271/2019-01-0145 (Published)	SCOPUS
5.	Performance improvement of a fin-tube heat exchanger using rectangular winglet as vortex generator	Sachin Gupta, Arvind Gupta, Munish Gupta	International Journal of Energy, Environment and Economics, Nova Science Publishers, Volume-25, Issue-04, 2017 (Published)	SCOPUS
6.	Heat Transfer Enhancement - A Review	Arvind Gupta, Sachin Gupta	IJMRS's International Journal of Engineering Sciences, Vol. 03, Issue 01, 2014 (Published)	Refereed

7.	Heat transfer improvement using vortex generator	Sachin Gupta, Arvind Gupta, Munish Gupta	Proceedings of the National Conference on Trends and Advances in Mechanical Engineering (TAME-2019) 2019	----
8.	A Review on techniques for heat transfer augmentation	Sachin Gupta, Arvind Gupta, Munish Gupta	Proceedings of National Conference on Recent Advances in Mechanical & Civil Engineering (RAMCE-2014) 2014	-----

APPENDIX A

Measurement of the mean velocity of airflow at two different probe points

No.	*Mean A	**Mean B	% Deviation
1	1.025	1.021	0.39
2	2.021	2.010	0.54
3	3.051	3.062	0.36
4	4.047	4.052	0.12
5	5.042	5.038	0.08
6	6.098	6.087	0.18

*Mean A: Mean velocity at 5mm below the position of the thermal probe

(Measured by Pitot-static tube)

**Mean B: Mean velocity at the position of the thermal probe

(Measured by Pitot-static tube)